

Lilian Telesphore Beichumila

Diagenesis and reservoir quality of deep marine Upper Cretaceous sandstone; Nise Formation in Vøring Basin, offshore Mid-Norway.

A mineralogical and petrographic approach.

Master's thesis in Petroleum Geoscience
Supervisor: Professor Mai Britt E. Mørk
July 2019

Lilian Telesphore Beichumila

Diagenesis and reservoir quality of deep marine Upper Cretaceous sandstone; Nise Formation in Vøring Basin, offshore Mid-Norway.

A mineralogical and petrographic approach.

Master's thesis in Petroleum Geoscience
Supervisor: Professor Mai Britt E. Mørk
July 2019

Norwegian University of Science and Technology
Faculty of Engineering
Department of Geoscience and Petroleum

 **NTNU**
Norwegian University of
Science and Technology

ACKNOWLEDGEMENT

First and foremost, I would like to thank Almighty God for giving me the strength, knowledge, ability and opportunity to undertake this master's thesis and complete it satisfactorily. Without His blessings, this achievement would not have been possible.

I feel great honor in expressing my special thanks to my supervisor, Professor Mai Britt E. Mørk for her valuable assistance, quick feedbacks and constructive discussions throughout this study. My gratitude is extended to Kjetil Eriksen for providing technical assistance during point count analysis and SEM studies.

I would like to express my warm thanks to EnPe-NORAD and Equinor Tanzania under the Angolan Norwegian Tanzanian Higher Education Initiative (ANTHEI) project for the financial support during my studies at Norwegian University of Science and Technology (NTNU).

My sincere thanks go to my family, friends and colleagues for their emotional support and love during my academic journey.

Last but not least, I would like to thank and congratulate myself for doing all this hard work.

NTNU, Trondheim.

02nd July 2019.

Lilian Telesphore Beichumila.

ABSTRACT

The present study deals with diagenesis and reservoir quality of deep marine (> 1.2 km water depth) Upper Cretaceous sandstones in Vøring Basin. Mineralogical and petrographical analysis has been done on the cored interval from well 6707/10-1. The study focuses in the petrographic understanding, diagenetic development and their influence on reservoir quality.

The studied samples are mineralogically and textually matured, mainly consist of quartz grains and classified as subarkose. The reservoir quality evolution was slightly controlled by compaction and cementation and improved through the partial to total dissolution of framework grains (mainly feldspars and micas) but the net gain in porosity was insignificant due to precipitation of authigenic clays.

The authigenic clays mineral content has been evaluated both in the optical microscope and scanning electron microscopy. The deep marine Nise Sandstone Formation contains kaolin as pore filling clay mineral along with partially leached feldspar grains. The occurrence of kaolin is in small amount since the Nise Formation was deposited in a distal setting (basin- floor fan system) and the sediments were isolated from meteoric water flushing. Kaolin is known for porosity reduction, but in these studied samples the amount was too low to reduce the reservoir quality.

The overall high IGV values (30.3 – 48.4%) have been observed in this study. High IGV values and well-preserved porosity indicate that mechanical compaction is not very significant in the cored interval. It has been observed that samples with higher carbonate cement ($\geq 18.2\%$) exhibits comparatively higher IGVs as compare to the samples without or lower carbonate cementation. This early carbonate cement helped to reduce the effect of mechanical compaction and preserve the high IGV values.

Upper Cretaceous sandstone deposited in the Vøring Basin are sourced from East Greenland and deposited from hyper-concentrated to concentrated density flows and turbidity flows which deposited clay free sediments. The longer transport distance and higher degree of sorting resulted to high porosity sandstones. The burial history shows that the sediments in the studied area experienced relatively low thermal exposure (have only recently exceeded 100°C). Consequently the sediments were not affected by the progressive and intense thermal subsidence to develop mesogenetic conditions such as extensive quartz overgrowth.

From this study it has been concluded that, the relatively high porosity values (average 24.41%) and the excellent reservoir quality of Nise Formation is due to the presence of limited quartz cement and to textural and mineralogical matured sandstones.

Contents

Chapter 1: Introduction.....	1
1.1 Background	1
1.2 Research objectives	2
1.3 Data and methods.....	2
1.4 Study Area.....	3
1.5 Structure of the thesis	6
Chapter 2: Geological framework	7
2.1 Introduction	7
2.2 Structural and tectonic settings of Mid-Norway.....	7
2.2.1 Tectonic setting of Vøring basin.....	8
2.3 Regional stratigraphy	10
2.3.1 Stratigraphy of Vøring basin.....	13
2.3.2 The Upper Cretaceous depositional system.....	15
2.4 Petroleum System of Mid-Norway	18
2.4.1 Petroleum system in Vøring basin	20
2.4.2 Exploration history of Vøring basin.	20
Chapter 3: Theoretical background	22
3.1 Introduction	22
3.2 Diagenesis	23
3.2.1 Near surface diagenesis.....	23
3.2.2 Mechanical compaction	26
3.2.3 Chemical compaction.....	28
3.3 Porosity Preservation Mechanisms.....	31
3.3.1 Grain coating.....	31
3.3.2 Fluid overpressure.....	33
3.3.3 Early hydrocarbon emplacement	34
Chapter 4: Methodology	35
4.1 Optical microscopy.....	35
4.1.1 Thin section analysis.....	35

4.1.2	Point count analysis	35
4.1.3	Intergranular volume.....	36
4.2	Scanning Electron Microscopy	37
4.3	Uncertainties.....	38
4.3.1	Thin section analysis.....	38
4.3.2	Point counting analysis	38
4.3.3	Intergranular volume.....	39
4.3.4	Scanning electron microscopy	39
Chapter 5:	Optical microscopy	40
5.1	Introduction	40
5.2	Results.....	40
5.2.1	Point count	40
5.2.2	Intergranular volume (IGV).....	50
5.2.3	Thin section observation.....	59
Chapter 6:	Scanning Electron Microscopy	66
6.1	Introduction.....	66
6.2	Results.....	66
6.2.1	Quartz overgrowth and porosity	66
6.2.2	Grain coating.....	67
6.2.3	Carbonate cement.....	68
6.2.4	Authigenic clays.....	70
6.2.5	Feldspar dissolution	72
6.2.6	Opaque minerals	74
6.2.7	Other minerals.....	76
Chapter 7:	Discussion.....	78
7.1	Introduction	78
7.2	Mechanical compaction.....	79
7.2.1	Intergranular volume.....	79
7.2.2	Textural characteristics	81
7.3	Chemical compaction.....	82
7.3.1	Carbonate cement.....	82
7.3.2	Authigenic clay	83
7.3.3	Authigenic quartz cement	84

7.3.4	Effect of Temperature history	85
7.3.5	Grain coating.....	86
7.3.6	Overpressure	87
7.3.7	Early Hydrocarbon emplacement	87
Chapter 8:	Conclusion	88
Chapter 9:	References	90

Chapter 1: Introduction

This thesis is performed as a part of a master's degree (M.Sc.) in Petroleum Geosciences, during the spring semester of 2019 at the Norwegian University of Science and Technology. It mainly describes the diagenesis and reservoir quality of deep marine Upper Cretaceous sandstone, Nise Formation in Vøring Basin offshore Mid-Norway.

1.1 Background

For the petroleum exploration point of view, the Norwegian Continental Shelf is distributed into three main provinces; North Sea, Mid-Norwegian continental margin and Western Barents Sea. These provinces were the part of a large epicontinental sea before continental break-up which was lying between the continental masses of Fennoscandia, Svalbard and Greenland ([Faleide et al., 2010](#)). This study covers the Nise Formation in Vøring Basin area from the Mid-Norwegian continental margin.

The Mid-Norwegian continental margin province has faced several stages of subsidence, uplift and erosion which effected the reservoir quality for petroleum accumulation. The updated technology and ideas are essential for interpreting and forecasting of reservoir quality which is important for successful exploration of petroleum in the uplifted area like the Mid-Norwegian continental margin.

According to [Worden and Morad \(2009\)](#), the reservoir quality of sandstones at any depth is mainly controlled by the initial depositional porosity and permeability, extent of mechanical and chemical compaction and quantity and type of pore-filling cement. The porosity reduction due to the mechanical compaction ceased when the chemical compaction starts. The degree of mechanical compaction may vary depending on textural characteristics and the composition of the sandstone. Quartz cementation is considered as the main porosity-reducing process at depths greater than 2.5km ([Paxton et al., 2002](#)).

The quartz cementation is mainly controlled by the temperature and kinetics. At temperatures above 80°C the precipitation of authigenic quartz cement will proceed until all pore-space is filled (Walderhaug, 1994b), and reservoir cut off is usually reached at approximately 3.5-4.5 km depth. Several porosity-preserving mechanisms may hinder the growth of authigenic quartz such as grain coatings, hydrocarbon emplacement and fluid overpressure. However, grain coatings (illite, chlorite, micro-quartz, detrital clay, and bitumen) are considered the most important (Taylor et al., 2010). The precipitation of authigenic clay minerals within the pore-space during burial may additionally influence the reservoir characteristics (Bjørlykke, 1998).

1.2 Research objectives

The main objective of my thesis research is to analyze the reservoir quality of Upper Cretaceous, Nise Formation in Vøring Basin from the cored reservoir interval in well 6707/10-1. During this analysis thin section samples made from cores are analyzed under optical microscope. Additionally, Scanning Electron Microscopy (SEM) analysis is also employed on carbon coated thin section slides. The focus of the study is to understand the diagenetic processes that have affected the deep marine sandstones, both the mechanical and chemical compaction. The thesis will also investigate the distribution and source of diagenetic materials and assess their influence on the reservoir quality.

1.3 Data and methods

A total of 25 thin section samples from an exploration well 6707/10-1 have been used in this study. It is a wildcat well which contain gas. The information about this well is given in [Table 1.1](#).

The reservoir properties from thin sections and carbon coated samples were investigated by mineralogical and petrographic analysis through:

- i. Optical microscopy.
- ii. Scanning Electron Microscopy.

Table 1.1: The description of the well 6707/10-1 from offshore Mid-Norway selected for the present study. Note that this exploratory well was drilled up to Cretaceous reservoirs with relatively low geothermal gradients but with greater water depth (fact pages NPD 2019). RKB – Rotary Kelly Bushing.

Well Name	Drilling Operator	NS UTM	EW UTM	Entry Date	Completion Date	Oldest age penetrated	Oldest formation penetrated	Content	Water Depth	Total Depth	Final V. Depth	B.H. Temp	Geo. Grad
		(m)	(m)						(m)	(m RKB)	(m RKB)	(°C)	(°C/km)
6707/10-1	BP Norway limited U. A	7440629.70	413490.42	19.04.1997	23.07.1997	Late Cretaceous	Kvitnos Formation	Gas	1274	5039	5026.5	114	22.68

1.4 Study Area

The Vøring Basin is situated on the Mid-Norwegian continental margin between latitude 65° and 67° north. This predominantly gas-prone hydrocarbon province extends out from the shelf to deep-water. From [Figure 1.1](#) to the east, Vøring Basin is delimited by the Trøndelag Platform and to the west, by the Vøring Marginal High. While to the north, the Vøring Basin is delimited by the Bivrost Lineament and by the Møre Basin to the south ([Blystad et al., 1995](#); [Brekke, 2000](#); [Mosar, 2000](#)).

Geologically, the Vøring Basin is a large sedimentary basin that consists of structural highs, grabens, and sub-basins ([Skogseid et al., 1992b](#)) mainly dominated by deep Cretaceous sequences and several magmatic rocks e.g., sills of the NE Atlantic margin and the North Atlantic igneous province ([Brekke et al., 1999](#)).

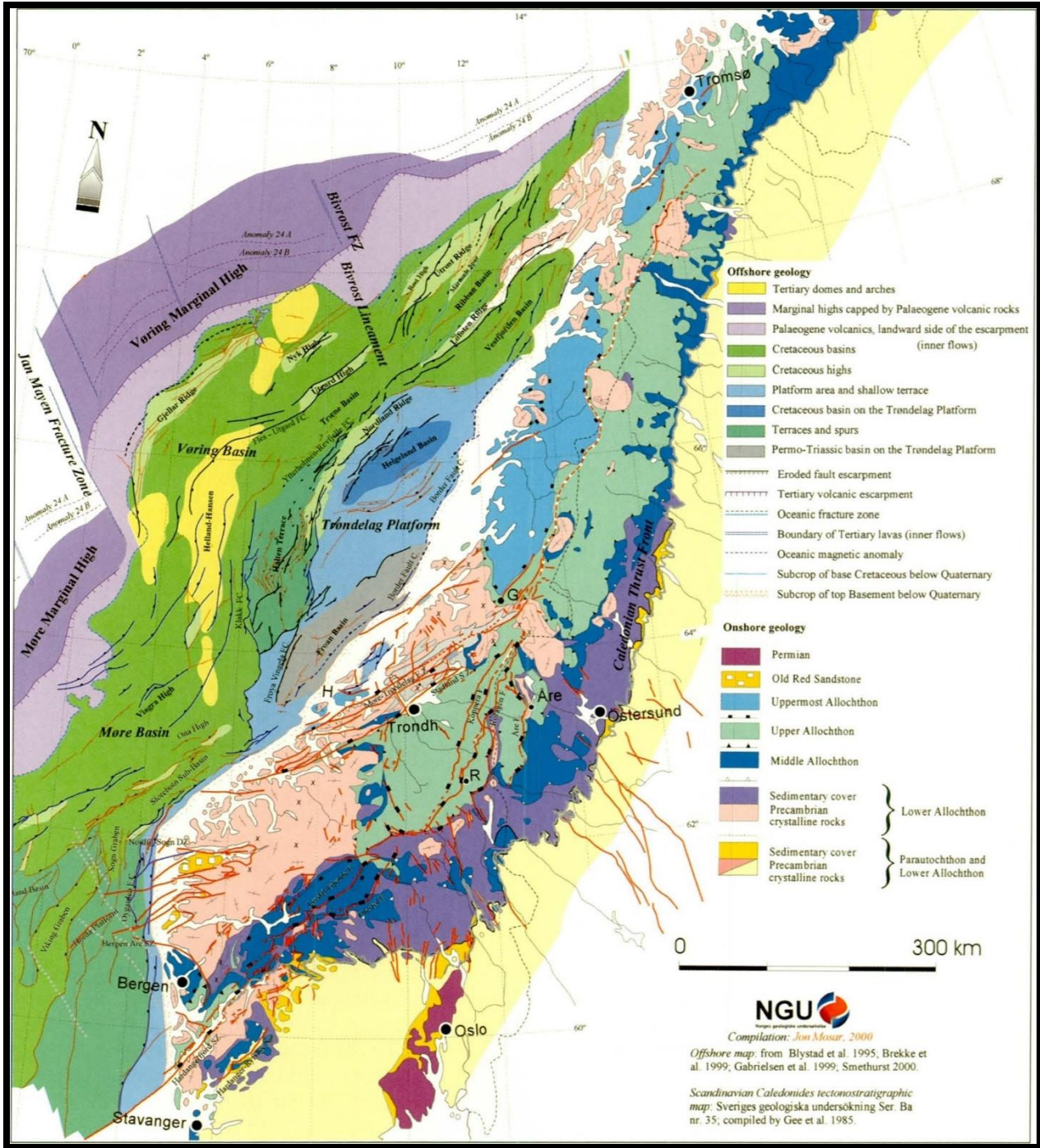


Figure 1.1: Simplified tectonostratigraphic map of the Atlantic Norwegian passive margin showing location of Vøring Basin. H = Hitra; R = Røragen and Trondh. = Trondheim. (Mosar, 2000).

The portion of the Vøring Basin represented in this study is located in the Nyk High from well 6707/10-1, 250 km offshore Mid-Norway (Knaust, 2009) which contains gas and so-called Nyk discovery well as presented in Figure 1.2. The Nyk cores cover 205 m of the Lower–Middle Campanian succession (3145–2967 m and 4145–4118 m) belonging to the Nise 1 sandstone and Nise 2 sandstone of the Nise Formation respectively (Fjellanger et al., 2005).

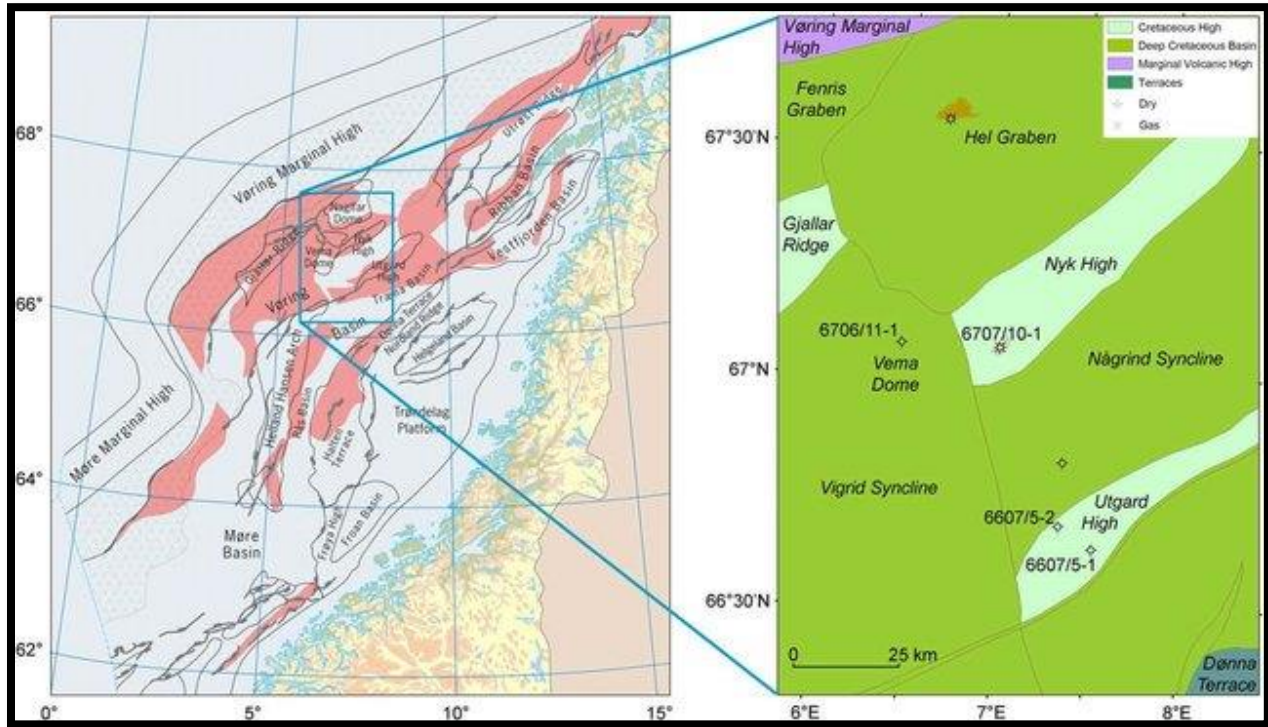


Figure 1.2: Regional map of a part of the offshore Mid-Norway region including the Vøring Basin with reservoir units of Upper Cretaceous rocks and the studied well (6707/10-1). The Dønna Terrace is located in the East of Vøring Basin while Vøring Marginal High marks the western limit. (Knaust, 2009)

1.5 Structure of the thesis

The thesis is divided into main eight chapters (**Figure 1.3**). Chapter 1, 2 and 3 are introduction to the thesis, highlight of tectonic evolution of the study area and theoretical background of the study. Chapter 4 deals with the methods used in the thesis while the results and interpretation of the findings from the study are presented in Chapter 5 and 6. Lastly, Chapter 7 and 8 contain discussion and conclusion of the overall study.

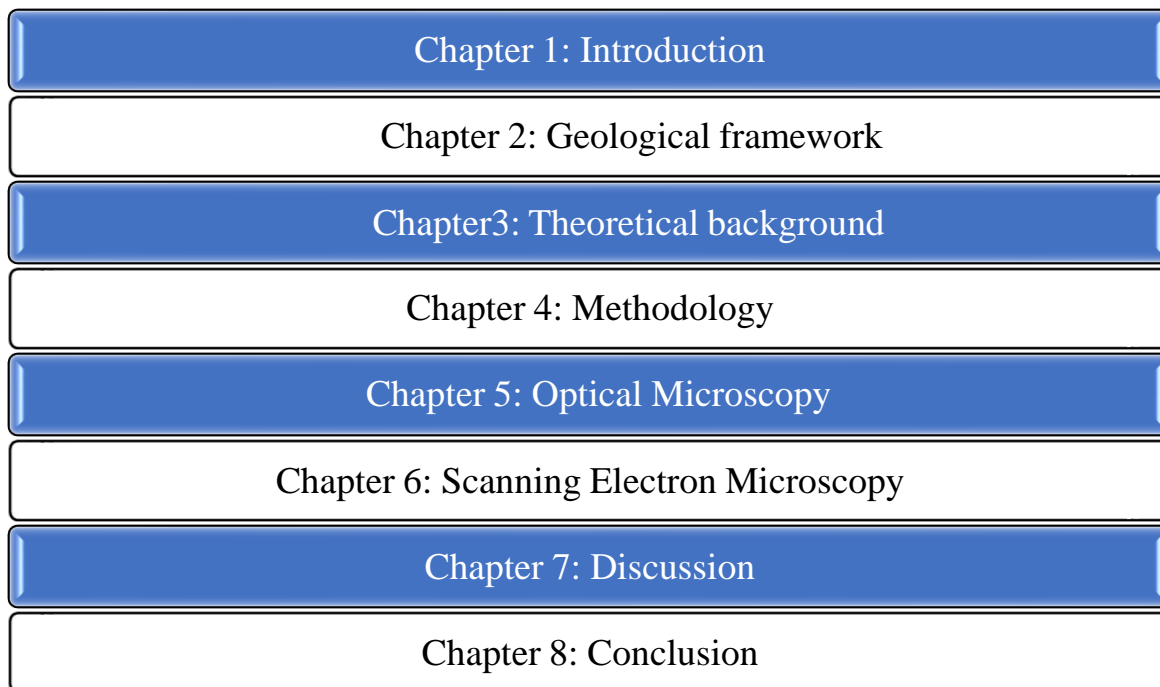


Figure 1.3: Structure of the thesis

Chapter 2: Geological framework

2.1 Introduction

This chapter summarizes the overview of the geological evolution and structural setting of the Norwegian Sea Continental Margin, with the emphasis on the Vøring Basin. The Norwegian Sea continental margin extends between latitude 62° and 69°30' north (Brekke et al., 1999). The structural style of the Mid-Norway was developed as a result of tectonic activity which influenced since Permo-Carboniferous times (Bukovics and Ziegler, 1985). The formation of supercontinent occurred by the collision of the Baltican and Laurentian plates in Silurian-Devonian of Paleozoic era. Thus, the basement underneath the current Mesozoic sedimentary strata was produced during Caledonian orogeny. The breakup of Pangaea during Late Paleozoic to Early Triassic resulted in the rifting of continents and extension of crust, while the second phase of extension occurred in Late Jurassic to Early Cretaceous when the Norwegian Continental Shelf was filled by marine sediments containing source and reservoir units. The final rifting event cause the formation of oceanic crust by sea floor spreading and opening of the Norwegian Greenland Sea in Early Cenozoic time (Faleide et al., 2008).

2.2 Structural and tectonic settings of Mid-Norway

The structural configuration of the region was controlled by three main rifting episodes within the Carboniferous to Permian, Middle Jurassic to Early Cretaceous (both extensional tectonics related to continental rifting), and a final major rifting episode in the Late Cretaceous to Paleocene, as a result of the onset of seafloor spreading within the North Atlantic (Faerseth & Lien, 2002).

The Carboniferous to Permian rifting is the main Post-Caledonian tectonic activity involved in forming the Norwegian Sea Continental Margin in the Paleozoic time (Blystad et al., 1995). In the Norwegian Sea, the extensional phase occurred in Late Permian to Early Triassic period that is implied by the breakup of supercontinent. During the Triassic period, continental and marine environments existed in the Norwegian-Greenland Sea areas and the basins received clastic input

from Scandinavian Caledonites (**Smelror et al., 2007**). Thick successions of alluvial conglomerates, sandstones and fine grained clastics were deposited in Middle Triassic to Early Jurassic rifting resulting from uplift and erosion (**Smelror et al., 2007; Gabrielsen et al., 2010**).

The second extension regime initiated in the Late Jurassic period and resulted in formation of horst and graben structures in the North Sea and the Mid-Norwegian Shelf. The Vøring and Møre basins were developed in the region that was precedingly influenced by erosion and exhumation (**Smelror et al., 2007**). The faulting continued in earliest Cretaceous followed by subsidence of the crust and deposition of thick successions of deep marine sandstone turbidites in various places of the Mid-Norway. Major uplifting occurred in Late Cretaceous-Early Paleocene that resulted in erosion of the basin margins and platform regions (**Blystad et al., 1995; Smelror et al., 2007**).

2.2.1 Tectonic setting of Vøring basin

The Vøring Basin was tectonically active in Late Cretaceous and acted as a rift basin along with widespread rifting of the Norwegian-Greenland Sea (**Ren et al., 2003**). The rifting of the Vøring Basin is described in **Figure 2.1** which points the onset of rifting in the start of Late Cretaceous with minor rifting events and major rifting phases.

In Early Paleocene, the extension of crust proceeded with breakup of continent and opening of the Norwegian Greenland Sea in the Early Eocene. The present continental margin is the result of outbuilding of large sediment deposits from mainland Norway (**Faleide et al., 2010**). The development of sill intrusive bodies, lava deposits and associated magmatism in the Vøring Basin, was at the highest level prior to and during the splitting of the Norway-Greenland continents (**Henriksen et al., 2005**).

The first phase of compression initiated at eastern margin basins of the Norwegian Sea while a second compression was evident in Middle Miocene (**Doré and Lundin, 1996; Smelror et al., 2007**). The deposition of fine-grained sediments in the Vøring Basin was prevalent after the second stage of compression with filling of sediments at the end of Miocene. Finally, glacial activity in Pleistocene eroded and deposited the sediments in the Norwegian Shelf (**Brekke et al., 2001; Smelror et al., 2007**).

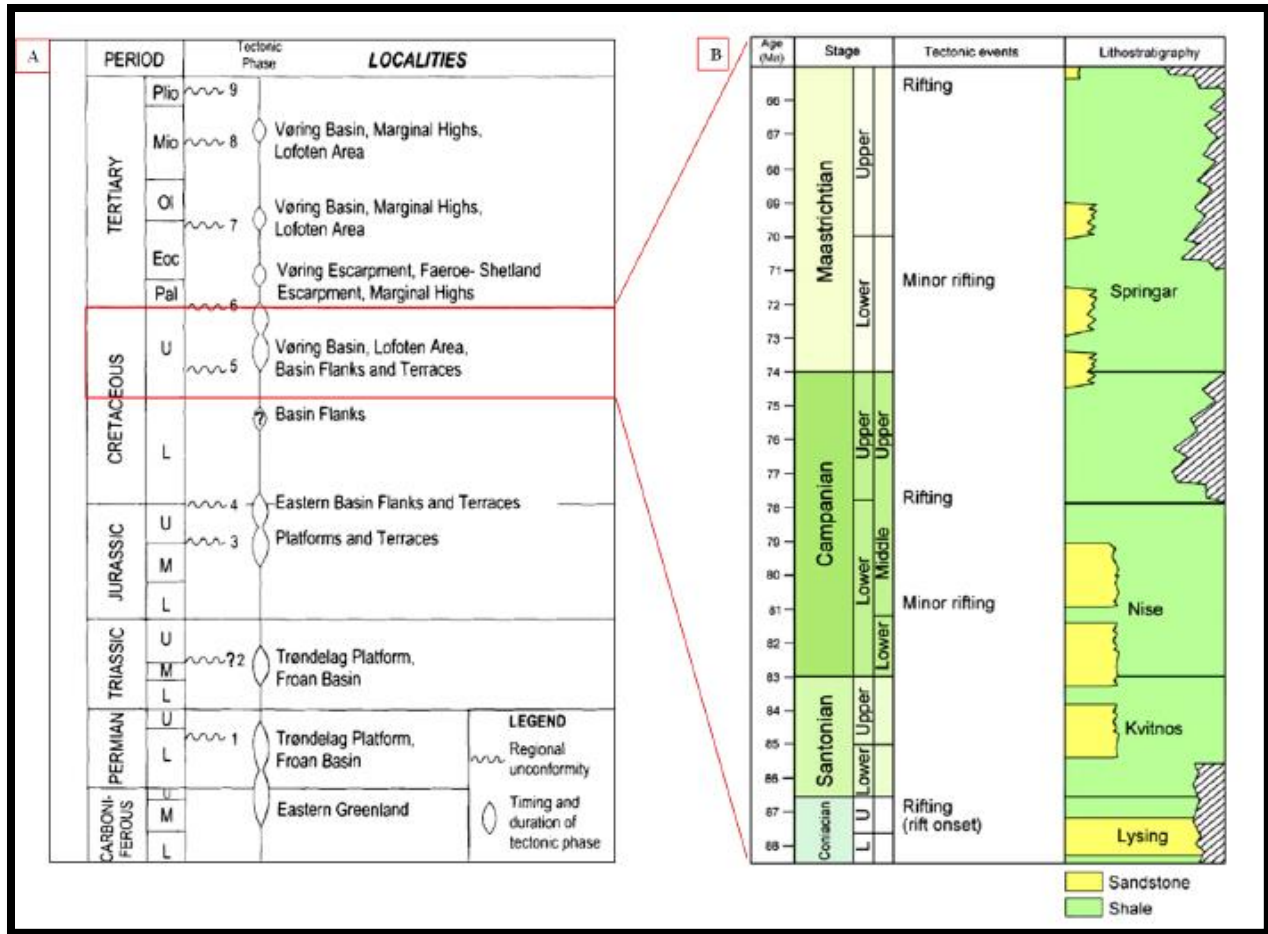


Figure 2.1: Tectonic development of the Norwegian Continental Shelf (A) and tectonic events emphasizing the Upper Cretaceous (B). The duration of each tectonic event and unconformable surfaces are mentioned with respect to age in this diagram (Brekke, 2000) whereas lithology (sandstone and shale) and stratigraphy (Lysing, Kvitnos, Nise and Springar Formations) are also illustrated in (B) part of the figure (from Knaust, 2009).

2.3 Regional stratigraphy

The exploration history of the offshore Mid-Norway was reaching a high point in 1981 with the discovery of the Midgard Field and drilling produced data of Tertiary and Mesozoic strata including Triassic deposits; however, the information regarding pre-Triassic strata was limited at this point (Dalland et al., 1988). With reference to Figure 2.2, the deposition of continental sediments in Middle Triassic to Early Jurassic times was evident from the Trøndelag Platform and the Halten Terrace. The Åre Formation contains evaporite succession, red beds which were overlain by clastic deposits of coal bearing delta plain facies (Whitley, 1992).

Shallow marine environments prevailed during the deposition of the Åre, Tilje, Ror and Tofte formations which together made the Båt Group (Dalland et al., 1988). Mainly sandstone and clay with interbedding of coaly claystone (having great source potential) and coal formed the Åre Formation (Heum et al., 1986; Forbes et al., 1991). The sand content greatly increases in the Tilje Formation consisting of only fine to coarse grained sandstone with shale and siltstone interbedding whereas, coarse grained-sandstone of the Tofte Formation has been deposited only in the western part of the Halten Terrace. Grey to dark grey mudstone along with interbedding of sand and silt formed the Ror Formation where coarsening upward sequence is present in sand and silt units (Dalland et al., 1988).

Middle Jurassic sedimentary deposits of the Fangst Group (the Ile Formation, the Not Formation and the Garn Formation) were deposited as a result of regression (Ehrenberg et al., 1992). Fine to medium grained sandstone laminated with siltstone and shale of the Ile Formation, having good reservoir properties, deposited over the entire Haltenbanken region while normally towards East the units thins out on the Trøndelag Platform (Dalland et al., 1988). The bioturbated mica rich, carbonate cemented sandstones units along with claystone define the Not Formation. Most parts of the Haltenbanken region contains good to excellent reservoir (Garn Formation) that may only be absent from structural highs because of erosion (Heum et al., 1986).

The Viking Group was deposited under marine conditions and contains three formations namely the Melke, the Spekk and the Rogn Formations. Melke Formation of open marine environment is mainly comprised grey to dark brown claystone with interbedding of limestone and siltstone (Ehrenberg et al., 1992). With high organic type II kerogen, the dark brown to grey shale of the Spekk Formation was deposited over the entire Haltenbanken region but may absent from structural highs. The shallow marine sand bar deposits of the Rogn Formation comprised siltstone and coarsening upward sequences from shale to sandstone with upward decrease in clay content and makes a good reservoir (Patience, 2003).

The Cromer Knoll and the Shetland Groups containing shale with few turbiditic sandstone deposits were preserved in shallow to deep marine environments during the Cretaceous period (Ehrenberg et al., 1992). The Tertiary claystone deposits form the Rogaland and Hordaland Groups in the Haltenbanken region, while the Kai Formation of the Nordland Group marks an unconformable contact with underlying Paleogene sedimentary strata. During Late Pliocene times, the Naust Formation containing alternate shale and poorly sorted sandstone was deposited over the Haltenbanken region (Ehrenberg et al., 1992).

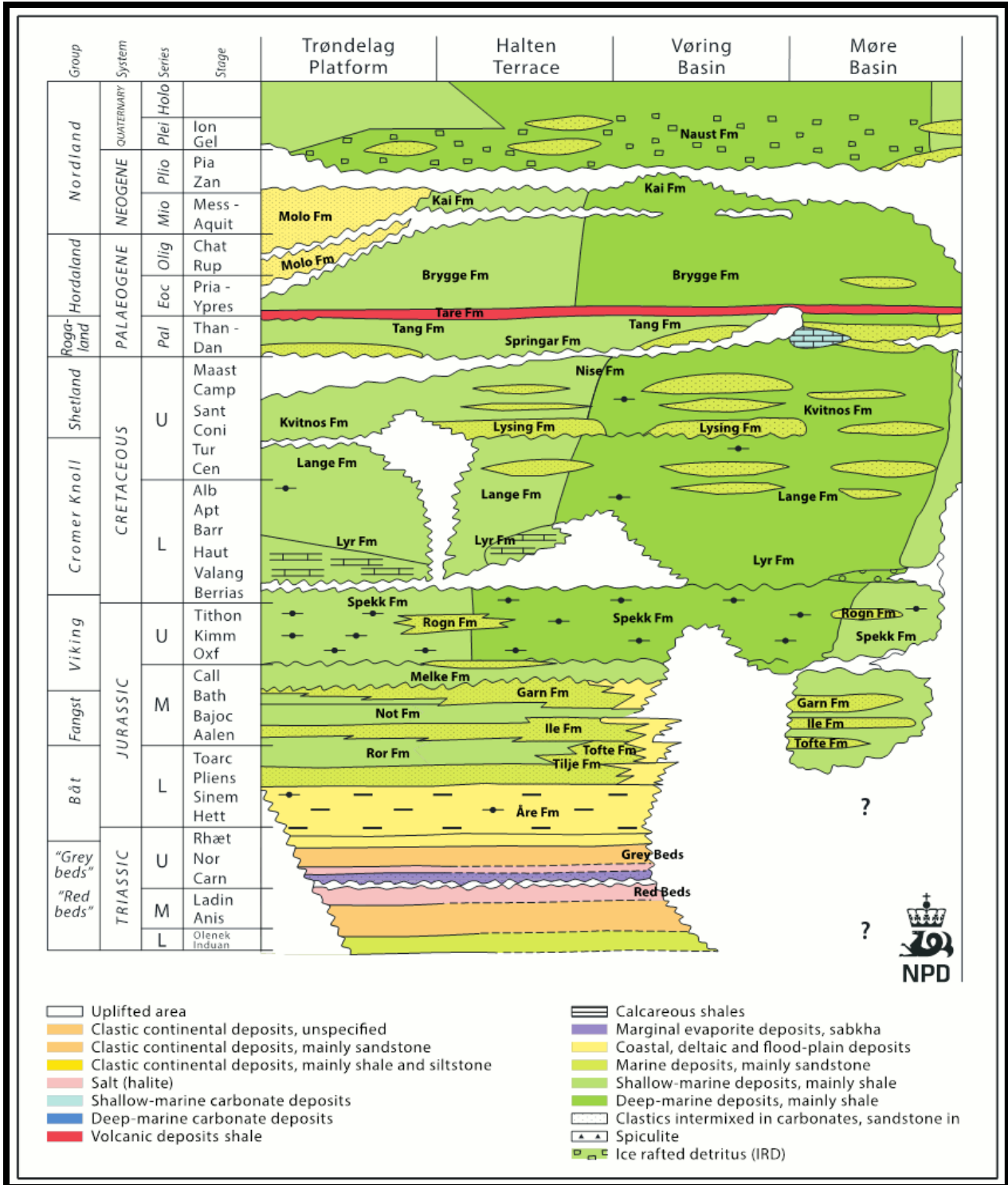


Figure 2.2: Lithostratigraphic summary for the Norwegian Sea shelf area (NPD).

2.3.1 Stratigraphy of Vøring basin

The Vøring Basin was formed during the Late Jurassic-Early Cretaceous rifting event, it is one among the deep Cretaceous basins which is filled up to 13 km of sediments, of which 8-9 km comprise the Cretaceous succession ([Blystad et al., 1995](#); [Osmundsen et al., 2002](#); [Brekke et al., 2001](#); [Brekke, 2000](#); [Skogseid et al., 2000](#)).

The Cretaceous evolution in the Norwegian sea is defined as a post-rift (thermal subsidence) period following Jurassic-Early Cretaceous rifting and precedes a Late Cretaceous-Paleocene rift episode ([Færseth and Lien, 2002](#)). The Cretaceous and Paleocene stratigraphy is shown [Figure 2.3](#) and stratigraphic nomenclature used is according to the formal stratigraphy for Mid Norway by [Dalland et al. \(1988\)](#).

With reference to [Figure 2.3](#), the stratigraphy of Early Cretaceous in Norwegian sea consists of Lyr and Lange formations, the sediments are dominated by deep marine mudstone and thin sandstone deposited in basin lows ([Færseth and Lien, 2002](#)). The Late Cretaceous stratigraphy is divided into Lysing, Kvitnos, Nise and Springar formations. Lysing Formation is dominated by deep marine sandstones deposited on regional basin slopes like Halten and Donna terraces ([Martinsen et al., 2005](#)). The Kvitnos, Nise and Springar formations are dominated by deep marine mudstone but thick local sandstones interval occurs in the Vøring Basin. These sandstones were deposited in a deep marine environment where local basin topography and subsidence were influenced by the early stage of Late Cretaceous-Paleocene rifting ([Færseth and Lien, 2002](#)). Sandstone of Paleocene age Tang Formation is deposited in locally deep sub basins in Møre Basin.

In general the Upper Cretaceous sandstone deposited in the Vøring Basin are sourced from East Greenland while Upper Cretaceous sandstone deposited in the Vestfjord Basin eastern Møre Basin and Halten/Dønna terrace are sourced from Mid-Norwegian margin ([Fonneland et al., 2004](#)). The Cretaceous and Paleocene form important reservoir intervals in the Møre and Vøring basins where sediments of up to 8km in thickness were deposited ([Faerseth and lien, 2002](#)).

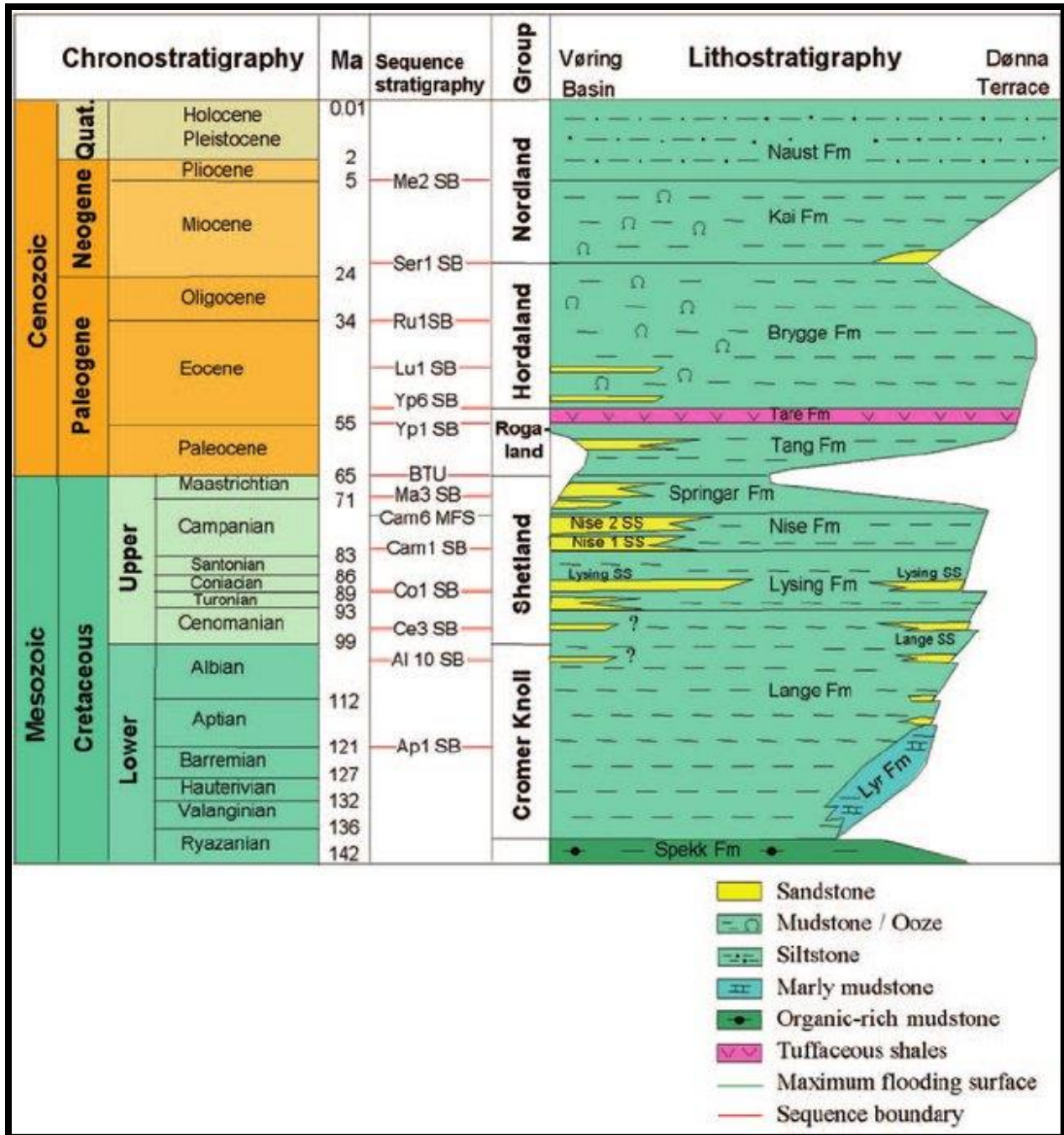


Figure 2.3: Stratigraphy of the Cretaceous–Cenozoic succession of the Vøring Basin, modified from Dalland et al., 1988.

2.3.2 The Upper Cretaceous depositional system

The Upper Cretaceous sandstones in the Vøring Basin were sourced from the Greenland craton and its paleo-shelf, prior to opening of the Norwegian–Greenland Sea (Fonneland et al., 2004, Martinsen et al., 2005). They were deposited in a deep-marine environment, where local basin topography and subsidence were influenced by the early stage of the Late Cretaceous/Paleocene rifting (Færseth and Lien, 2002).

Fjellanger et al. (2005) performed sedimentological core descriptions of several exploration wells drilled in the Vøring Basin as the basis for interpretation of sedimentary processes and depositional environments. They grouped the Campanian–Maastrichtian sandstones into six main sedimentary facies (Figure 2.4) based on cores from wells 6707/10-1, 6706/11-1, 6607/5-2 and 6704/12-1.

This study is focusing in well 6707/10-1 which cover 205 m cores of the Lower–Middle Campanian succession (3145–2967 m and 4145–4118 m) belonging to the Nise Formation. All six main facies groups are identified in the logged interval of this well (Figure 2.5).

Facies interpretation of cores by Fjellanger et al. (2005), shows that the Campanian-Maastrichtian deposits (including Nise Formation) are dominated by stacked, massive, partly graded sandstones interpreted as deposited from hyper-concentrated to concentrated density flows (Facies C1 and C2) and to some extent also turbidity flows (Facies T1) forming sheet-like basin-floor fan systems. Figure 2.6 shows the depositional development of Nise Formation from Nyk High with dominant facies.

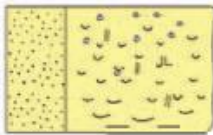


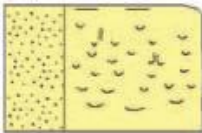

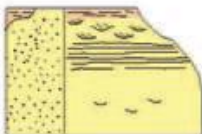

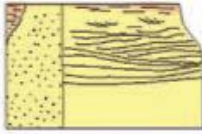


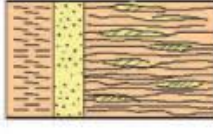

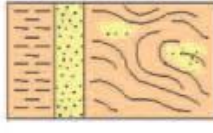
Facies	Observations	Process	Description	Core photo
C1	Massive sandstone or faint inverse graded sandstone	Hyper-concentrated density flow		<p>Facies C1</p>  <p>Facies T1</p> 
C2	Massive or top-only graded sandstone	Hyper-concentrated to concentrated density flow		<p>Facies C2</p> 
T1	Graded sandstone with Tabcde Bouma divisions	Concentrated density flow and turbidity flow		<p>Facies T2</p> 
T2	Stratified sandstone	Concentrated density flow and turbidity flow modified by currents or waves		<p>Facies H1</p>  <p>Facies S1</p> 
H1	Heterolithic sandstone and mudstone	Low density turbidity flow / bottom current		<p>Facies S1</p> 
S1	Overtuned / brecciated deposits	Slumping		<p>Scale: Core width 10 cm</p>

Figure 2.4: Main sedimentary facies recognized in the Campanian–Maastrichtian basin-floor fan deposits in the Vøring Basin (Fjellanger et al., 2005).

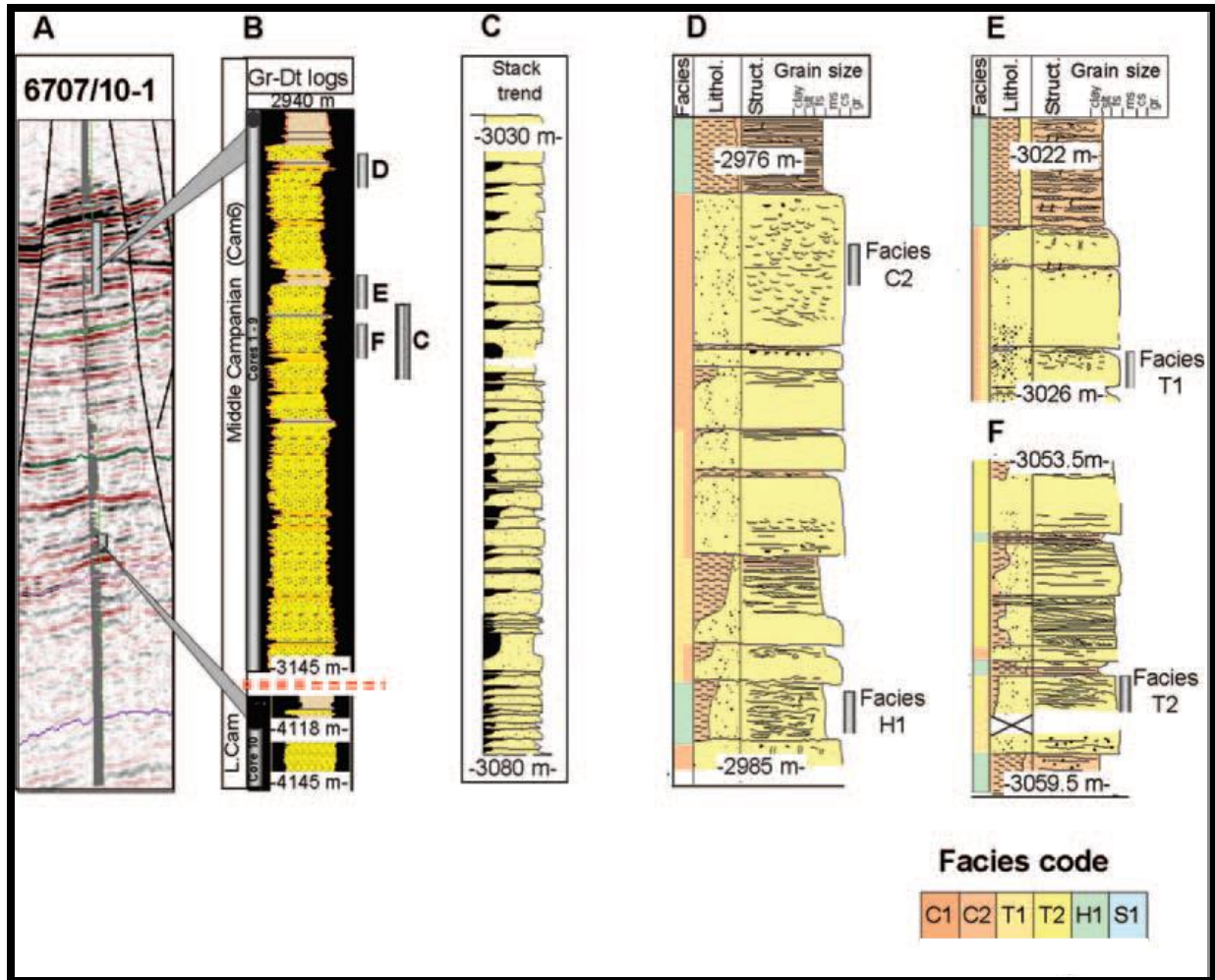


Figure 2.5: Key sedimentary facies described from the cores in Well 6707/10-1 drilled on the Nyk High. (A) Seismic section at the well location of the Lower–Middle Campanian succession. (B) Wireline logs of the cored interval. (C) Simplified core description showing the lack of trends in the stacking of the sandy density-flow deposits. (D–F) Core descriptions showing the dominance of hyper-concentrated and concentrated density-flow deposits and examples of key facies (Fjellanger et al., 2005).

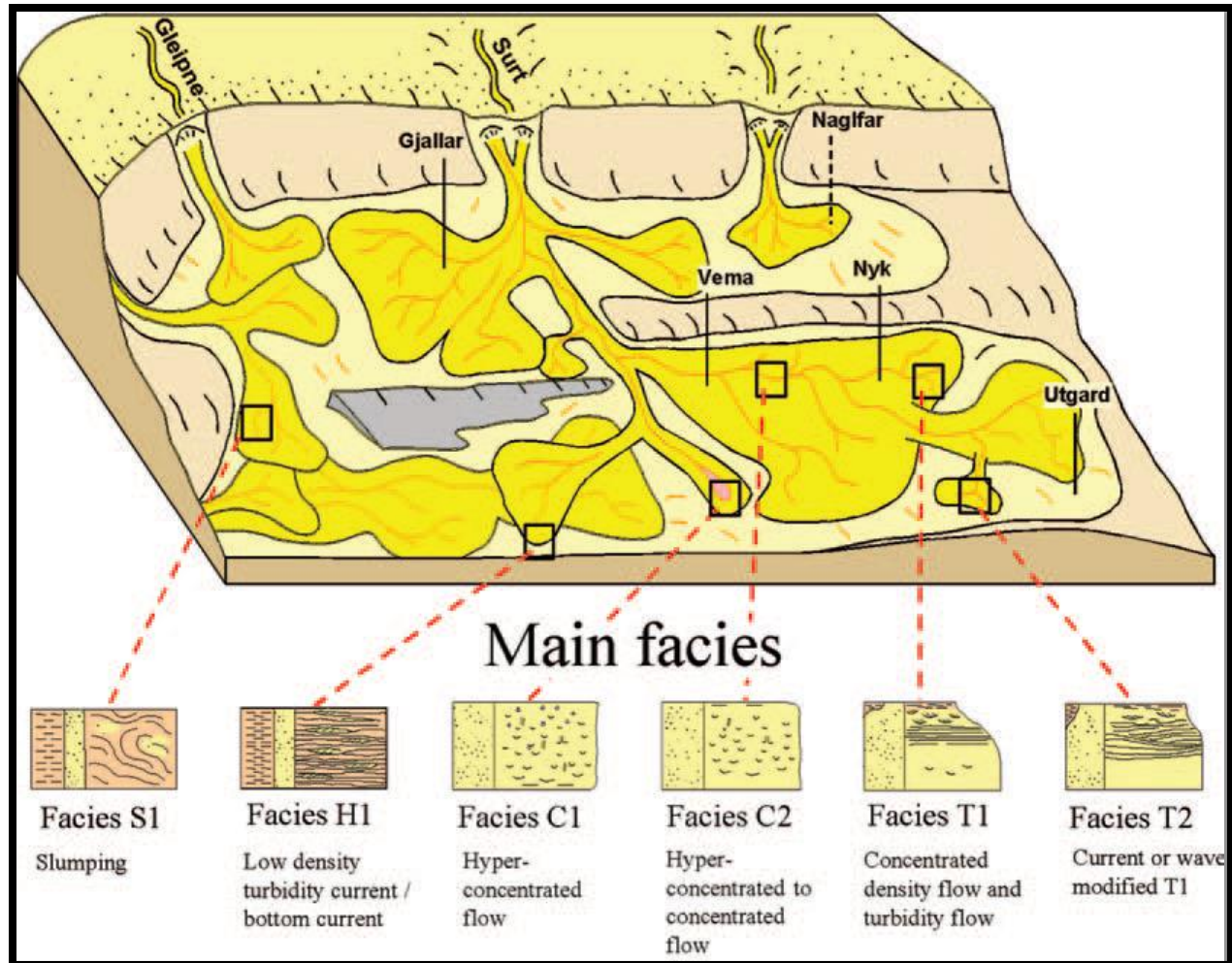


Figure 2.6: Schematic illustration of the depositional environments of the Campanian–Maastrichtian fan systems in the Vøring Basin. Illustrations of typical locations for the six main facies are included (Fjellanger et al., 2005).

2.4 Petroleum System of Mid-Norway

Source rocks

In the Mid-Norway region, three major rock units of Jurassic age have been identified as organic rich source rocks namely the Spekk, the Melke and the Åre formations (Karlsen et al., 2004; Karlsen and Skeie, 2006). The maturity of Lower Jurassic Åre Formation increases as we move from the East towards the West in the Vøring Basin. In Early Triassic period, the Åre Formation

achieved the oil generation window in region of the Halten Terrace ([Campbell and Ormamsen, 1987](#); [Karlsen et al., 1995](#)). According to [Karlsen et al. \(1995\)](#), the Åre Formation in the Midgard and the Draugen fields has been contemplated as immature. The shale units with silt and clay intercalations represent the organic rich Melke Formation (having 1 to 4 % TOC), but the Melke Formation has unsubstantial oil potential than Spekk and Åre formations ([Heum et al., 1986](#); [Cohen et al., 1987](#)). The Spekk Formation of Late Jurassic age is considered to be thick and relatively mature in the region except the eastern area of the Trøndelag Platform while it becomes over mature towards the West in the Vøring Basin ([Karlsen et al., 1995](#)).

Reservoir rocks

[Faleide et al. \(2010\)](#) stated the sand units with alternate shale layers of Early and Middle Jurassic age named as Åre, Tilje, Tofte, Ile and Garn formations are believed to be reservoir rocks in the offshore Mid-Norway region. These formations constitute the Jurassic Fangst Group in the Smørbukk and Heidrun fields as reservoir whereas; the reservoirs in the Njord Field belonged to the Båt Group. [Karlsen et al. \(1995\)](#) suggested that only one formation (Rogn Formation) of Late Jurassic age has been considered to be reservoir in Darugen Field.

Much of the exploration to date has focused on the Early to Middle Jurassic sandstone sequence in the shelf area of the basin, but in recent years attention has also turned to the exploration potential of the frontier Late Cretaceous to Paleocene deep-water reservoirs named Lysing, Kvitnos, Nise, Springar and Tang formations ([Brekke et al., 1999](#); [Kittelsen et al., 1999](#)).

Traps

According to [Faleide et al. \(2010\)](#) the rotated fault blocks in horst and graben system of Jurassic age acted as trap in the Halten region, where these structures were conceived by extensional tectonics but the upwelling of salt in Triassic period resulted in some salt induced structures that formed the Smørbukk Sør and Tyrihans South Field ([Jackson and Hastings, 1986](#); [Karlsen et al., 1995](#)) whilst towards the East (Trøndelag Platform) the mechanism of trapping had failed to

occur and in the Draugen Field and hydrocarbons were trapped in the gentle anticlinal structures (Provan et al., 1992; Karlsen et al., 1995).

2.4.1 Petroleum system in Vøring basin

In the Vøring Basin, the presence of gas has been found in several wells, but only minor oil presence. Brekke et al. (1999) stated that the source rock in this basin may be associated with water circulation from two different periods. The first phase was during the Early Cretaceous in the Hel and Fenris Grabens and a second phase in the Paleocene-Early Eocene at the time when the Vøring Basin was close to Lofoten and Vesterålen (Skogseid et al., 1992a).

The Jurassic and Early Cretaceous layers are too deep as hydrocarbon plays, except on the Vøring Marginal High that has possible hydrocarbon accumulations beneath the Paleogene sills (Brekke et al., 1999). The most promising reservoirs are the Turonian, Coniacian, and Early Campanian sandstones that are trapped in rotated fault blocks. The second promising reservoirs could be found in the Vema Dome, the Nyk High, Någrind and Vigrid Synclines which are associated with the Early Paleocene sandstones (Brekke et al., 1999; Kittelsen et al., 1999).

The massive magmatic activity in Paleogene in the Vøring Basin has probably altered the reservoir quality. Rapid subsidence and deposition of marine shales during Late Paleogene-Neogene in the western part of the Vøring Basin led to the formation of cap rocks in this basin, whereas the traps are generally associated with Eocene-Miocene compressional domes and stratigraphic closure (Brekke et al., 1999).

2.4.2 Exploration history of Vøring basin.

The Upper Cretaceous deep-water plays of the Vøring Basin were first drilled on the Utgard High by wells 6607/5-1 and -2 operated by Esso in 1987 and 1992, respectively, the targets were at the time interpreted as being of Jurassic age but were later shown to represent distal parts of Lower–Middle Campanian (Nise Formation) deep-water deposits. In 1993, IKU cored three shallow wells in the Vøring Basin, two on the Nyk High and one on the Naglfar Dome. The cores proved the

presence of Campanian–Maastrichtian deep-water sandstones in this part of the Vøring Basin (Fjellanger et al., 2005), as well as ash-bearing Tertiary deposits (Mørk et al., 2001).

In 1997, BP drilled well 6707/10-1 on the Nyk High and discovered gas in central parts of a Lower–Middle Campanian basin-floor fan system (Kittelsen et al., 1999). The sandstones in the Nyk well are of very good reservoir quality. The well also penetrated deep-water sandstones of Maastrichtian age above the Campanian target, but they were not successfully cored. In 1997–1998, Statoil drilled well 6706/11-1 on the Vema Dome. The same good quality Lower–Middle Campanian reservoir sandstones were penetrated, but hydrocarbons were not encountered.

During the summer of 1999, Saga Petroleum completed the drilling of well 6704/12-1 on the Gjallar Ridge. The well was dry but showed the presence of a sand rich Upper Cretaceous interval, 750 m of which were of Late Campanian–Early Maastrichtian age (Springar Formation) and 250 m of Early–Middle Campanian age (Nise Formation) (Fjellanger et al., 2005).

Chapter 3: Theoretical background

3.1 Introduction

This study focuses on samples from the deep marine Upper Cretaceous sandstones, sampled at depths between 2.9 to 4.1 km. The great burial depth interval is expected to have involved several diagenetic processes. This chapter briefly mentions the main diagenetic processes and on how they affect the reservoir quality of the sandstone.

The properties of sandstone are “continuously” changing from the time of deposition, through burial at greater depth and during uplift while these properties depend on its composition at shallow depth, temperature and stress history during burial. The initial composition of sandstone depends upon its provenance, depositional environment and transport. Diagenetic processes occur, near the surface and during deep burial, several different diagenetic processes which act continuously on the sandstones just after their deposition to the present are reported . The initial or primary clastic composition and the depositional environment are the two most important factors to predict reservoir quality at depth (**Figure 3.1**) (Bjørlykke and Jahren, 2010).

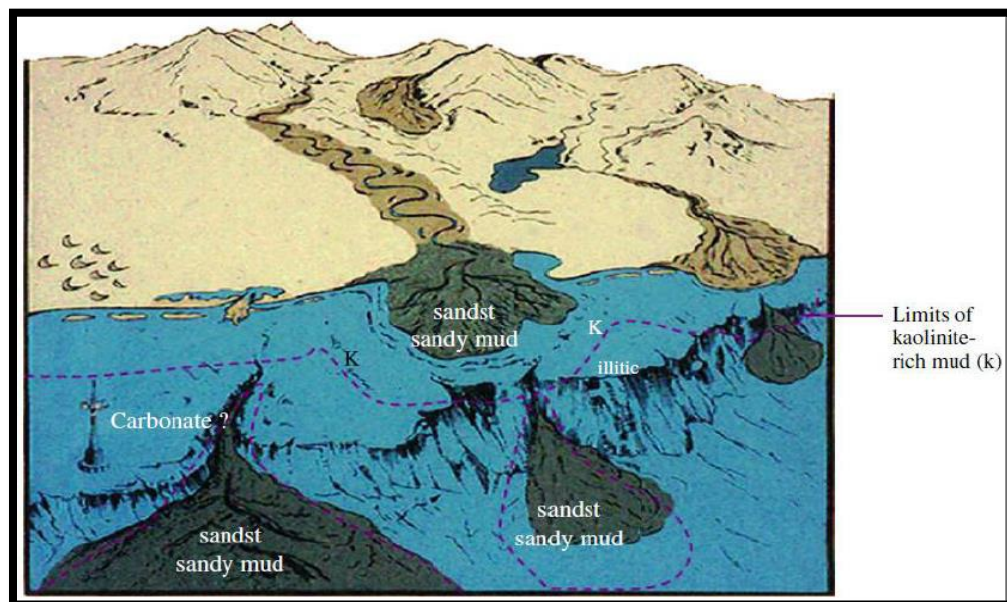


Figure 3.1: Schematic illustration of a sedimentary basin on a continental margin (Bjørlykke, 2010)

3.2 Diagenesis

After deposition, diagenetic processes occur to modify the composition of sediments therefore affect the reservoir quality of the rock. The main diagenetic processes include; near surface diagenesis, mechanical compaction, chemical compaction and formation of authigenic minerals and cements (**Bjørlykke and Jahren, 2010**). Mechanical compaction is the main mechanism for the porosity loss at shallow depths, while chemical compaction is pronounced at greater depths and porosity is lost primarily by the precipitation of quartz cement and authigenic clay minerals. Some diagenetic products can be potential in porosity preserving mechanism. Burial diagenesis involves depth and temperature dependent reactions. The geothermal gradient considered in this study is 30°C/km.

3.2.1 Near surface diagenesis

Near surface diagenesis includes the processes which are influenced by sea-water and meteoric water. Composition of sediments starts to alter immediately, after their deposition by various near surface diagenetic processes. Transportation of solids which are dissolved by fluid flow and diffusion is more effective near the surface (depth less than 1 to 10 m). Sediments are more prone to change their bulk composition at shallow depth as compare to the greater burial (**Bjørlykke and Jahre, 2010**). The initial composition of clastic sediments is altered by the addition of newly formed components within the basin such as biogenic carbonates and silica, authigenic minerals like carbonates, phosphates, glauconite, sulphides and iron and the formation of kaolinite by the leaching of feldspar and mica (**Figure 3.2**).

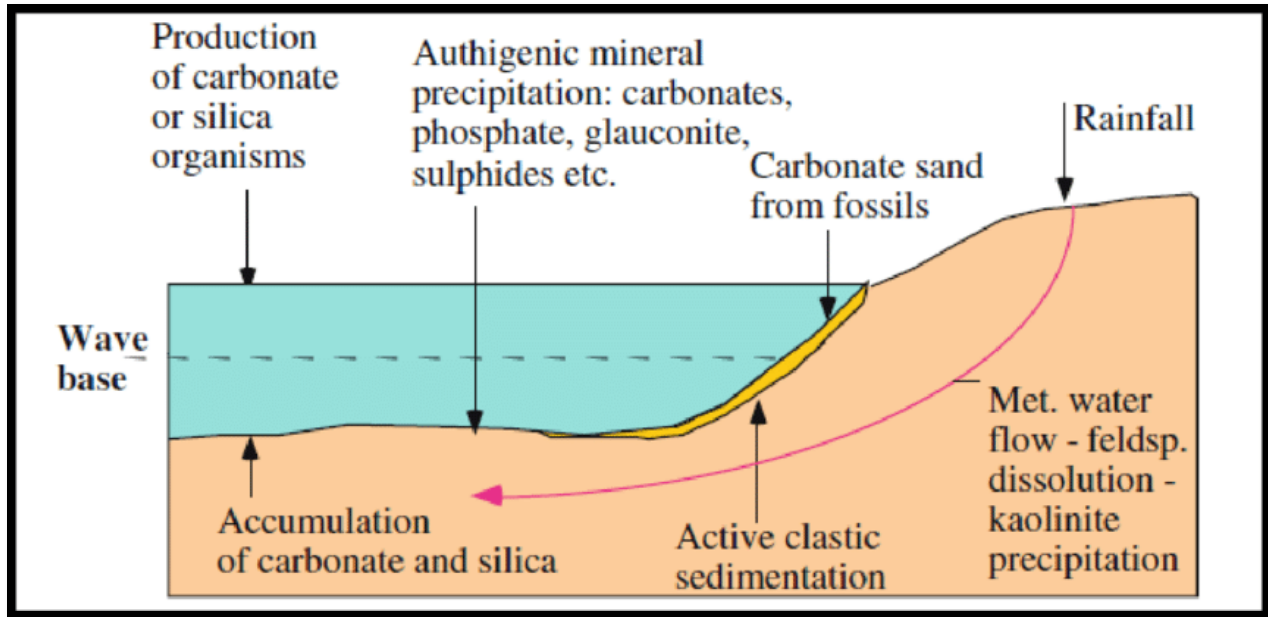
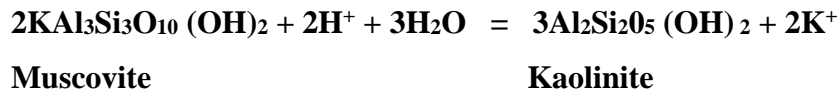
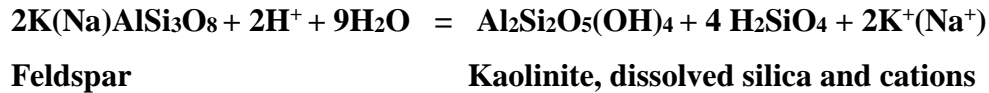


Figure 3.2: Diagenetic processes in shallow marine environment (Bjørlykke and Jahren, 2010).

Oxidizing conditions occur in the upper few centimeters of seabed and reducing conditions prevail in deeper part of the basin. At certain depth where there is no free dissolved oxygen in the pore water, sulphate reducing bacteria uses the sulphates and generate sulphides like pyrite (Bjørlykke and Jahren, 2010).

Shallow marine diagenesis is strongly influenced by the deposition of biogenic silica and carbonate on the sea bed. Bioturbation changes the textural composition of the sediments, it destroys the laminations of the clay, increases the vertical permeability and hence enhances the reservoir quality. Siliceous organisms like diatoms and siliceous sponges which are composed of opaline silica, can act as source for micro-quartz coatings on detrital quartz grains at greater burial depths (Bjørlykke, 1998). Biogenic carbonate is the main source of calcite cement. In the Mesozoic era, evolution of pelagic planktonic calcareous organisms occurred and increased the supply of carbonate to deeper parts of the basin, before this, all the carbonate produced by the benthic organisms was confined to the shallow water facies. Upper Jurassic and younger sandstones are heavily cemented by calcite due to the rain of calcareous algae and foraminifera on the seafloor. (Bjørlykke and Avseth, 2010).

Formation of kaolinite from dissolution of feldspars and micas is another reaction common at shallow burial. The reactions are facilitated by meteoric water which is normally undersaturated with mineral. Rainwater dissolves CO₂ and SO₂ from the air and alters slightly into carbonic acid (H₂CO₃) and sulphuric acid (H₂SO₄), seeps into ground and is mixed with ground water. This meteoric water starts to dissolve carbonates first and then other unstable minerals like feldspar and mica. According to [Bjørlykke, \(2010\)](#), leaching of minerals like feldspars and mica and then precipitation of kaolinite is controlled by the flux of groundwater which is flowing through the rock per unit of time. Na⁺ and K⁺ are leached away from silicate minerals like feldspar and mica come into solution. This process can be expressed by the following reactions:



The reactions above cannot take place in closed system because removal of cations, silica and availability of protons are necessary to complete the reaction. Meteoric water has tendency to flow along the most permeable beds in the basin. Therefore meteoric water has ability to flow deep into the sedimentary basins. Many of the Norwegian Sea reservoirs that exhibit lower salinities (<50%) as compare to the normal Sea water, represent influx of meteoric water ([Bjørlykke, 1998](#)).

From the reactions it is evident that low K⁺/H⁺ ratios will drive the reactions to the right, and that the precipitation of kaolinite requires that the reaction products Na⁺, K⁺ and silica are constantly removed, and new freshwater is supplied. Dissolved silica and aluminum generated, combines to precipitate the kaolinite. Silica released from dissolution of feldspar does not precipitate as quartz, but it remains in the solution because temperature is low near the surface. When concentration of silica becomes very high in porewater, kaolinite becomes unstable and smectite is precipitated instead ([Bjørlykke, 2010](#)).

Depending on the elevation of the groundwater table; the potentiometric head, meteoric water flow can extend far out into the basin, however the flux of meteoric water decreases strongly in the deeper parts of the basin. The mineral leaching will be most intense at the surface or near the seafloor as meteoric water becomes gradually less undersaturated and loses its leaching capacity. If the kaolinite is altered to illite at greater depths, it will severely reduce the permeability (Bjørlykke, 1984).

Dissolution of feldspar and mica generates secondary porosity but the precipitation of authigenic clays like kaolinite reduces the porosity so there is small net gain in pore space. Authigenic kaolinite occurs as pore-filling mineral and this reduces the porosity. The smaller pores (<0.005 mm) which are present between the kaolinite crystals are too small to be filled with oil because of the high capillary entry pressure which is required to infiltrate these pores. Thus, there is higher water saturation in the reservoir rock (Bjørlykke and Jahren, 2010).

3.2.2 Mechanical compaction

During burial, sandstones experienced compressive forces due to increase in overburden. It induced compaction in sandstones which results to expulsion of pore water and reduction of rock bulk volume. Mechanical compaction includes reorientation, rotation and fracturing of brittle grains and deformation of ductile grains, accounting for most of the early porosity loss (Berner, 1980). Sandstones consisting of more ductile components are severely affected by mechanical compaction and show high porosity loss (Rittenhouse, 1971). Mechanical compaction is controlled by effective stress (difference between lithostatic pressure and pore pressure) and its magnitude depends upon the strength of grains and their framework (Figure 3.3).

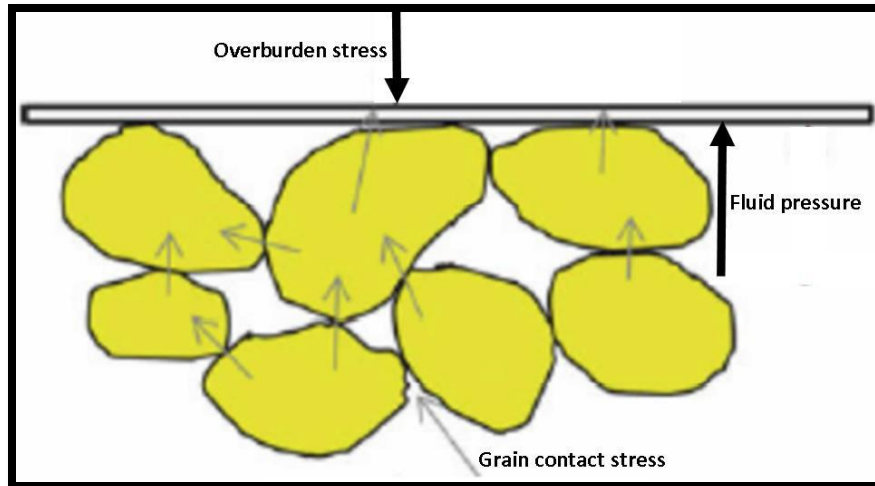


Figure 3.3: The effective stress from the overburden ($\sigma'v$) is carried by the mineral grain framework and pore pressure (Bjørlykke and Jahren, 2010).

Sandstone deposited at less than 2km burial are still loose unless subjected to an early cementation, probably carbonate cement. The responsible mechanism for porosity loss at shallow depth is the mechanical compaction (Bjørlykke and Avseth, 2010). From Figure 3.4, studies of experimental compaction of loose sand with an initial porosity 40-42% reveals that porosity can be reduced to 25-35% at stresses of 20 – 30 MPa which corresponds to 2 - 3 km of burial depth of normally pressured rocks depending on the geothermal gradient. The experimental data also shows that under same circumstances, well sorted coarse-grained sand is more compressed than fine-grained sand (Chuhan et al., 2002; Mondol et al., 2007). This is because there are fewer grain contacts and more stress per grain contact in coarse-grained sand, resulting more grain fracturing.

In sedimentary basins with normal geothermal gradient, grain framework is stabilized by quartz cementation and prevents the further mechanical compaction at a burial depth of about 2 to 3 km (70-80°C). At further greater depths, compaction is influenced by both effective stress and temperature. Overpressure reduces the vertical effective stress and helps in preserving the porosity due to mechanical compaction (Osborne and Swarbrick, 1997).

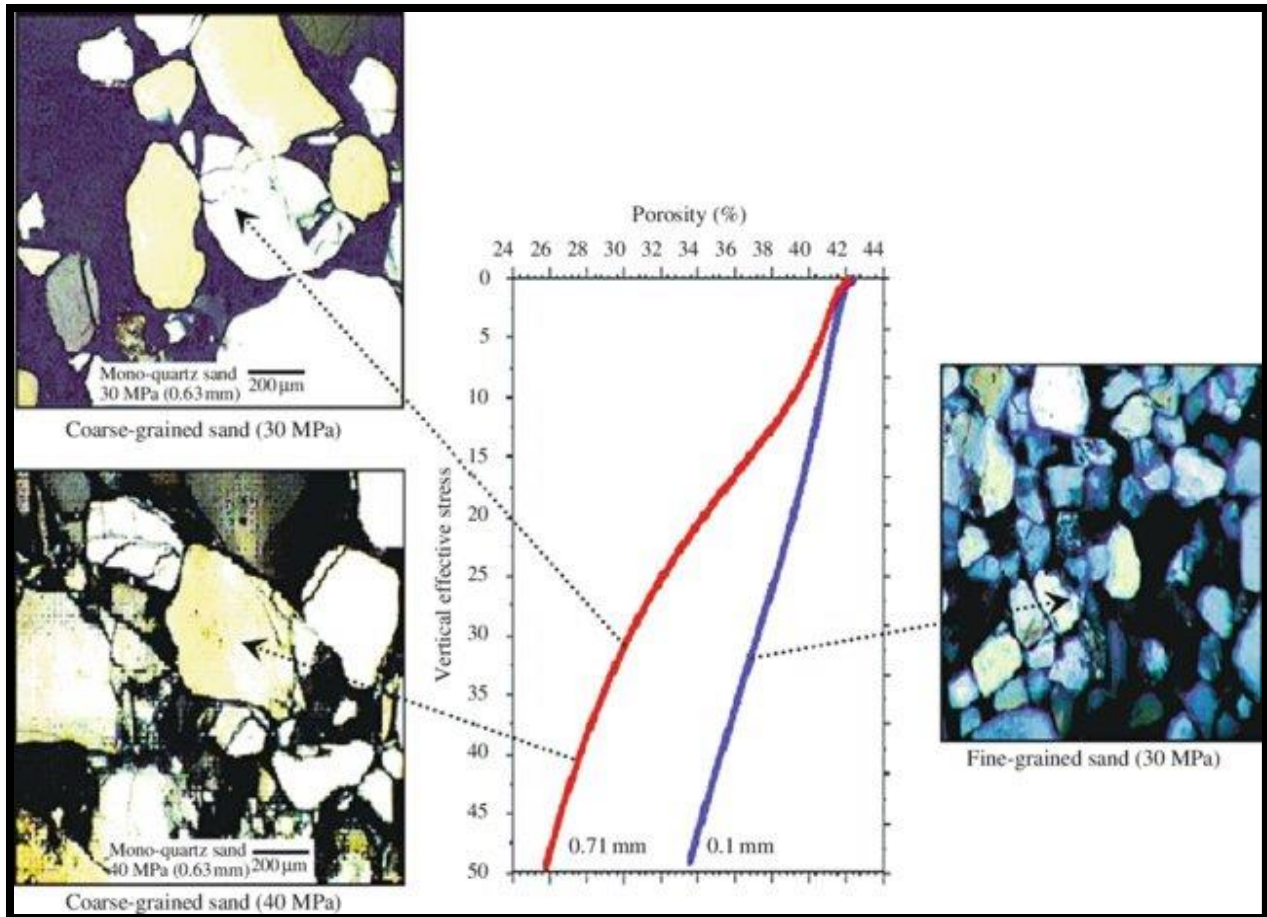


Figure 3.4: Experimental compaction of loose sand grains, coarse-grained sand is more compressible than fine-grained sand (Chuhan et al., 2002).

3.2.3 Chemical compaction

Chemical compaction normally starts from 2 to 3 km depending on the temperature gradient. It increases the strength of the rock and stops mechanical compaction. Temperature is the main controlling factor in chemical compaction and other factors are primary mineral composition, pore-fluid composition and time-temperature history etc. (Oelkers et al., 1996; Bjørlykke, 1998; Peltonen et al., 2008). The zone where mechanical compaction ceases, and chemical compaction starts is called the transition zone (Figure 3.5). The chemical compaction will continue during the uplift as long as the temperature is above 70-80°C but the rate is slower because of the lowering

of temperature due to upliftment (Bjørlykke and Jahren, 2010). Once the quartz growth has started it will continue to precipitate and fill the pores until nearly all porosity is lost (if silica is available).

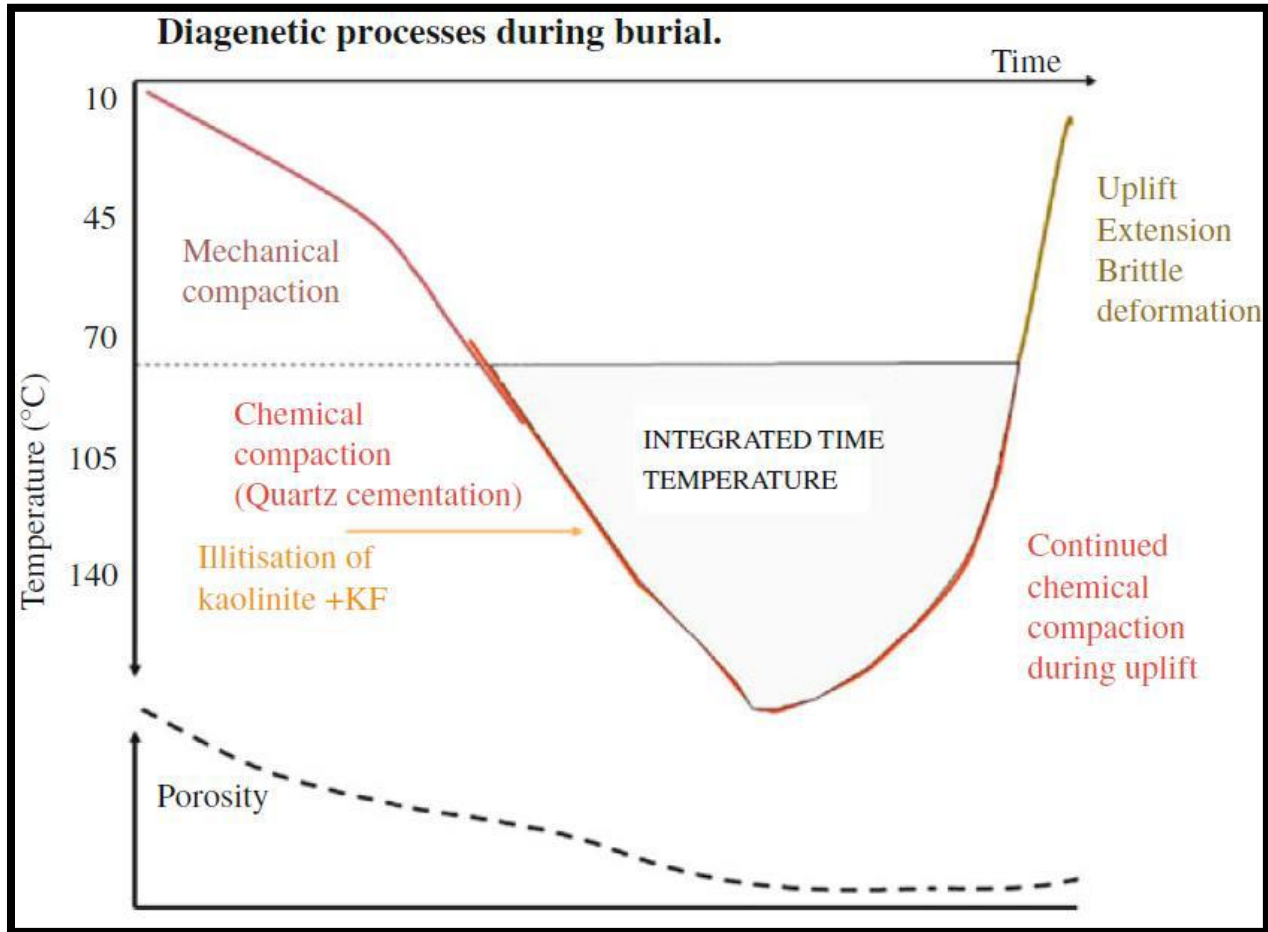


Figure 3.5: Diagenetic processes mainly quartz cementation as a function of temperature and time. Note that quartz cementation will continue also during uplift as long as the temperature exceeds 70-80 (Bjørlykke and Jahren 2010).

A strong reduction in reservoir porosity and permeability occurs from about 3-3.5 km to 4-4.5 km (120-160°C), mostly due to the precipitation of quartz cement and illite. A clean well sorted sand has best porosity down to 3.5-4 km, but then loses porosity rapidly due to quartz cementation. Sandstones with some clay content, will lose more porosity at mechanical compaction, but may preserve more porosity with depth due to retarded quartz growth (Bjørlykke and Avseth, 2010).

Quartz overgrowth

In sandstone reservoirs quartz cementation is found to be the main porosity reducing factor at temperature ranges between 70-80°C. Various petrographic studies have been done to analyse the source of quartz cementation. **Fuchtbauer, (1983)** mentioned the five possible sources of silica cement as quartz dissolution associated to the siltstones, feldspar to clay minerals replacement, pressure solution and stylolite, smectite to illite alteration and dissolution of the volcanic glass. Among these sources, stylolitization and quartz pressure solution have received dominate attention (**Oelkers et al., 1996**).

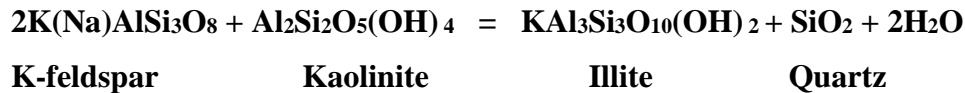
The main factor controlling the rate of quartz precipitation is temperature, as it increases exponentially with rise in temperature. The quartz cementation is also dependent on grain surface available for precipitation (**Oelkers et al.,1996**). Once cementation has started and the overgrowth is formed, quartz cementation will fill the pore space until surface area for further growth decreases. Overall, the reaction is surface-controlled as the rate limiting step is the nucleation of quartz. Porosity can be modeled as available surface area proportional with an exponential function of the time-temperature integral (**Walderhaug, 1994a**).

Authigenic clay

The transition of mechanical to chemical compaction in sandstones starts from 70 - 80°C while in shales it depends upon the stability of the primary minerals and burial history. The alteration from smectite to illite start from 60 - 70°C (**Bjørlykke, 1998; Peltonen et al., 2008**).

Smectite + K-feldspar = Illite + Quartz

If kaolinite and K-feldspar are present together in a reservoir and the temperature reaches 120 - 130°C, illitisation starts (**Storvoll and Brevik, 2008**). The transition of kaolinite to illite is an important reason for reduced reservoir properties in sandstones. (**Bjørlykke et al., 1992**). The illitisation reaction can be written as:



3.3 Porosity Preservation Mechanisms

The diagenetic processes described in this chapter affect the reservoir quality of the sandstones. However quartz cementation and mechanical compaction are the main porosity-destroying processes in quartz rich sandstones during their progressive burial. There are certain coatings of minerals which, if developed on the grain surfaces prior to quartz cementation can hinder the formation of quartz over-growth and help in preserving the porosity. Clay coating and micro-quartz coating have been accepted by many workers as porosity preserving agents in deeply buried sandstones reservoirs (Aase et al., 1996). Bloch et al. (2002) suggested three mechanisms which help to preserve the anomalously high porosity; grain coating minerals, fluid over-pressure and early hydrocarbon emplacement.

3.3.1 Grain coating

Grain coatings present on the surface of quartz grains prior to the onset of quartz cementation, preserve porosity by preventing quartz cementation. The grain coating only affects the precipitation of quartz cement and will therefore have no effect on porosity where the reservoir quality is controlled by other cements such as carbonates. Also, in immature sandstones, where quartz cementation is negligible, grain coatings will have no effect on the porosity (Bloch et al., 2002). Authigenic clay minerals and microcrystalline quartz have been found to be the most effective grain coatings (Taylor et al., 2010).

According to Storvoll et al. (2002), the following criteria must be fulfilled for grain coatings to effectively preserve primary porosity;

- The quartz grain must be fully covered before significant quartz cementation starts (2-3km).
- The coating must be continuous and cover the entire grain.
- The coating must be present on most of the grains in the sample.

Clay coating

The clay coatings are very important in preserving the porosity in sandstones and are identified in a lot of studies ([Ehrenberg, 1993](#); [Storvoll et al., 2002](#); [Bloch et al., 2002](#); [Heald and Larese 1974](#); [Thomson, 1979](#); [Smith, 1985](#)). These authors demonstrate that the deeply buried sandstones which have poorly developed clay coatings are very highly quartz cemented whereas the same sands with extensive clay coatings have very low amount of quartz cement. The authigenic chlorite coatings are the most important and effective in retarding the extensive quartz cementation in sandstones. The main reason being that chlorite form continuous layers around the detrital quartz grains which helps in preventing the quartz overgrowth ([Taylor et al., 2010](#)).

At Haltenbanken, offshore mid Norway, the Tilje and Garn Formations are reported to have extensive chlorite and illite coatings ([Ehrenberg, 1993](#); [Storvoll et al., 2002](#)). These coatings are believed to be the reason for the good reservoir quality in the oil and gas discoveries on the Haltenbanken, and porosities are preserved up to 25% at greater burial depths of more than 5km depth. The precursor of chlorite formation in marine sandstones is from the alteration of an earlier iron silicate phase which were formed on the sea floor or could be the iron and magnesium rich smectite. Illite is also reported to form an effective coating which prevents the quartz overgrowth ([Heald and Larese, 1974](#); [Storvoll et al., 2002](#)) and precursor of illite could be smectite.

Micro-quartz coating

Micro-quartz, like chlorite coats, forms on the surface of the detrital quartz grains and retard or inhibit the pore-filling quartz overgrowths ([Bloch et al., 2002](#)). The random orientation of minute micro-quartz crystals, covering the detrital quartz grains interfere with the formation of macro-quartz overgrowth ([Heald and Larese, 1974](#)) and is found to be the main cause for higher porosities and good reservoir quality at depths up to 5 km.

Experimental data ([Heald and Renton, 1966](#)) and morphology of micro-quartz crystals ([Williams et al., 1985](#)) indicate quick crystallization of micro-quartz phase from pore fluids with high saturation of silica. The silica is probably originated by dissolution of volcanic glass shards and sponge spicules, as a result of increase in temperature and burial ([Aase et al., 1996](#); [Ramm et al., 1997](#)).

Precipitation of micro-quartz occurs at low temperature (60 - 65 °C). At this time pore water is highly supersaturated with respect to dissolved silica through the dissolution process of Opal A and Opal CT and at the same time quartz growth rate is slow resulting in nucleation of many small crystals (Bjørlykke and Jahren, 2010). At higher temperatures, unstable silicates like Opal A, Opal CT and smectite have already dissolved. At this point, pore water is saturated with respect to silica and insufficient to precipitate quartz on the micro-quartz surfaces (Aase et al., 1996).

Due to its smaller crystal size, it is difficult to identify microcrystalline quartz in thin section using standard light microscopy, but it can be easily identified using SEM. Micro-quartz coat consists of a layer of about 1 - 15µm prismatic quartz crystals with c-axis haphazard direction. The c-axis orientations of micro-quartz crystals (Haddad et al., 2006) can prevent their change into bigger syntaxial quartz overgrowths.

3.3.2 Fluid overpressure

Fluid overpressure is expressed as the amount of pore-fluid pressure greater than the hydrostatic pressure (Dickinson, 1953). Fluid overpressure can develop 1) where pore volume reduction rate is higher than the rate of fluid release, 2) where pore fluid expansion rate is higher than the rate of fluid escape and 3) where large-scale movement occur (Swarbrick, 1999; Bloch et al. 2002).

At grain contacts fluid overpressure has the ability to reduce the effective stress by bearing some of the mass of the overlying sediments. Decrease in effective stress prevent mechanical compaction therefore the porosity lost due to mechanical compaction, is held open by overpressure, resulting in preserved porosity at deeper burial depths. Otherwise, it would be destroyed during the compaction process. Early overpressure provides a potential for porosity preservation until significant quartz cementation occurs (~80°C) (Walderhaug, 1994b). Overpressures may also limit quartz cementation by delaying the onset of intergranular pressure solution, eliminating a primary source of silica although the development of overpressure at later stage has a minor effect on porosity (Taylor et al., 2010).

3.3.3 Early hydrocarbon emplacement

The porosity preservation due to early emplacement of hydrocarbons in sandstones is still unclear in literature. Many authors have suggested that early infill of hydrocarbon in the pore space inhibited the quartz overgrowth and helped in preserving the porosity ([Selley 1978](#); [Rothwell et al., 1993](#), [Emery et al., 1993](#); [Gluyas et al., 1993](#); [Marchand et al., 2000, 2001](#)). Also, several workers have claimed to have seen an effect of less quartz cementation in the oil leg of sandstone reservoirs, but they have yet to prove that early onset of hydrocarbon saturation can retard quartz cementation.

An observations of hydrocarbon inclusions within quartz cement by [Walderhaug \(1990\)](#); [Bloch et al. \(2002\)](#) and [Karlsen et al. \(1993\)](#) prove that cementation continues despite a presence of hydrocarbon. According to [Giles et al. \(1992\)](#); [Ramm and Bjørlykke \(1994\)](#) and [Walderhaug \(1994a\)](#), there is very little correlation found between good reservoir quality and presence of hydrocarbons in the Norwegian and North Sea and reservoir quality remained the same across the water contact. An observed change in the amount of quartz cement in the water leg and the oil-leg, might be caused by overlooked grain coatings ([Aase and Walderhaug, 2005](#)).

[Worden and Morad \(2000\)](#) suggested that in water wet sandstone reservoir, hydrocarbon emplacement will have no effect on the quartz cementation because the grains surface will be coated by water. However in oil wet systems, where surface of quartz grain will be coated with hydrocarbon the oil emplacement will hinder or retard the quartz cementation. The fact that quartz grains normally are water wet, suggests the diffusion and precipitation of silica should be able to begin regardless the hydrocarbon has pre-filled the pore space. This strongly suggests that hydrocarbon content has no influence on the reservoir quality.

Chapter 4: Methodology

This study has been divided into two levels of investigation with different resolutions related to the tool to be used to evaluate the diagenetic processes and reservoir quality of Upper Cretaceous Nise Formation. During the analysis Optical microscopy and Scanning Electron Microscopy (SEM) techniques are employed.

4.1 Optical microscopy

4.1.1 Thin section analysis

The goal is to estimate the mineralogical and textural characteristics of samples from deep marine Upper Cretaceous sandstones, Nise Formation from Vøring Basin. In this study 25 samples (polished thin-sections impregnated with blue epoxy) were available. All the thin sections have been studied under a Nikon Optiphot-Pol petrographic microscope in order to extract detailed information. During study enough time was spent to identify and classify the minerals in order to minimize the error. The thin-sections were examined with respect to mineral compositions, sorting, grain shape (roundness), average grain size and framework connection. Other observations were also noted, and included such as authigenic clay minerals, quartz overgrowth and sutured/composite grains.

To support the documented observations pictures of thin sections are taken with high magnification microscope. The grain size measurements are based on the scale of Udden-Wentworth grain size scale ([Wentworth, 1922](#)) whereas the maturity of sandstone from the sorting and roundness classification schemes is available in [Adams et al. \(1986\)](#) and [Folk \(1951\)](#).

4.1.2 Point count analysis

The main reason for performing point counting is to estimate the composition and porosity of the samples. An automatic counter (Swift) attached with a mechanical stage, POL is used with Nikon Optiphot-Pol petrographic microscope for point counting. The mechanical stage and point

counting attachment projects a grid across the thin section by moving the section through the field of vision along a straight line at equal intervals. Each point is marked by the center of cross-hairs for each step. For each thin section three hundred points are counted in ten rows with thirty counting each row, with regards to rock composition (quartz, feldspar, lithic fragments), detrital and authigenic matrix, cement (quartz and calcite) and porosity (primary and secondary).

The data from the count was then transferred to Excel to generate diagrams. The resultant rock composition was plotted into a petrophysical ternary diagram, using the Tri-Plot program (Copyright © Todd A. Thompson, 2004).

4.1.3 Intergranular volume

Intragranular volume (IGV) is an important parameter for measuring compaction in sandstone, it can be calculated from the information gathered in point counting. It is equivalent to measure of the space between framework grains and averages around 40-45 volume percent in sandstones. IGV varies to a limited degree with sorting and does not vary with particle size. It should be noted that the 2D representation through a thin section gives an apparent variation in grain size. Grain contacts may also be out of the plane of the thin section (Lundegard, 1992; Ehrenberg, 1995).

From the point counting results intergranular volume (IGV) has been measured. Paxton et al. (2002) defined the intergranular volume as the sum of matrix, intergranular cement and pore spaces between the grains where, matrix is termed as clay and silt size particles between the grains (Figure 4.1). The results from calculated IGV were presented as bar chart diagram and divided into components like cements, matrix (detrital + authigenic clays) and primary porosity. To investigate the influence of textural parameters, composition and amount of quartz cement on the IGV values, these parameters were plotted against IGV.

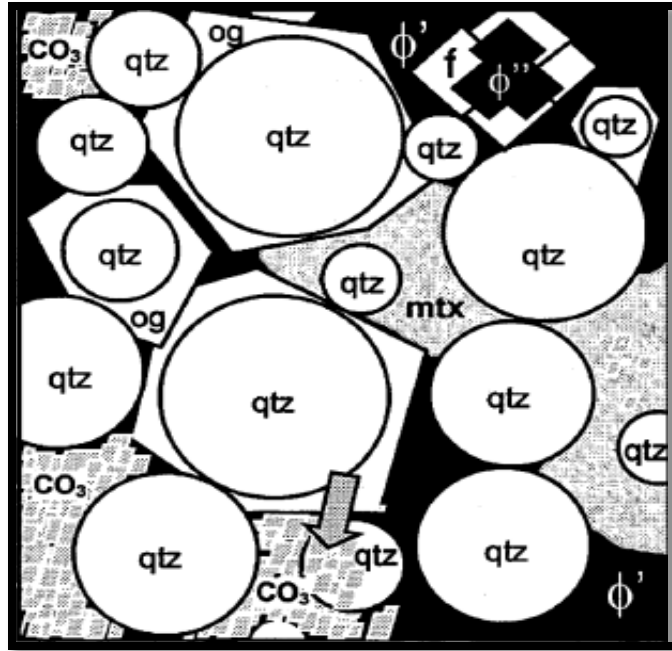


Figure 4.1: Sum of cement, matrix and porosity are termed as inter granular volume (Paxton et al. 2002).

4.2 Scanning Electron Microscopy

Scanning electron microscopy (SEM) has ability to achieve very high-resolution micrographs of the samples. To confirm the observations under optical microscopy, SEM study was completed by using JEOL JSM-6460LV Scanning Electron Microscope with a LINK INCA Energy 300 Energy Dispersive X-ray (EDX) system.

In this study 7 selected thin sections from well 6707/10-1 were carbon coated and analyzed under Scanning Electron Microscope. Backscattered electron imagery (BEI) makes it possible to distinguish materials of differing elemental composition, as the backscattered coefficient is proportional to the number of electrons detected, leaving lower atomic elements appear darker than the heavier atomic elements (Tucker, 1988). With the Energy Dispersive X-ray microanalysis (EDS) the energies of the emitted X-rays can be shown as series of peaks, spectra, distinct for individual elements within the material (Bishop et al., 1992). The data collected from SEM analysis in the end integrated with the optical microscope observation to minimize the errors.

4.3 Uncertainties

4.3.1 Thin section analysis

The method in one way or another is subjective, the common grain shape and roundness is based on the overall impression of the interpreter. Roundness is difficult to determine because compaction and cementation may have affected the shape and all rounded opaque minerals are identified as pyrite which might be another ore mineral. Two of the thin sections (at depth 3068m and 3076m) turned to be bad samples (not well impregnated with blue epoxy) which resulted to the difficulties in distinguishing missing grains, porosity and extinct quartz.

4.3.2 Point counting analysis

The samples are point counted from the middle part of thin section, the motive is to avoid counting on the edges of the thin-sections as these grains may be disturbed or damaged during preparation and could generating false porosity estimation in the sample. This also applies for the thin sections which are badly prepared, missing grains and containing many air bubbles.

The amount of quartz cement is uncertain in some cases due to weakly developed dust rims, which led to the difficulties in separating overgrowths from detrital quartz grains. The difference between quartz grains and untwinned albite is almost impossible to detect in a thin section. Albite is therefore assumed to be extensively undercounted if present, which would influence the feldspar count negatively.

Also, there are uncertainties in counting secondary porosity because secondary porosity was created during the dissolution of feldspars and unstable grains. During this process grains are partially dissolved and in other case authigenic clays precipitated in pores. Therefore, point counting of secondary porosity could be uncertain.

Most of the opaque minerals were probably pyrites, recognized by their round shape, but there were also other opaque phases present, especially within the pore space. It is likely that these opaque phases are either hydrocarbon residue or iron oxides. Within the pore space, the opaque phases would in several thin sections mask other pore-filling minerals or detrital, and lead to an underestimation of detrital or authigenic clay.

4.3.3 Intergranular volume

The main insecurity in the method is the inaccuracy of the point count. Badly prepared thin sections resulting in ripped out grains and pore-filling clay minerals, may influence the point count values and subsequently the calculated IGV-values.

4.3.4 Scanning electron microscopy

In the SEM it is difficult to make a proper quantitative analysis; the area of view is so small that the observer cannot know precisely what the content of the entire sample is. If something has not been observed in the sample, it does not necessarily mean that it is not present. In BEI, as in thin section, the albite and quartz look close to identical because of the similar amounts of electron emission, and thus the two minerals display the same grey shade. The albite content estimation is undermined, it can therefore be difficult to get an impression of albite content.

Chapter 5: Optical microscopy

5.1 Introduction

A mineralogical and petrographic analysis was performed on the samples to investigate the relationship between diagenetic processes and reservoir quality of deep marine Upper Cretaceous sandstone, Nise Formation in Vøring Basin. In this chapter the mineral contents and the textural relationships within the rock are described in detail. The main focus is on degree of compaction and diagenetic cements in Nise Formation. Other factors that affect reservoir quality, such as the grain size, sorting and overall grain composition, were analyzed in the thin section analysis.

The dataset consists of 25 thin section from well 6707/10-01 in Aasta Hansteen discovery. All thin sections have been point counted using a polarization microscope to gain information about the composition of the sandstones as well as the porosity of the samples. Data obtained from thin section analysis by point counting is further employed to calculate Inter-granular volume (IGV) and perform petrographic classification of sandstones using [Dott \(1964\)](#).

5.2 Results

5.2.1 Point count

A point counting was performed on all 25 thin-sections taken from well 6707/10-1 at 2976.45 m to 4134.45 m depths. The main purpose of the point count was to get a quantitative analysis of the sandstone composition and quality. The point counting was achieved in a scheme with respect to detrital framework grains, matrix, cement and porosity employing 300 points per sample. Results from the point count are displayed in [Table 5.1](#).

[Table 5.2](#) displays the textural characteristics and calculated IGV of the point counted samples. Also, the samples which were selected for further investigation in SEM are marked with # symbol.

Table 5.1: Summary of point count analysis of samples from Nise Formation in well 6707/10-1.

POINT COUNT												
Well 6707/10-1												
Depth (m)	Framework (%)				Matrix (%)		Cement (%)		Porosity (%)		Total rock volume (%)	Calculated IGV%
	Quartz	Feldspar	Lithic fragment		Authigenic clay	Detrital clay and opaque	Quartz	Carbonate	Primary	Secondary		
			Glauconite	Micas								
2976.45	46.50	9.20	2.00	1.00	1.70	3.30	2.60	5.30	25.70	2.60	100	38.60
2983.57	40.40	5.20	3.00	2.40	2.30	2.60	0.00	36.80	0.30	7.10	100	42.00
2986.62	41.00	13.00	3.20	2.00	2.30	2.30	2.70	3.30	27.90	2.30	100	38.50
3003.42	38.30	1.30	3.10	2.90	3.70	0.70	0.00	32.00	12.00	6.00	100	48.40
3010.40	39.00	10.30	3.10	2.00	4.50	1.60	5.10	0.00	33.10	1.30	100	44.30
3013.55	47.50	10.40	2.70	1.40	0.30	1.30	0.90	0.30	35.10	0.00	100	37.90
3033.58	43.60	11.50	3.30	2.10	1.30	1.60	1.60	6.40	28.70	0.00	100	39.60
3038.69	44.00	4.70	3.20	1.80	0.30	4.00	0.00	22.30	19.70	0.00	100	46.30
3046.56	43.90	4.20	2.60	1.30	1.00	2.60	1.00	6.50	35.80	1.30	100	46.90
3049.53	44.00	6.50	3.70	1.80	0.30	3.30	4.20	4.90	28.30	2.90	100	41.00
3068.56	45.20	4.10	3.30	1.10	1.00	3.40	1.40	32.40	6.90	1.40	100	45.10
3076.82	47.60	1.90	6.00	1.20	1.30	1.60	0.00	18.20	21.60	0.60	100	42.70
3087.50	38.40	10.00	6.40	1.00	3.40	1.90	0.90	4.40	32.10	1.60	100	42.70
3093.45	40.40	9.80	6.30	1.30	0.60	0.90	0.60	7.60	31.50	0.90	100	41.20
3100.73	41.70	7.70	6.20	0.80	0.00	2.70	1.30	13.30	19.70	6.70	100	37.00
3107.63	47.30	5.70	5.10	0.60	0.70	3.30	0.30	2.00	33.00	2.00	100	39.30
3112.94	44.60	6.40	5.40	0.70	1.90	4.50	1.30	4.80	26.30	4.20	100	38.80
3122.50	56.20	4.80	1.80	0.60	2.40	1.30	0.30	2.40	29.00	1.10	100	35.40
3145.40	53.50	6.40	3.10	1.50	0.90	0.90	0.60	1.40	30.30	1.40	100	34.10
4118.70	47.70	8.20	3.30	1.00	3.30	0.70	0.30	5.30	28.30	2.00	100	37.90
4119.60	48.70	0.70	4.10	1.20	16.00	0.00	0.00	20.80	5.90	2.70	100	42.70
4128.30	48.60	4.60	0.80	0.10	4.50	0.90	0.60	12.60	20.70	6.50	100	39.30
4129.25	48.00	5.60	3.80	0.20	1.00	3.60	0.70	6.60	29.50	1.00	100	41.40
4132.58	53.10	6.20	4.30	0.40	1.90	3.70	0.60	2.80	24.80	2.20	100	33.80
4134.45	58.10	4.20	4.50	0.30	0.90	0.60	1.50	3.30	24.00	2.70	100	30.30

Table 5.2: Summary of textural characteristics and calculated IGV of samples from Nise Formation in well 6707/10-1. Also, SEM analysis was performed in selected samples marked with #.

TEXTURE AND CALCULATED IGV					
Well 6707/10-1					
Depth (m)	Average grain size	Sorting	Grain Shape	Calculated IGV%	SEM Analysis
2976.45	Medium	Moderately sorted	Sub-angular	38.60	#
2983.57	Veryfine	Well sorted	Sub-rounded	42.00	#
2986.62	Medium	Moderately sorted	Sub-angular	38.50	
3003.42	Veryfine	Well sorted	Sub-rounded	48.40	#
3010.40	Fine	Well sorted	Sub-rounded	44.30	
3013.55	Medium	Moderately sorted	Sub-rounded	37.90	#
3033.58	Medium	Moderately sorted	Angular	39.60	
3038.69	Veryfine	Well sorted	Sub-angular	46.30	#
3046.56	Fine	Well sorted	Sub-rounded	46.90	
3049.53	Medium	Moderately sorted	Sub-rounded	41.00	
3068.56	Veryfine	Well sorted	Sub-angular	45.10	
3076.82	Veryfine	Well sorted	Sub-angular	42.70	
3087.50	Fine	Well sorted	Sub-rounded	42.70	
3093.45	Medium	Moderately sorted	Sub-rounded	41.20	
3100.73	Course	Moderately sorted	Sub-angular	37.00	
3107.63	Medium	Moderately sorted	Sub-rounded	39.30	
3112.94	Medium	Moderately sorted	Sub-rounded	38.80	#
3122.50	Medium	Poorly sorted	Sub-rounded	35.40	
3145.40	Medium	Moderate	Angular	34.10	
4118.70	Course	Poorly sorted	Sub-rounded	37.90	
4119.60	Veryfine	Well sorted	Sub-rounded	42.70	#
4128.30	Course	Poorly sorted	Rounded	39.30	#
4129.25	Fine	Well sorted	Sub-angular	41.40	
4132.58	Medium	Moderately sorted	Rounded	33.80	
4134.45	Medium	Moderately sorted	Sub-rounded	30.30	
			AVERAGE IGV=	40.21	

Point count results

In **Figure 5.1** the results of the point count are presented in a graph, subdivided into the three main constituents; grain, cement and primary porosity. All samples are plotted according to their measured depth (m). For further simplification data has been categorized due to their grain size (VF for very fine-grained, F for fine-grained, M for medium-grained and C for coarse-grained samples).

From the figure, there seems to be a relationship between the grain size and the sample constituents. The largest amounts of cement (including authigenic clays), are found in very fine-grained samples results to less grains and low porosity. The fine to medium-grained samples have the highest detrital grain count, and a correspondingly low cement content and high porosity. Course-grained shows similar results, but with slightly less grains and more cement.

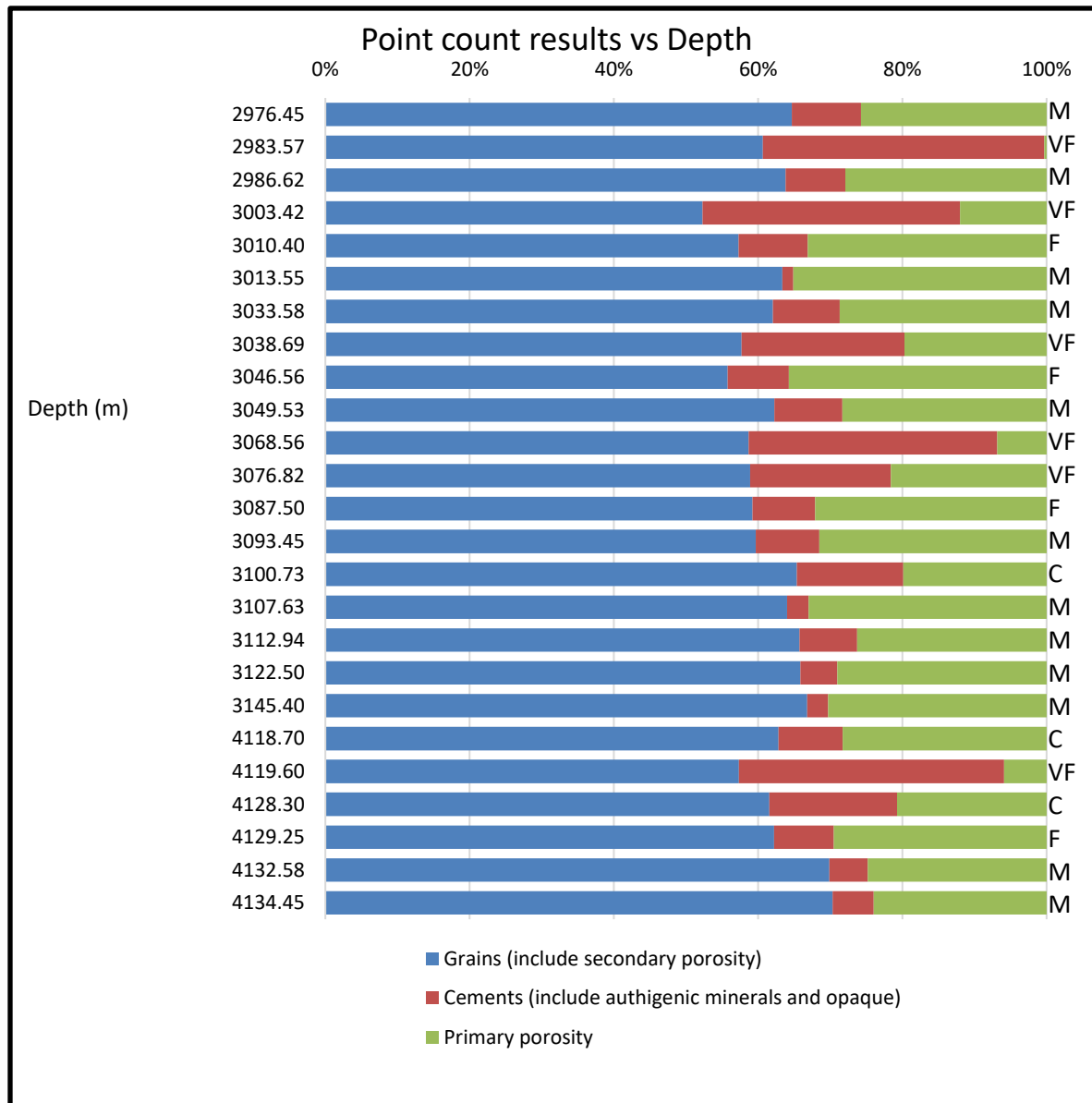


Figure 5.1: Point count results with respect to the sample depths, divided into three constituents, grains, cements and primary porosity. The right column shows the variation in grain size.

Sandstone classification

Most sandstone classifications are based on petrographic model analyses. In this study Dott's classification scheme (Dott, 1964) and arenites-classification scheme by Folk (1974) are used, (Figure 5.2 and Figure 5.3) based on relative proportional of matrix, quartz, feldspars and rock fragments.

The counted rock composition has been divided into the three components; quartz, feldspar and rock fragments and plotted on the ternary diagram to determine type of sandstone (Figure 5.4). All samples have less than 15% fine-grained matrix thus lie within the definition of arenites. The samples contain significant amount of quartz and feldspar with little rock fragments. From Figure 5.4 it has been observed that majority of the samples (several of the points overlap) plot within the subarkose area.

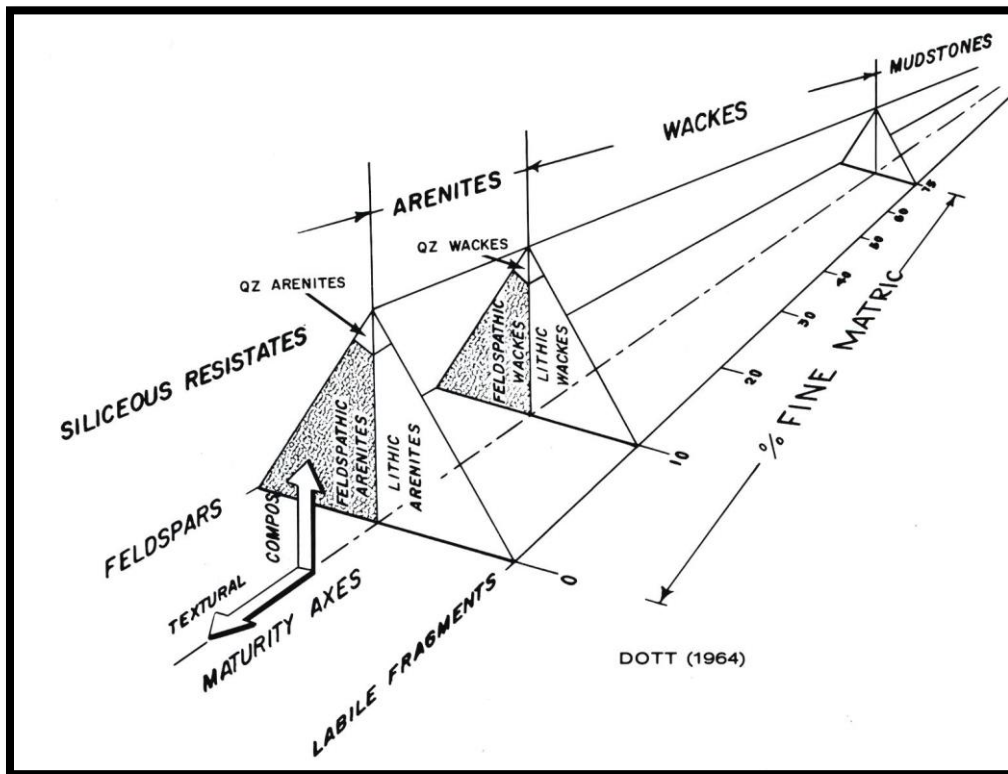


Figure 5.2: Sandstone classification by Dott 1964

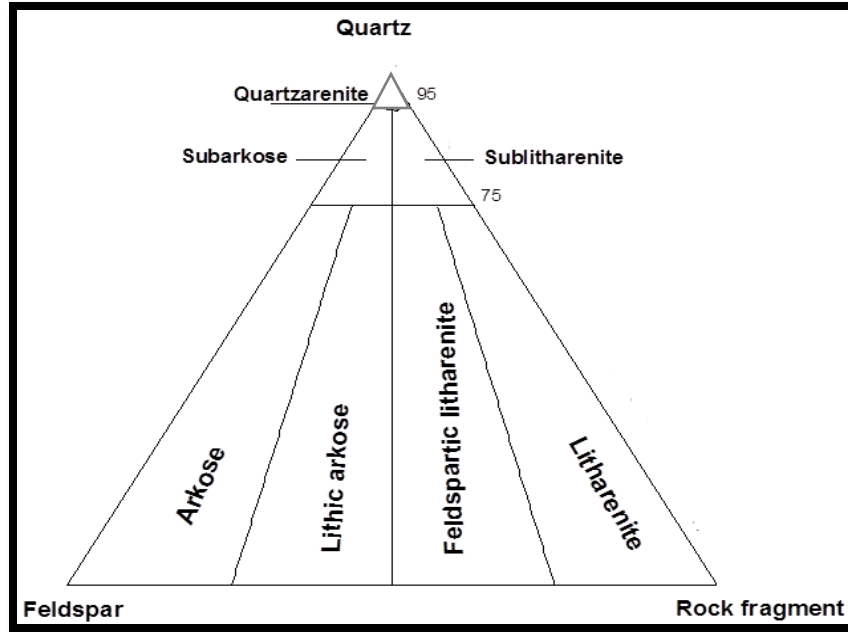


Figure 5.3: QFL ternary classification plot (Folk 1974)

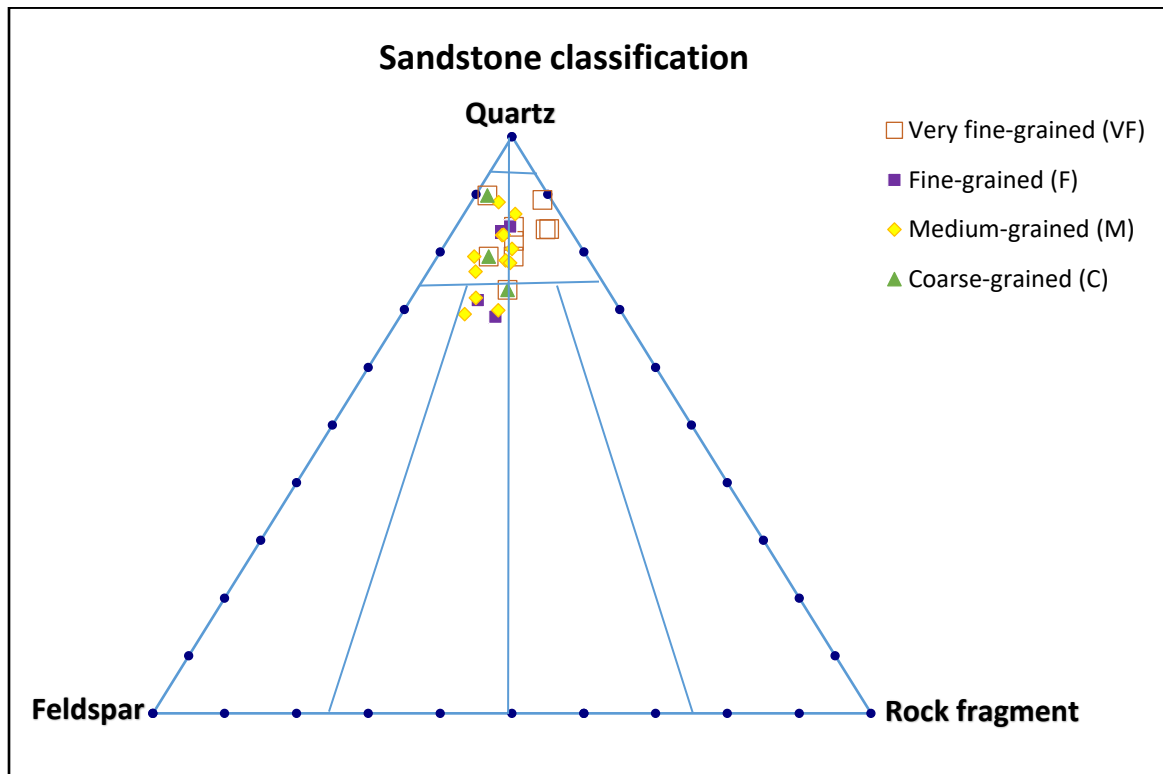


Figure 5.4: Petrographic classification of Nise Sandstones Formation. All the samples have been plotted and color-coded according to their grain sizes.

Primary porosity

Primary porosity is found to be the most abundant pore type during the point count analysis. The average counted primary porosity of Nise Formation according to this study is 24.41%, the lowest porosity values are observed in very fine-grained samples due to high amount pore filling carbonate cement. (Table 5.3). The histogram (Figure 5.5) represents the porosities of the samples with increasing depth and ranges from 0.30% in cemented sandstones to as much as 35.8% in clean sandstone.

Table 5.3: Calculated mean count percentage for primary porosity, for Nise Formation and for each grain size unit.

Mean porosity (%)			
Nise Sandstone Formation			
24.41			
VF	F	M	C
11.07	31.63	28.72	22.90

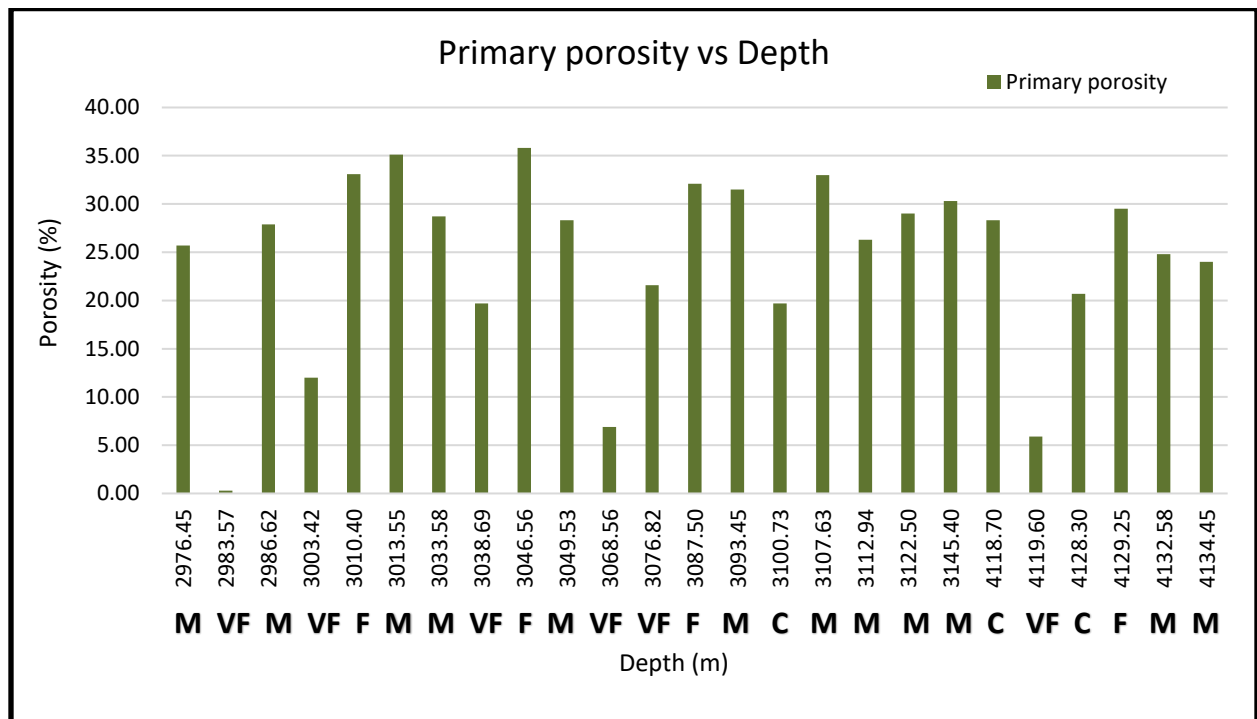


Figure 5.5: Histogram of the counted percentage of primary porosity vs depth, the values are shown according to their grain size with respective depths.

Low primary porosity is often related to advanced diagenesis of the sandstone. At great depths this is mainly due to the precipitation of quartz cement. To see if there is any such relationship within these samples, the counted percentage of primary porosity and quartz cement is displayed together in **Figure 5.6**.

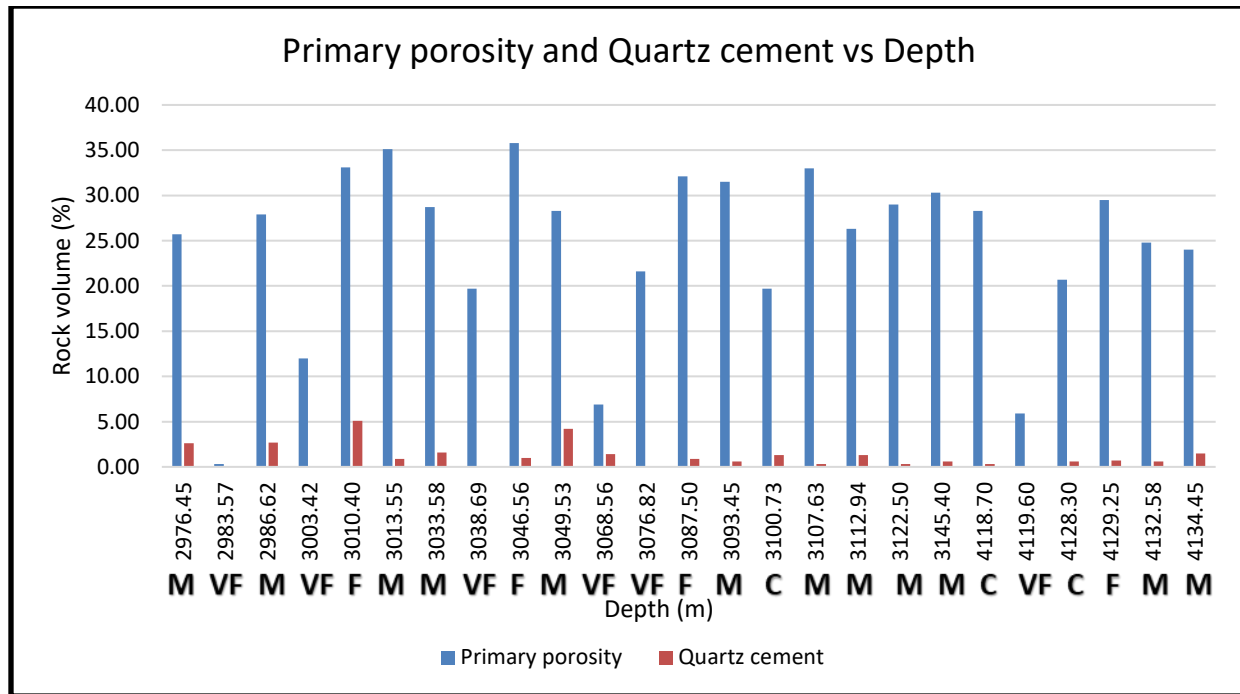


Figure 5.6: Histogram with comparison of quartz cement and primary porosity percentage, arranged by increasing depth with respective grain size.

Variable content of quartz cement is observed from samples as syntaxial overgrowth, the counted quartz cement varies between 0.3% - 5.1% of the total rock volume. Nevertheless the quartz cement in these samples is very limited and difficult to point count because of the very weak dust rims that differentiate detrital quartz grain and the quartz cement. The amount of quartz cements seems to be one of the reasons for low primary porosity, note from **Figure 5.6** presence of low quartz cement in some samples indicates anomalously higher porosities.

Another reason for porosity lost is due to early emplacement of carbonate cement. The sample from depth 2983.57 m and 4119.60 m are marked by extremely low values of primary porosity and lack of quartz cement due to extensive carbonate cement. Other samples with low porosities are at depth 3068.56 m and 3003.42m and both samples have higher carbonate cement content. All of this carbonate cemented samples are associated with very-fine grain size which were observed to be the lowest porosity samples (**Figure 5.7**).

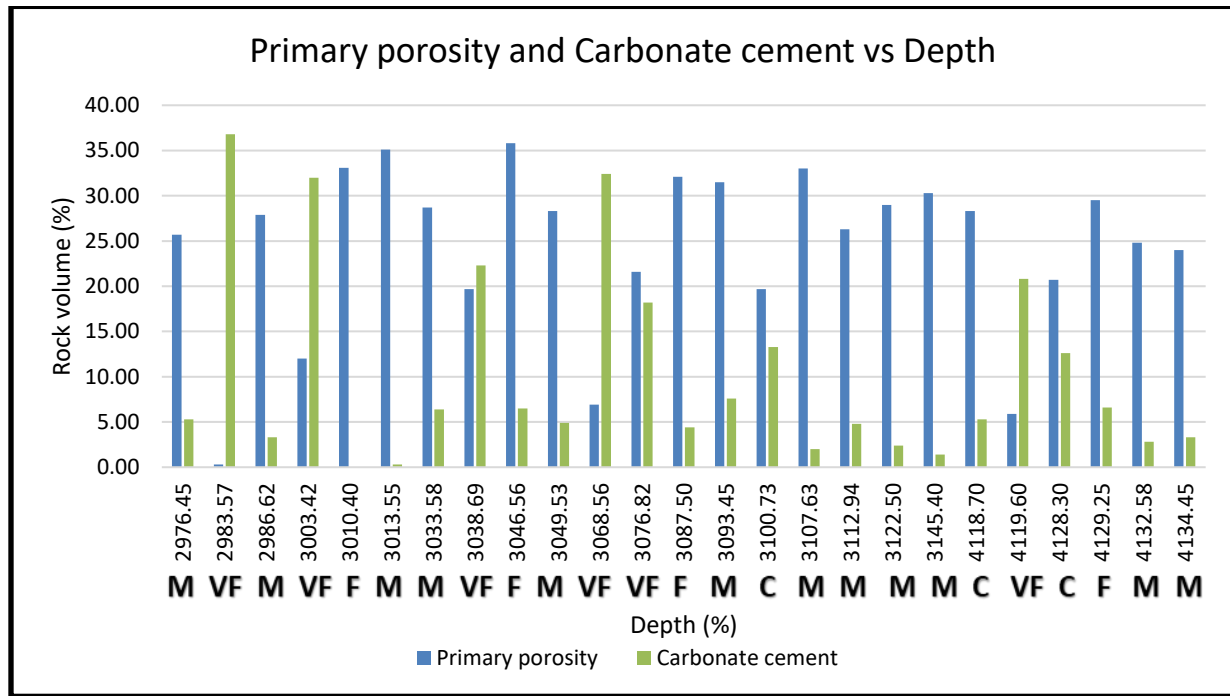


Figure 5.7: Histogram with comparison of carbonate cement and primary porosity percentage, arranged by increasing depth with respective grain size.

Secondary porosity

Specific point counting results were compared to investigate if the secondary porosity from framework grain dissolution has any significant influence on the total porosity and permeability. The analysis of partially dissolved grains in SEM (**Chapter 6:**) revealed that the observed secondary porosity in thin-section is most likely caused by the leaching of feldspar. A diagram was generated in order to define the relationship between feldspar and secondary porosity in the

point counting results (**Figure 5.8**). The two graphs show opposite trends, indicating that secondary porosity is associated with dissolution of feldspars. Decrease in feldspar content correspond to increase in secondary porosity means the feldspar has been dissolved to produce secondary porosity.

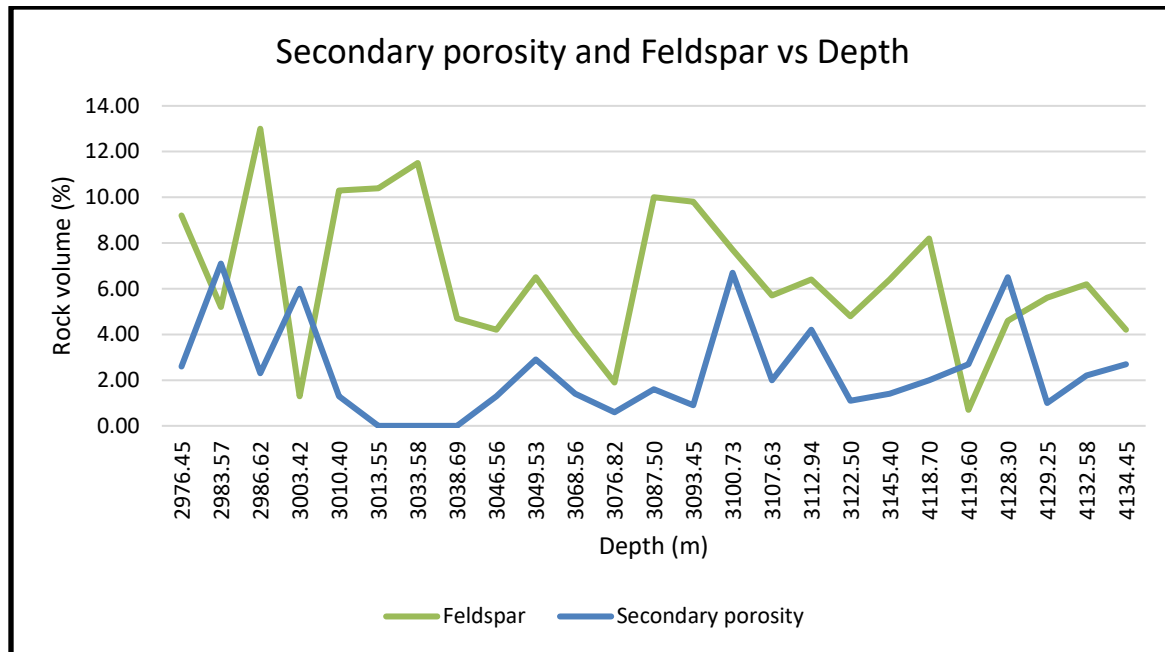


Figure 5.8: Rock volume percentage of feldspar and secondary porosity compared and plotted against depth.

Leaching of feldspar is commonly associated with precipitation of the authigenic clay minerals such as kaolinite and illite. A significant amount of authigenic clays have been observed during point counting and it was observed that most of the clay is kaolinites which were later on confirmed by the SEM analysis (**Chapter 6**). Secondary porosity from framework grain dissolution was compared to the content of authigenic clays in order to investigate if the grain dissolution observed in the samples had a significant contribution to the porosity. The comparison shows that the percentage of authigenic clay content increases in accordance with the secondary porosity (**Figure 5.9**). Therefore the net gain in total porosity is almost zero because the dissolved pores are filled with authigenic clays which reduce the porosity of the sandstone.

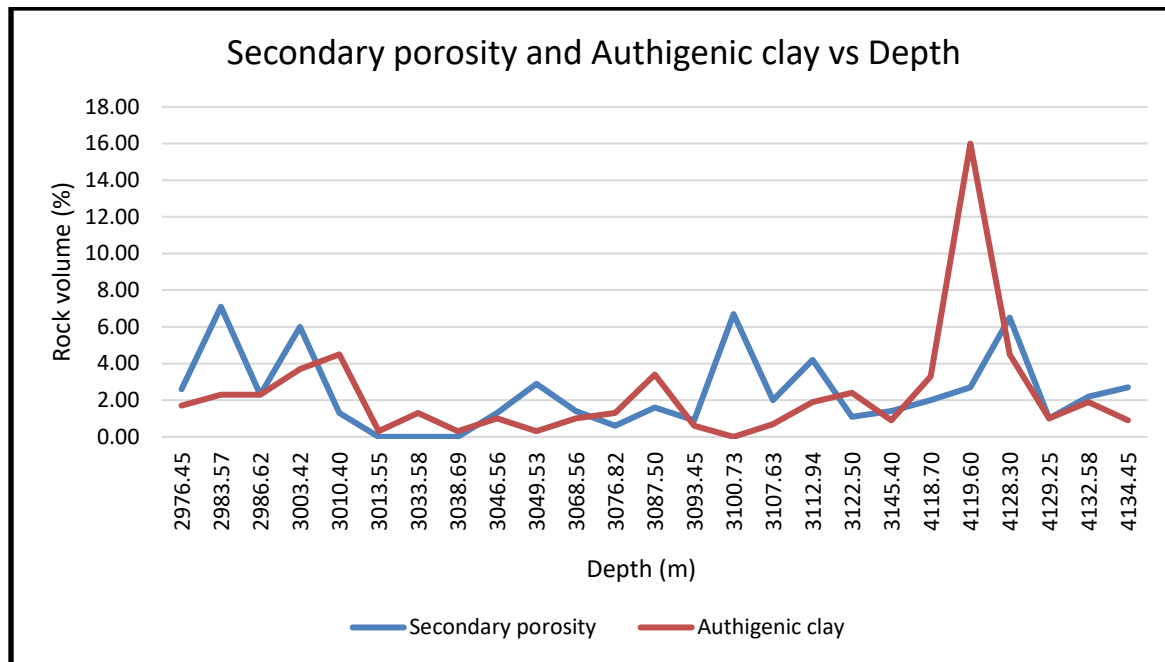


Figure 5.9: Rock volume percentage of authigenic clay and secondary porosity compared and plotted against depth.

5.2.2 Intergranular volume (IGV)

Intergranular volume (IGV) has been calculated from point counting to get the estimation of compaction and cementation to the porosity loss. Calculated IGV is the sum of matrix, cement and porosity for each sample.

Figure 5.10 shows the overview of the calculated values of intergranular volume divided into its constituents and arranged according to depth. Generally, from the figure it appears that the highest IGV-values are found in the samples from the shallowest depths. The pore space of the shallower samples has high contents of quartz cement and carbonate cement, but also higher primary porosity than the deepest samples.

The average IGV value for all sample is 40.21% while some of the samples show slightly higher values (up to 48.40%) than the average values. These higher values are because of the early carbonate and quartz cementation. In some samples the values are little lower than the average values which shows the higher mechanical compaction and low cementation.

So presence of higher amount cement especially carbonate cement could be the reason of higher average of IGV in Nise Sandstone. Early carbonate cementation squeezes the frame work grains apart and helps in less compaction hence greater IGV value. Deeper samples are expected to have lower IGV values, but some samples have higher IGV values. The reason is higher authigenic clays content and primary porosity count as compared to shallower ones. Grain plucking during the preparation of thin section samples could generate the pseudo porosity so higher porosity count results in the higher IGV values.

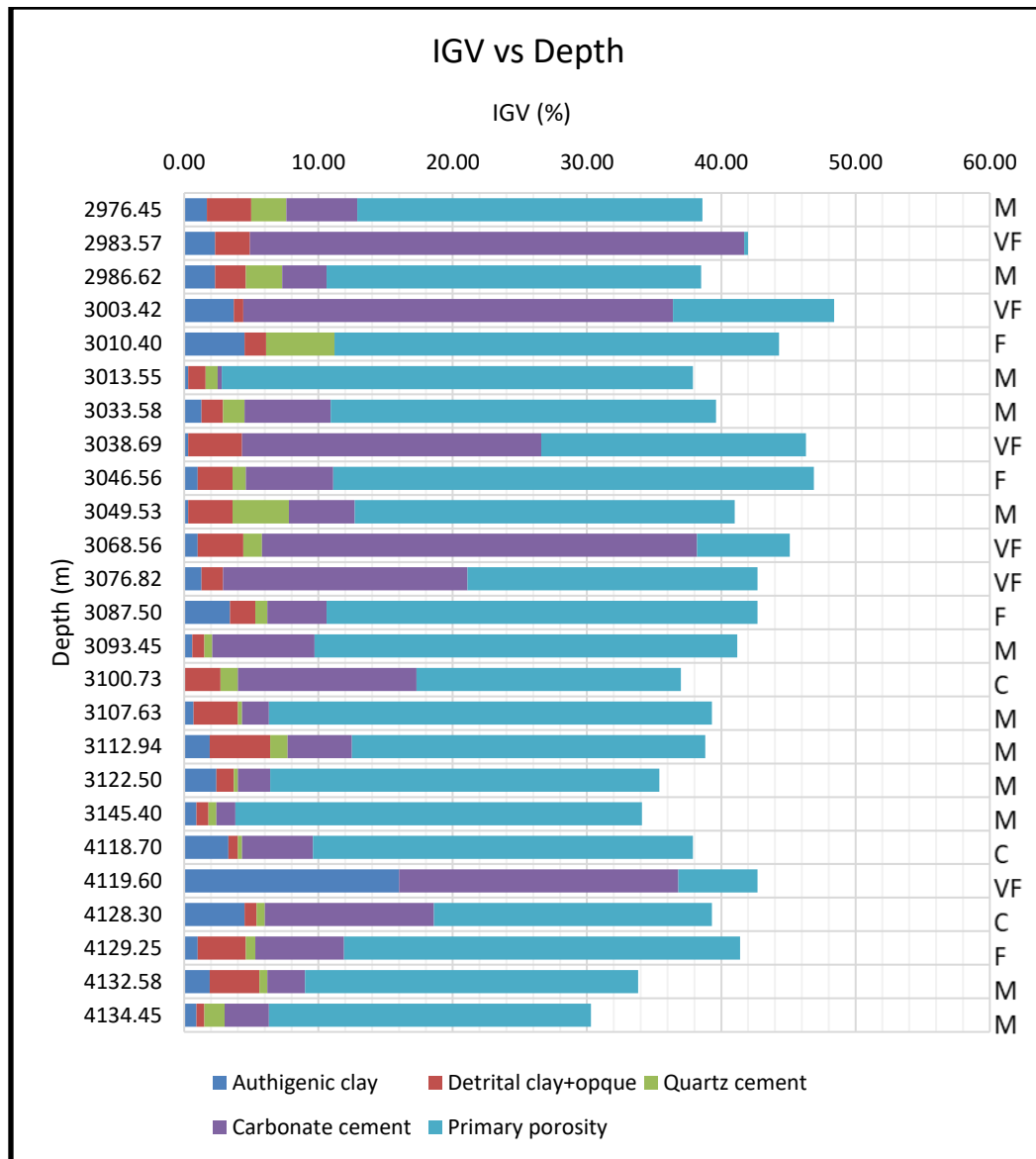


Figure 5.10: Overview of calculated IGV, arranged by increasing depth. Color coding illustrates the content of the various components of the IGV. The right column shows the variation in grain size.

Textural characteristics

A visual estimation of grain size, shape and sorting, was performed for all the thin sections under the microscope. This analysis was done to see if the mentioned parameters vary between the sandstone samples and if it had any corresponding or noticeable effect on the intergranular volume (IGV) calculated from the point count. The results were also used to get an estimate on the maturity of the sandstone.

Calculated IGV values were plotted against the sorting, average grain size and grain shape in three separate diagrams (Figure 5.11, Figure 5.12 and Figure 5.13). The most confident linear trends could be seen for the sorting and grain size (Figure 5.11 and Figure 5.12), displaying that IGV value increases slightly with better sorting and decreasing grain size.

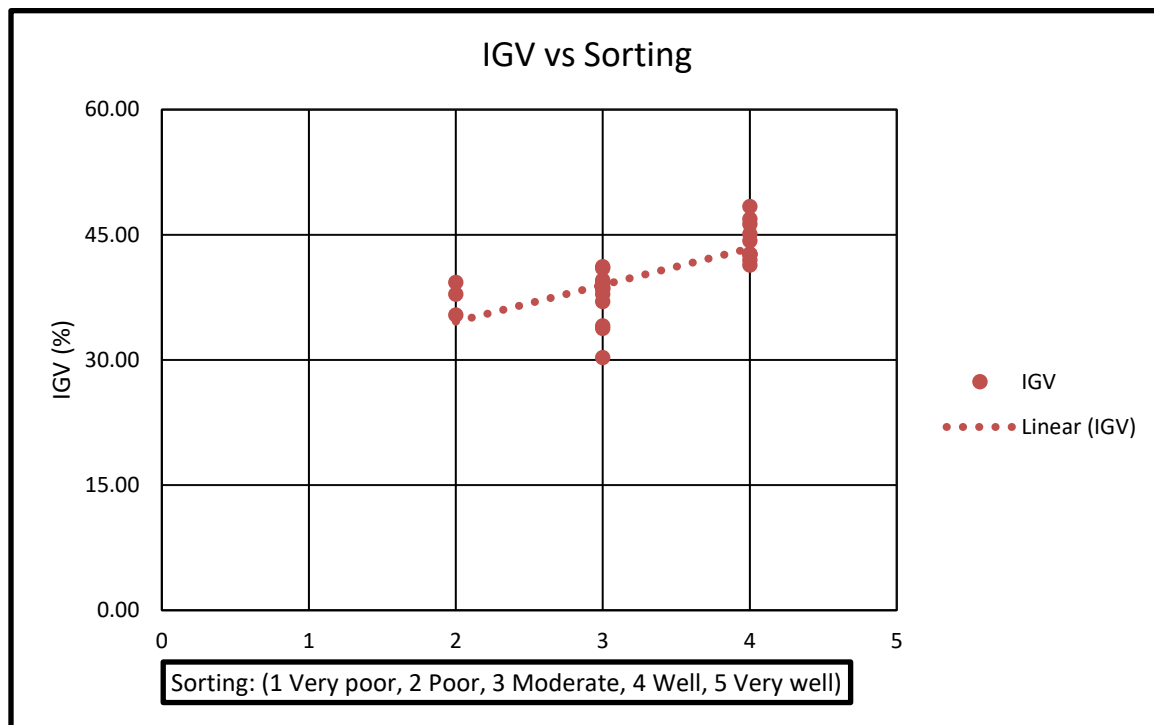


Figure 5.11: Cross plot showing the correspondence between the degree of sorting and calculated IGV. The IGV value increases with better sorting.

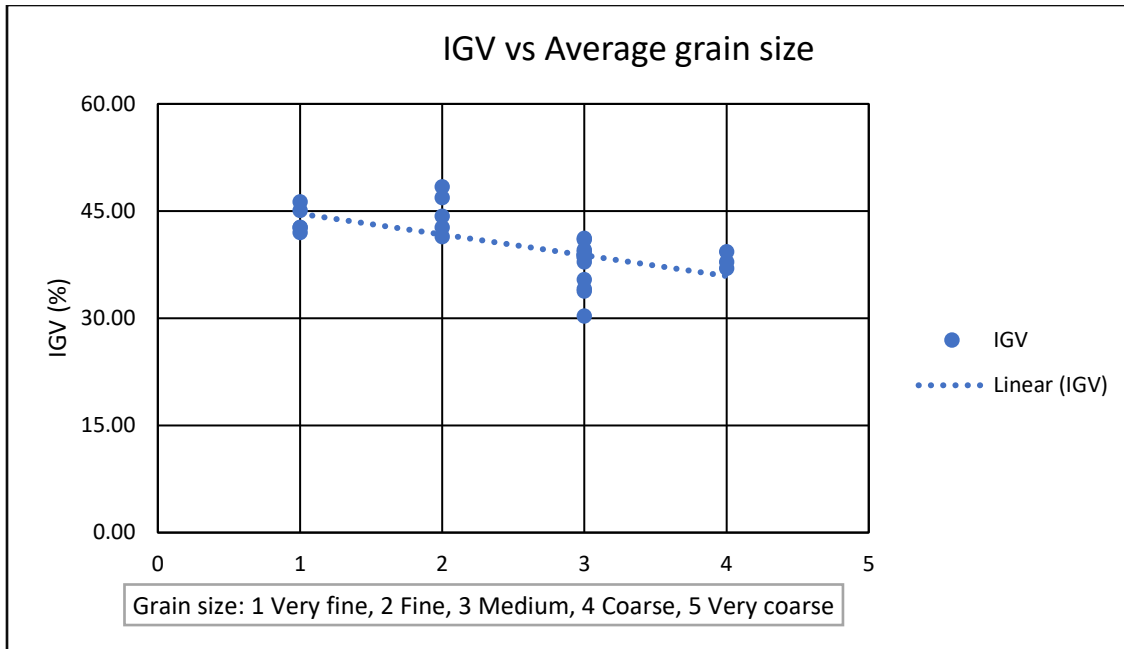


Figure 5.12: Cross plot showing the correspondence between average grain size and calculated IGV. The IGV value increases with the decrease in grain size.

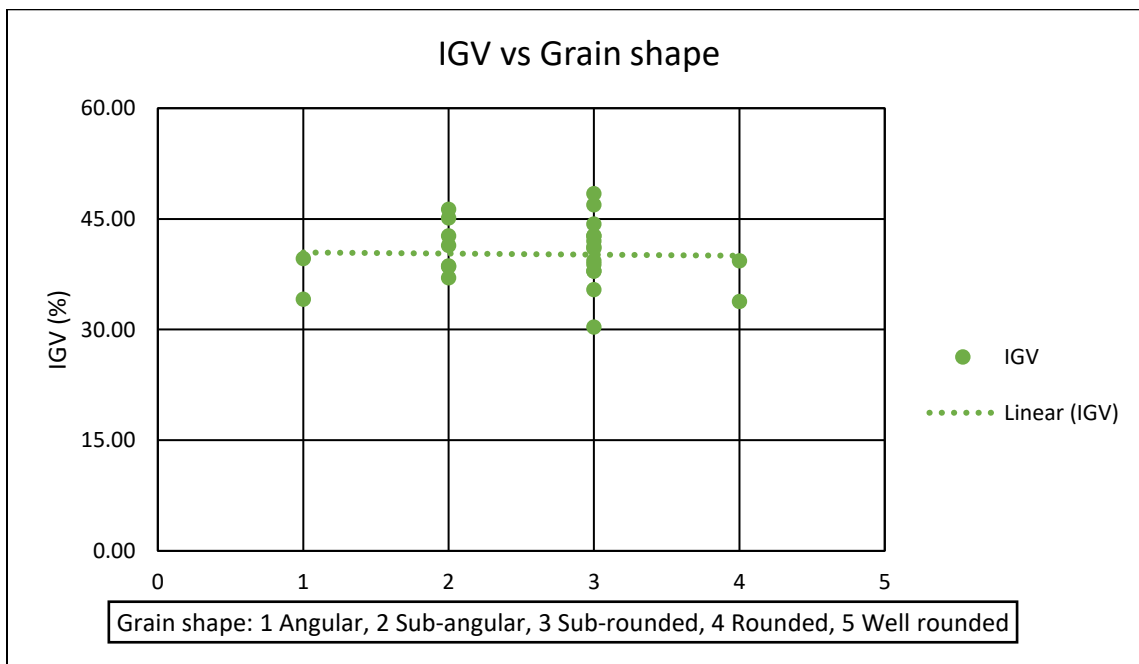


Figure 5.13: Cross plot showing the correspondence between the grain shape and calculated IGV. Overall no considerable variation has been observed.

Textural maturity

According to **Folk (1951)**, there are four stages of textural maturity described by the three sequential events; (1) Clays removal (2) sorting of the sand grains (3) high roundness achievement. The four stages of textural maturity are shown in **Table 5.4**. The sorting and roundness results from the textural sample analysis were combined to get an estimate on the maturity of the Nise Sandstone.

Table 5.4: Stages of sediment maturity (Folk 1951).

1 Immature stage	2 Sub-mature stage	3 Mature stage	4 Super mature stage
Sediments have considerable clay and mica; the grains are poorly sorted, and grains are angular.	Sediments have very little clay; grains are poorly sorted and angular.	Sediments don't have any clay; grains are well sorted and sub angular.	Sediments are without clay, grains are well sorted and rounded.

Following the definition by **Folk (1951)** the sorting and angularity of the samples were compared. None of the samples contained significant amounts of detrital clay, clay content can therefore be disregarded, and the immature stage may be excluded (**Table 5.4**). Thus the studied samples fall under the texturally mature stage, as majority are subangular to sub-rounded and moderate to well-sorted grains.

Detrital clay

Detrital matrix was one of the parameters counted in the point count, the amount of detrital clay is compared to the calculated IGV values in order to investigate whether or not a difference in detrital clay content has influenced the mechanical compaction. **Figure 5.14** shows that there is apparently no correlation between the calculated IGV-values and the amount of detrital matrix.

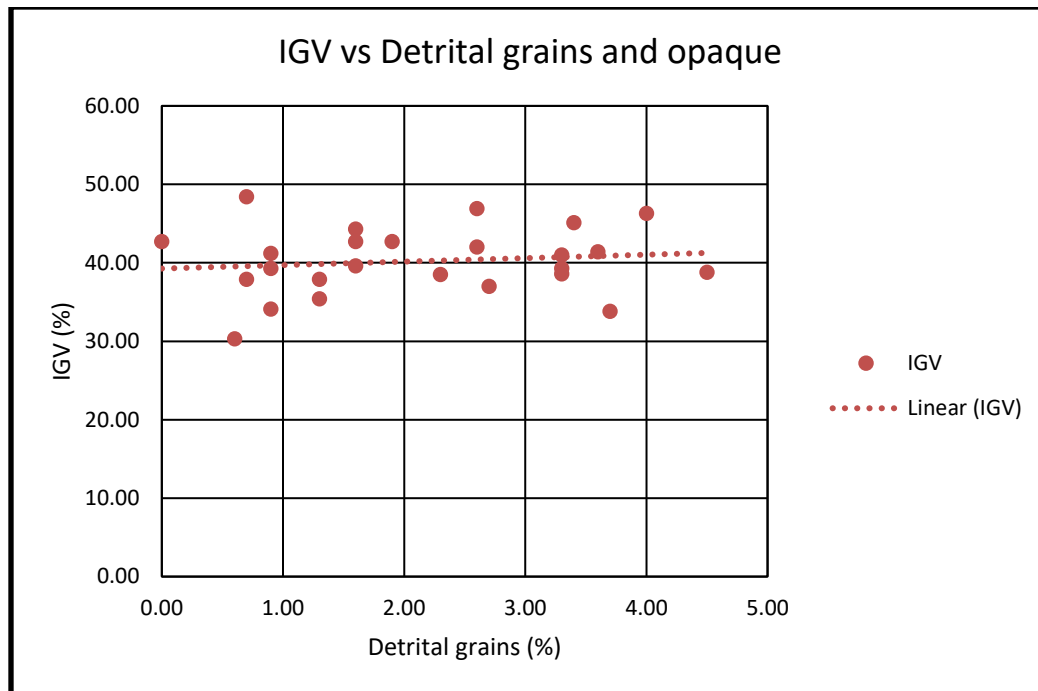


Figure 5.14: The correlation between IGV-values and the detrital matrix count.

Secondary porosity

Secondary porosity was plotted against the corresponding IGV-values in order to investigate any relationship between the two. The plot ([Figure 5.15](#)) shows that the secondary porosities are generally low and corresponds to IGV-values ranging from 30 - 50%. No trend can be seen in the plot. Secondary porosity was not included in calculating the IGV, but this relationship shows that generation of secondary porosity can cause increase in IGV, if this secondary porosity is well developed and get connected with the primary porosity it can enhance the total porosity.

Quartz cement

The IGV-values were plotted against the amounts of quartz cement, to check if the precipitation of quartz cement has any noticeable influence on the calculated IGV. In the plot ([Figure 5.16](#)), no apparent trend is observed between the two parameters. Quartz cementation is the major factor in decreasing the porosity at greater depths, but it does not decrease the IGV.

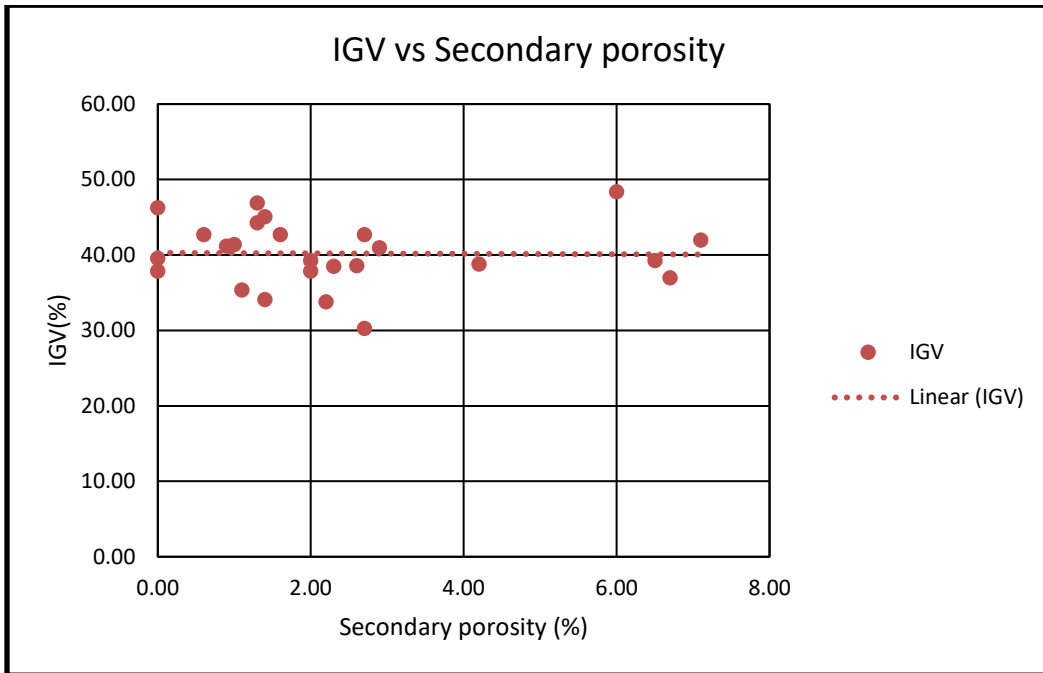


Figure 5.15: The correlation between IGV-values and the counted secondary porosity.

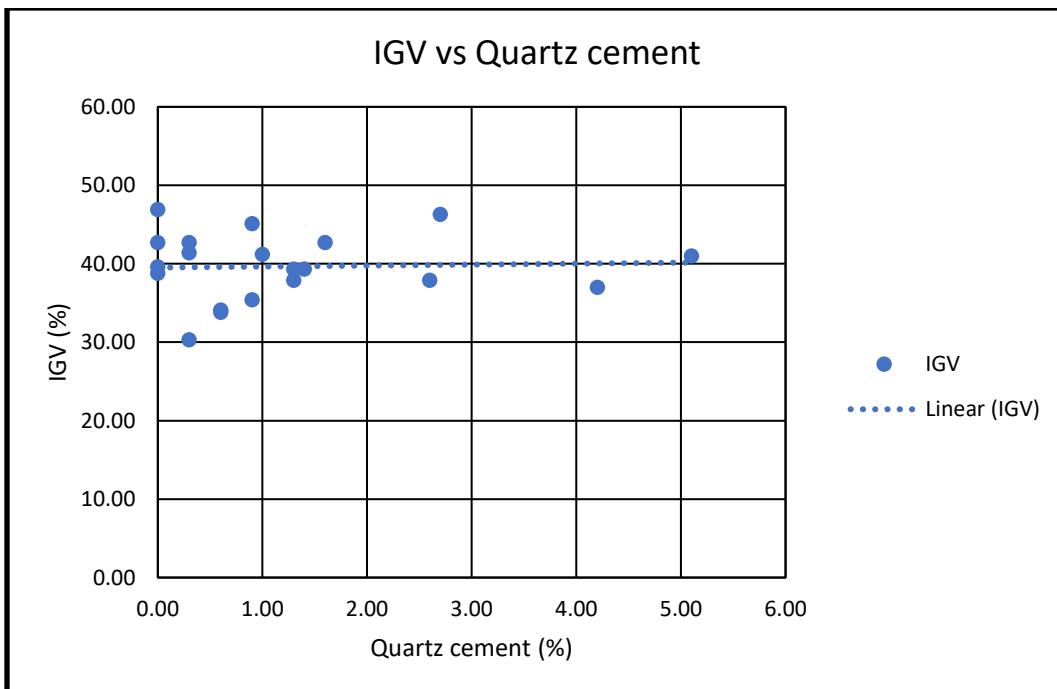


Figure 5.16: The correlation between IGV-values and the quartz cement.

Carbonate cement.

The IGV-values were plotted against the amounts of carbonate cement, to check if the precipitation of carbonate cement has any noticeable influence on the calculated IGV. In the plot (Figure 5.17), similar trend is observed between the two parameters. Increase in carbonate cement also shows increase the IGV. Samples with higher carbonate cement shows higher IGV value therefore less mechanical compaction.

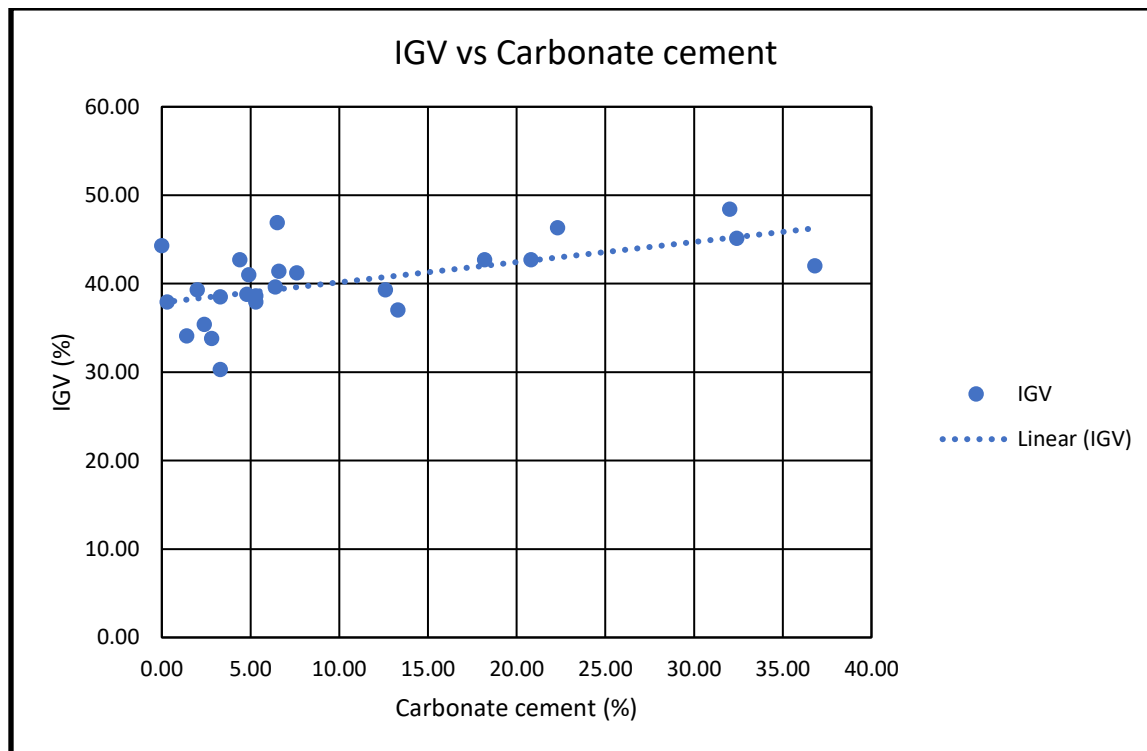


Figure 5.17: The correlation between IGV-values and carbonate cement.

5.2.3 Thin section observation

Pictures of selected thin-sections were taken in an optical microscope with an attached camera. The images were taken in order to illustrate some of the observations made in the point count and textural analysis.

Detrital composition of sandstones

In a ternary compositional plot ([Figure 5.4](#)), the Nise sandstones are classified as subarkoses, have mostly quartz as basic grain framework with lesser amount of feldspars and very little rock fragments. K-feldspar is observed to be more abundant than plagioclase. Other detrital grains occur in relatively small amounts and these include micas, glauconite and opaque minerals. In this study micas and glauconite are grouped as lithic grains ([Figure 5.18](#)). Most of the examined samples were, subangular to sub rounded, moderately to well-sorted, medium to fine grained sandstones. But some variation in grain size was noted (very fine -grained and course- grained) ([Figure 5.19](#)).

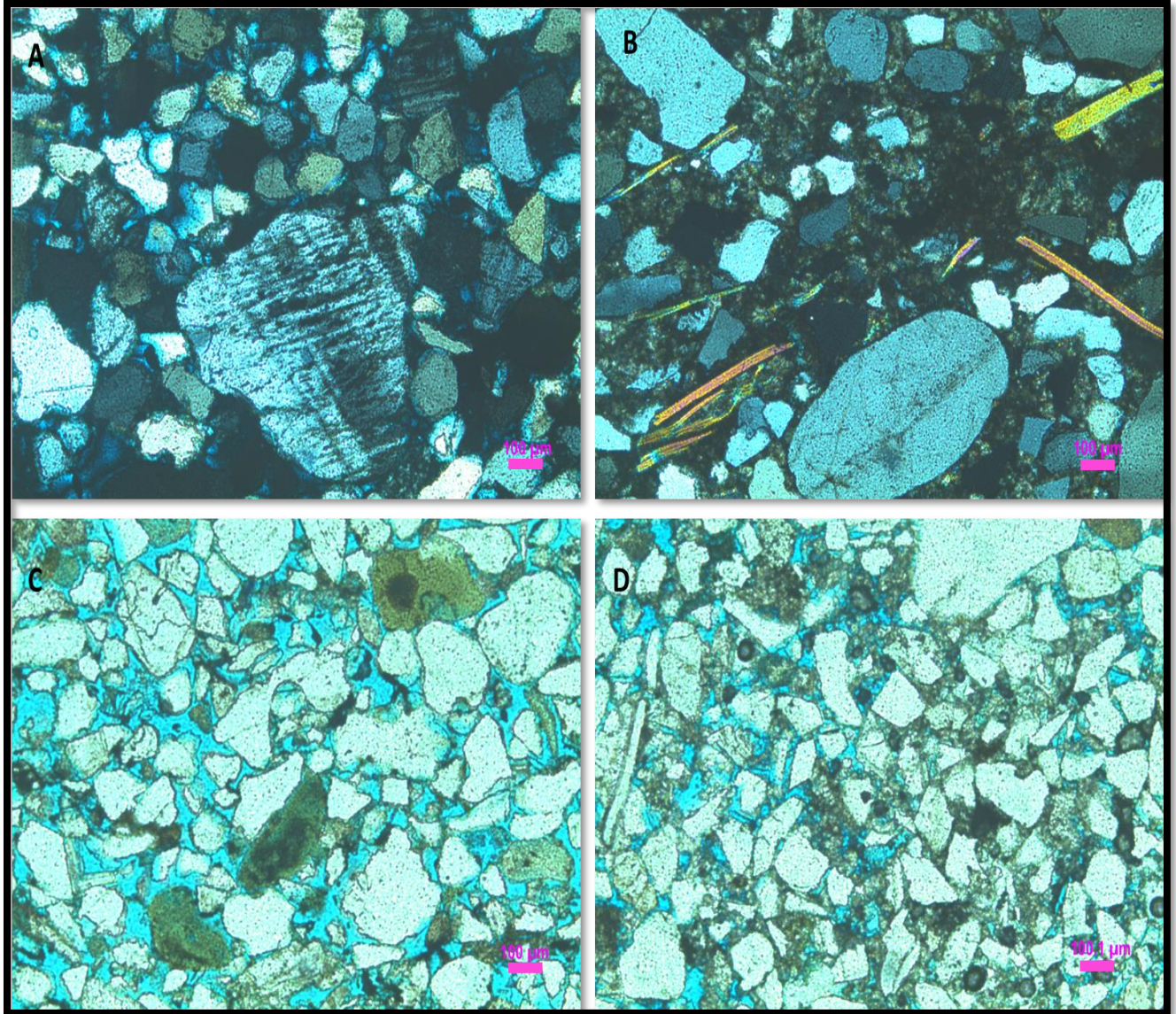


Figure 5.18: Images taken with optical microscope at magnification of 5X from sample depth (A) 2976.45 m showing twinned K-feldspar crystals in cross polarized light. (B) 2983.57 m showing straight micas with dusty yellow color in cross polarized light. (C) 3112.94 m showing glauconite minerals in green color. (D) 3038.69 m showing opaque minerals like pyrite in small rounded black grains and non-rounded black grains are identified as detrital clay minerals. Note the abundant quartz grains in all samples. Blue epoxy between the grains showing porosity, seen in plane polarized light and black in crossed polarized light. The pink scale bar in the lower right corner equals to 100 μm .

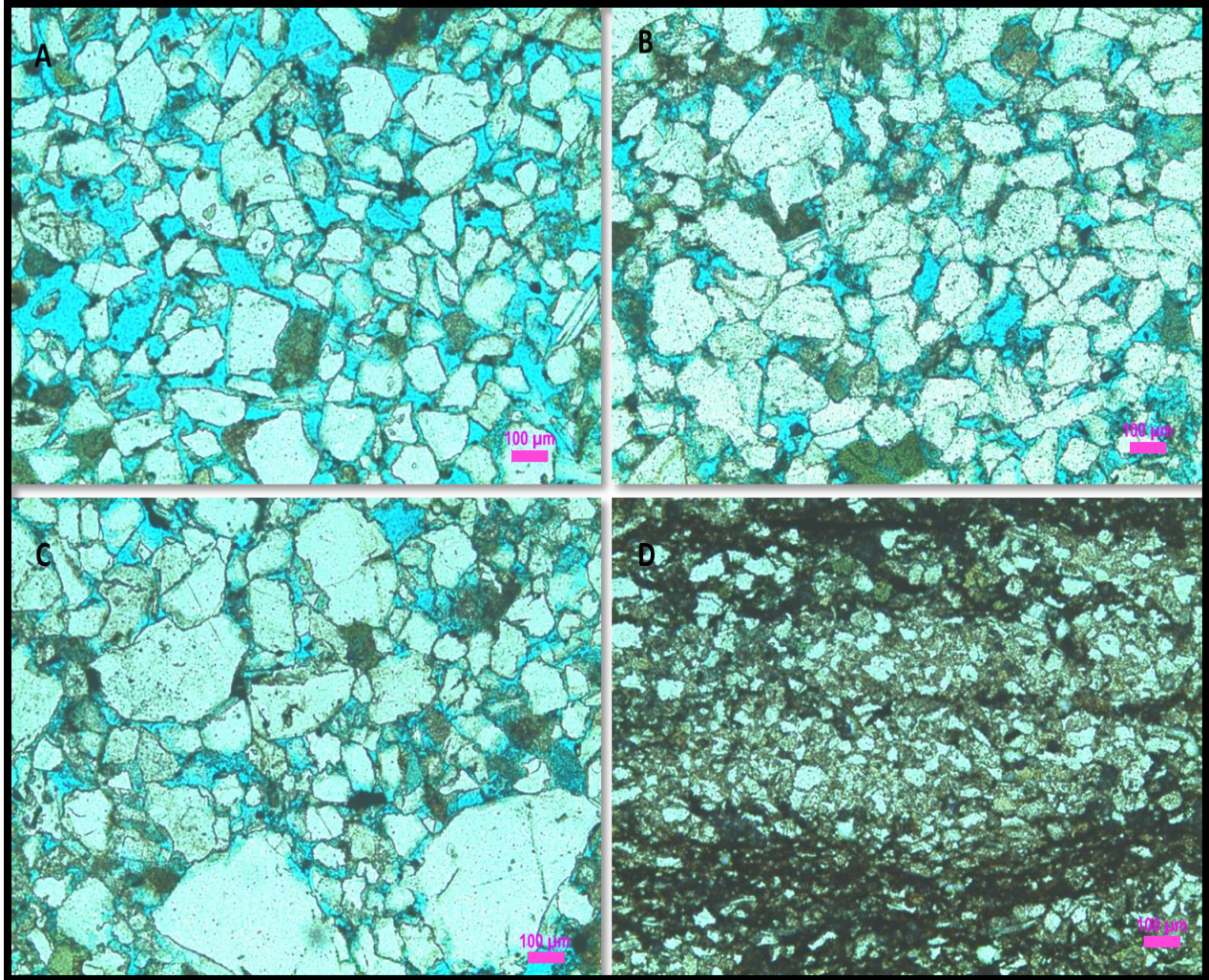


Figure 5.19: Images taken with optical microscope at magnification of 5X (plane polarized light) from sample depth (A) 3145.40 m and (B) 4134.45 m showing medium- to fine-grained sandstone. (C) 4118.70 m showing coarse to fine-grained sandstone. (D) 4119.60 m showing very fine-grained sandstone. Blue epoxy between the grains showing porosity, seen in plane polarized light. The pink scale bar in the lower right corner equals to 100 μm .

Porosity

The primary porosity range is from 0.3% to 35.8% (24.41% average) and controlling factors are compaction and cementation. Most of the samples contain well-connected intergranular pores and the intergranular contacts between the framework grains range from point to straight. Secondary

porosity occurs too as moldic and oversized pores, ranging from trace to 7.1% in modal abundance which are interpreted to result from the partial to total dissolution of framework grains (primarily feldspars). Secondary intragranular porosity occurs within glauconite that contains abundant internal microcracks generated during shrinkage (**Figure 5.20**).

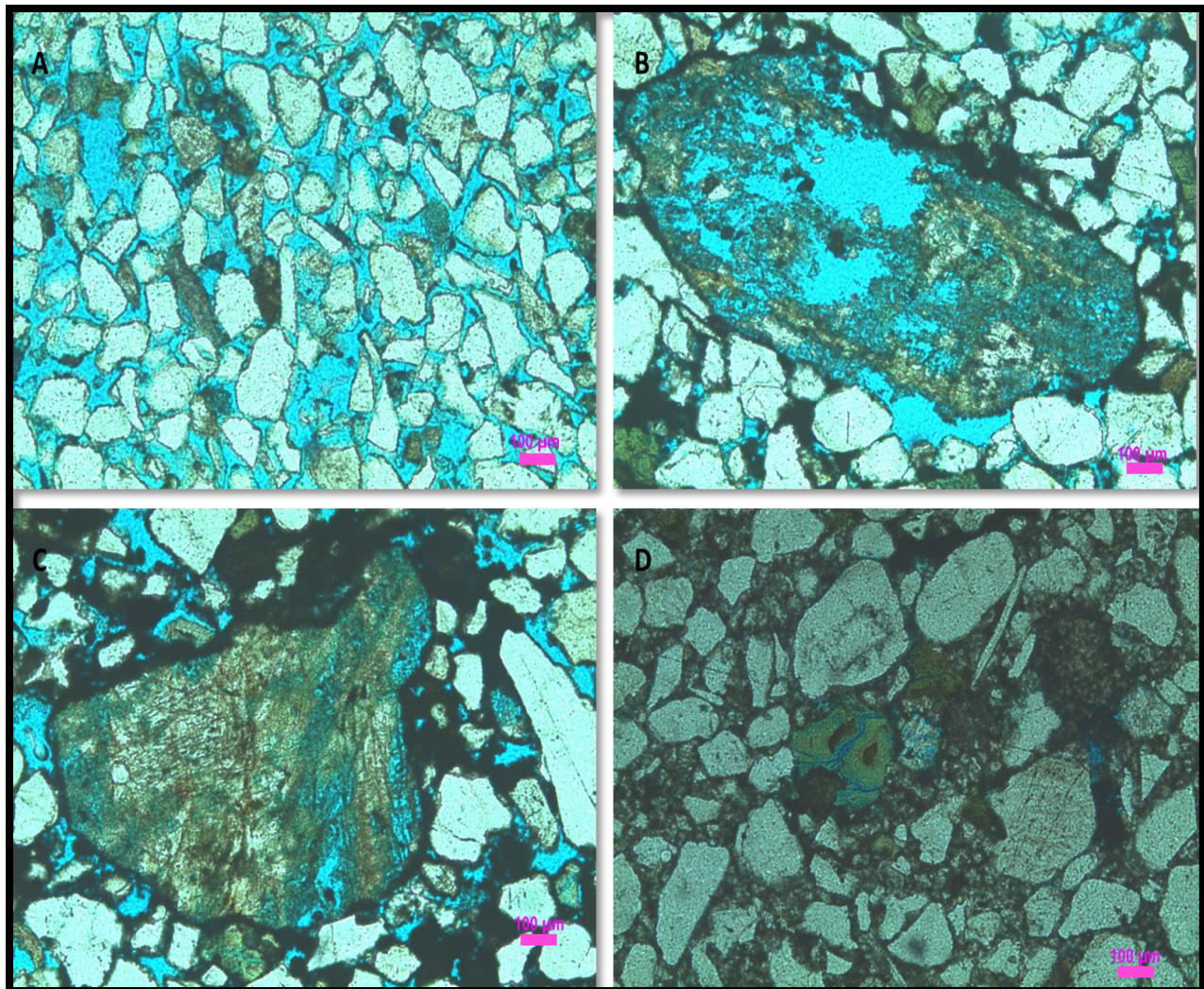


Figure 5.20: Images taken with optical microscope at magnification of 5X (plane polarized light) from sample depth (A) 3107.63 m showing well connected intergranular pores with point to straight grain contact. (B) and (C) 4128.30 m showing secondary porosity due to dissolution of feldspar grains. (D) 2983.57 m showing secondary porosity in glauconite due to micro-cracks

generated during shrinkage. Blue epoxy between the grains showing porosity, seen in plane polarized light. The pink scale bar in the lower right corner equals to 100 μm .

Diagenetic minerals

Quartz cement.

One of the most common diagenetic minerals in the Nise sandstones is quartz cement. Quartz cement occurs as syntaxial overgrowths on detrital quartz grains. Occasionally, sub-rounded quartz grains show remnants of inherited quartz overgrowths indicating recycling of quartz sandstones in the source area. Some few samples have extensive quartz over growth developed with clear dust lines (Figure 5.21).

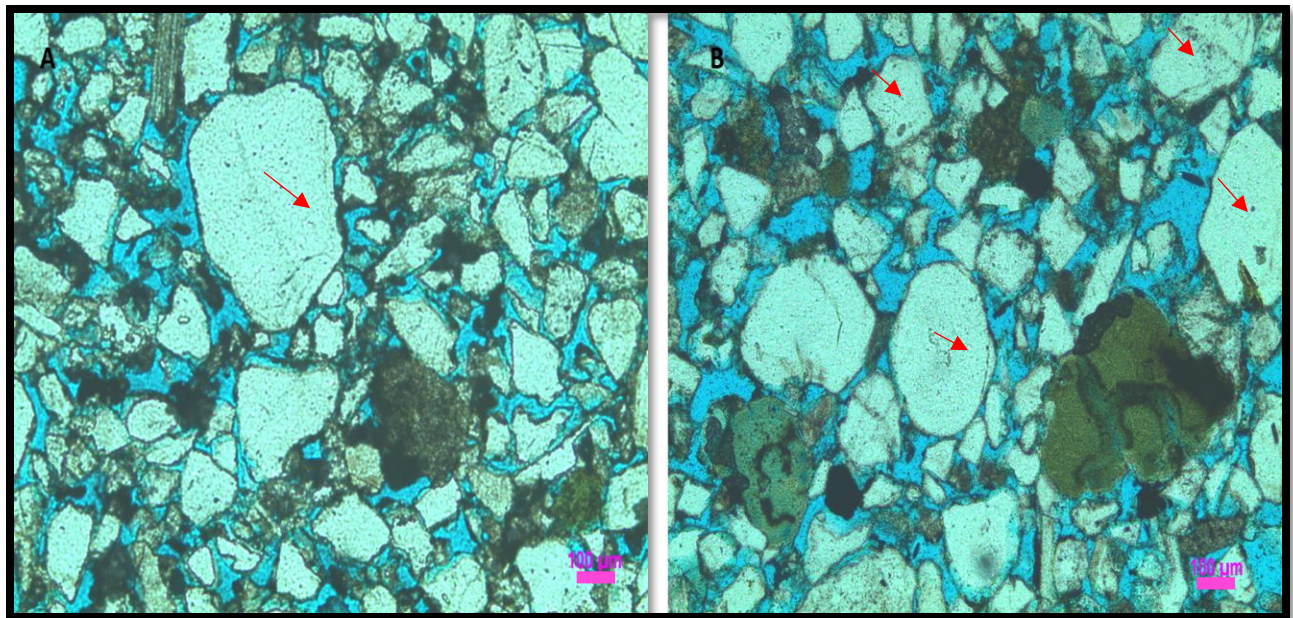


Figure 5.21: Images taken with optical microscope at magnification of 5X (plane polarized light) from sample depth (A) 3033.58 m and (B) 3112.94 m showing quartz over growth developed with clear dust lines indicated by red arrows. Blue epoxy between the grains showing porosity, seen in plane polarized light. The pink scale bar in the lower right corner equals to 100 μm .

Carbonate cement

Carbonate cement in the Nise sandstones range from 0.3% to 36.8 % (average 10.23%). It was confirmed from SEM studies (**Chapter 6:**), Fe-dolomite and ankerite cement are the most abundant diagenetic carbonate cement in Nise Formation, occurring as pore filling cement (**Figure 5.22**) and also observed as grain-replacive cement, replacing the detrital grains example feldspars in **Figure 5.23**.

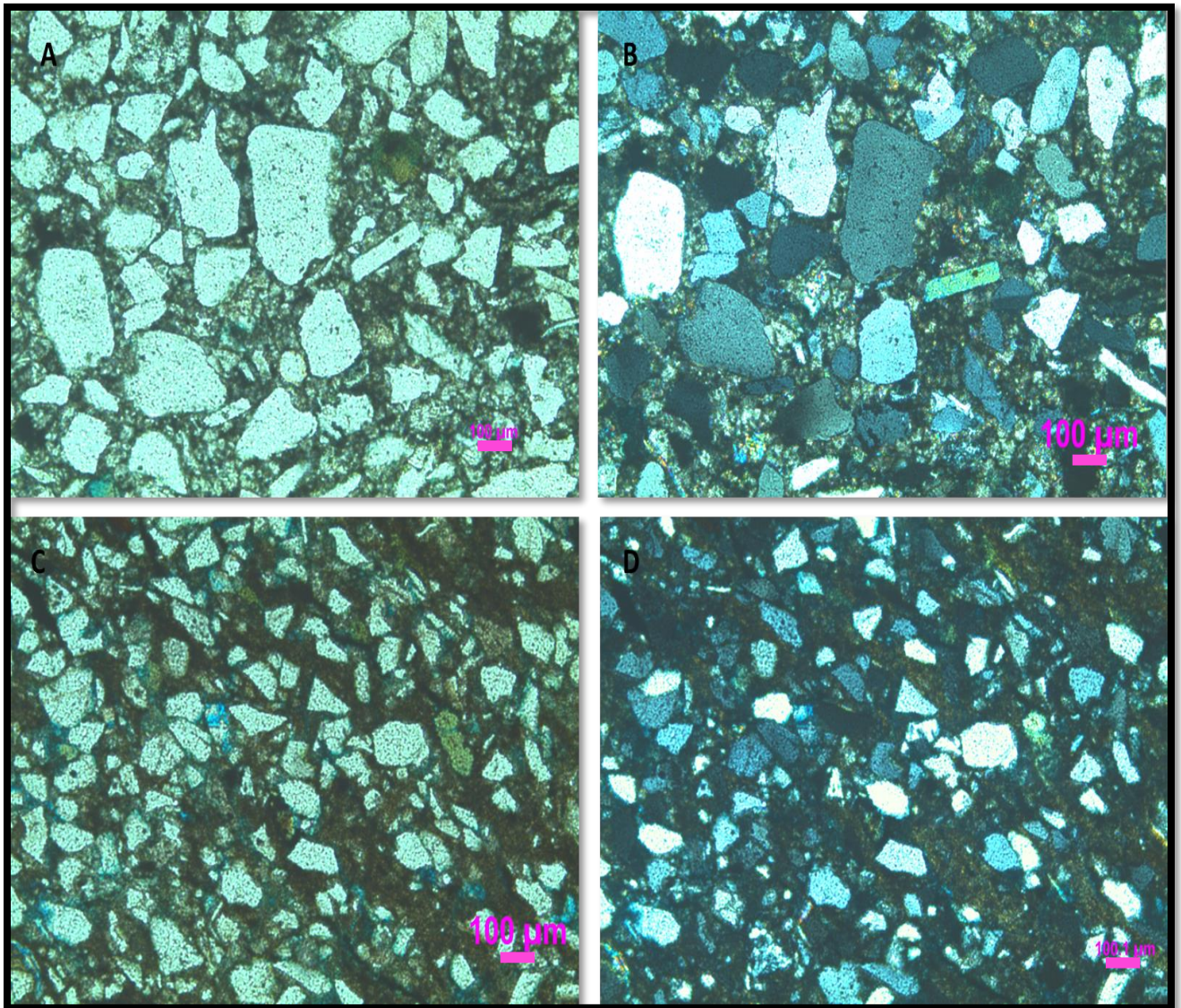


Figure 5.22: Optical photomicrograph showing carbonate pore filling cement at sample depth (A) and (B) 2983.57 m in plane and cross polarized light. (C) and (D) 3003.42 m in plane and

crossed polarized light, dark carbonate cement indicates presence of Iron which was later confirmed in SEM to be ankerite and Fe-bearing dolomite. The pink scale bar in the lower right corner equals to 100 μm .

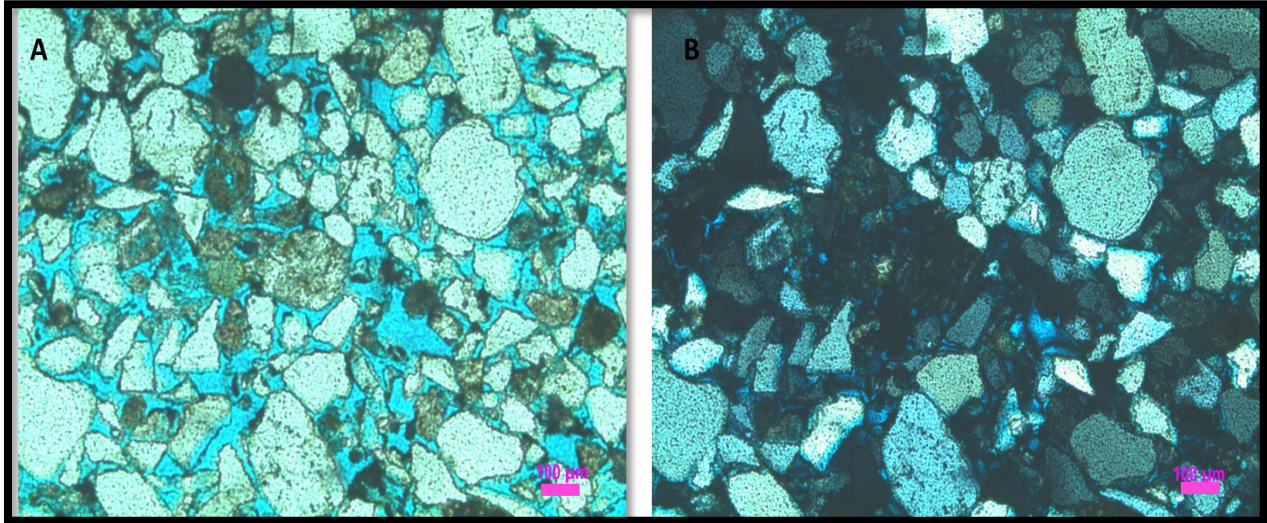


Figure 5.23: Images taken from sample depth 3112.94 m with optical microscope at magnification of 5X (A) and (B) in plane and crossed polarized light, showing dissolution of feldspar grains and then replaced by carbonate cement. The pink scale bar in the lower right corner equals to 100 μm .

Chapter 6: Scanning Electron Microscopy

6.1 Introduction.

Scanning Electron Microscopy technique is employed to investigate the mineralogy of the samples into more detail with emphasis on mineral content, porosity, cementation, authigenic clays and grain coatings. In this study, 7 selected thin sections from well 6707/10-1 were carbon coated and analyzed under Scanning Electron Microscope. This investigation is performed to cross check the results which are being obtained in the optical microscopy. Minerals have been identified with the help of Backscatter Electron Image (BEI) and Energy Dispersive Spectrometer (EDS). The following observations are made on the basis of this investigation.

6.2 Results

6.2.1 Quartz overgrowth and porosity

Quartz cementation was one of the parameters counted during point counting. To get a visual estimation, samples have been analyzed in SEM to confirm the results of optical microscope.

In this sample the grains are large and mechanically compacted rather than chemically cemented. **Figure 6.1** shows a picture of sandstone that may appear cemented, but they have none or little quartz overgrowth. This may indicate that the quartz grains have been compacted together rather than cemented by quartz overgrowth. Therefore the porosity loss is mainly by compaction than quartz cementation. Several of the samples show a large amount of open pore-space which in BEI is shown in black color.

Figure 6.2 shows the EDS analysis of quartz grains.

6.2.2 Grain coating

An attempt was made to examine various coatings present in the samples that could be a reason for limited amount of quartz cement and preserved porosity. None of the examined samples showed grain coating. It should be noted that it is very difficult to get an accurate estimation of the quantity of coating using this method.

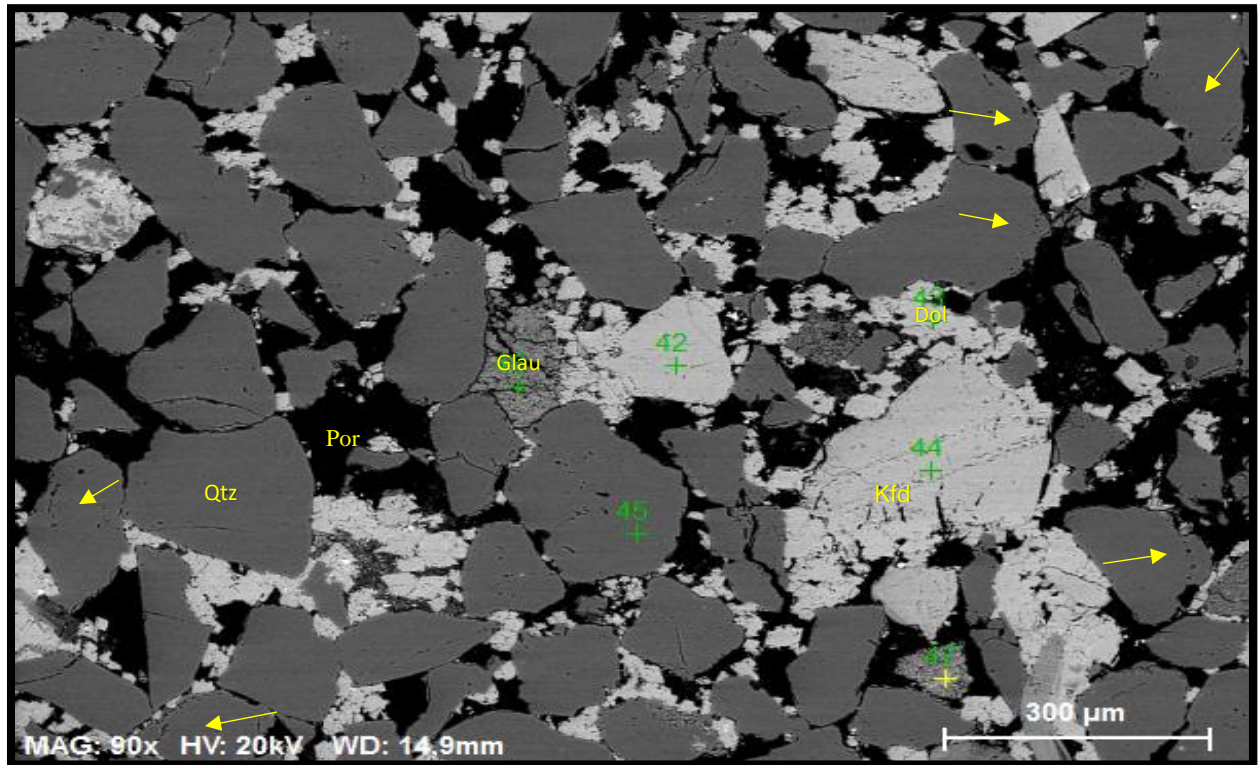


Figure 6.1: A backscattered electron image showing an overview of porosity and grains in a sample depth 3038.69 m. Note the yellow arrows show quartz cement identified by dust rim around the quartz grain. Por = Porosity, Qtz = Quartz, Glau = Glauconite, Kfd = K-feldspar and Dol = Dolomite.

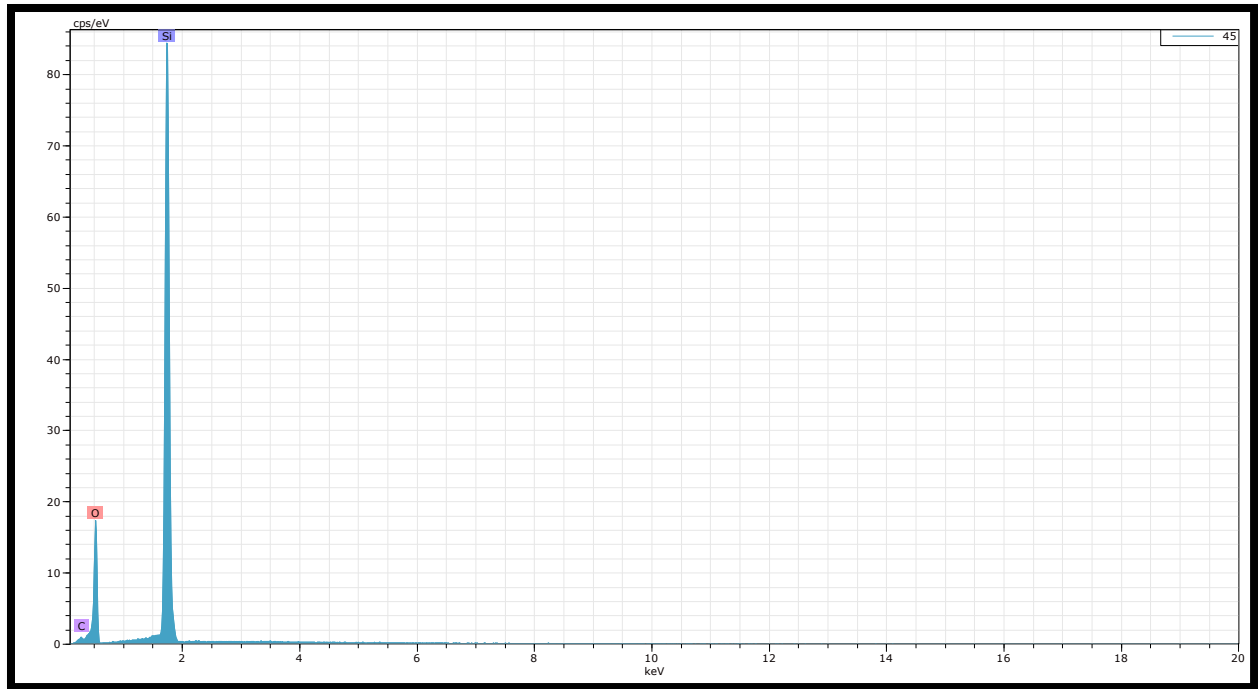


Figure 6.2: EDS image showing spectrum for quartz mineral (SiO_2) from sample depth 3038.69 m.

6.2.3 Carbonate cement

Point count results show considerable amount of carbonate cement in some of the samples. The samples from depth 2983.57 m and 4119.60 m show 36.8% and 20.7 % carbonate cement when analyses with optical microscope. Same samples, when scanned, BEI confirm the high percentage of carbonate cement.

The SEM studies prove that dolomite and ankerite cement are the most abundant diagenetic carbonate cement in Nise Formation. Dolomite and ankerite cement have poikilotopic texture forming scattered patches and occur as pore filling cement. In BEI ankerite is observed to be very bright as compared to dolomite since is heavier than dolomite (Figure 6.3). Also, the EDS analysis in Figure 6.4 indicates presence of ankerite and Fe-bearing dolomite cement (Ferroan-dolomite), they differ in Mg/Fe ratio.

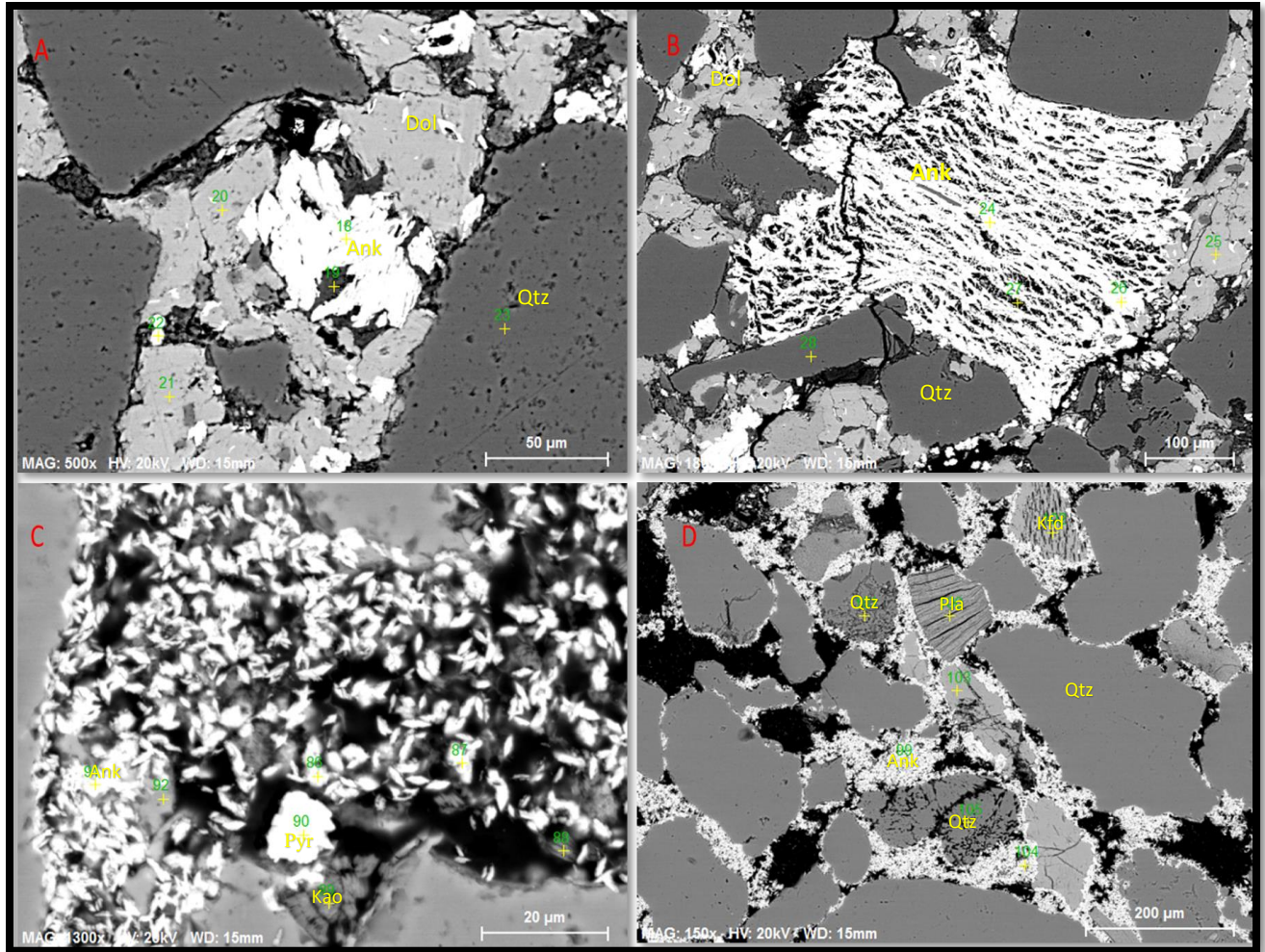


Figure 6.3: Backscattered electron image from sample depth 2983.57 m (A) and (B) showing poikilotopic dolomite and ankerite cements. (C) 4119.60 m showing pore filling ankerite cement. (D) 4128.30 m an overview of carbonate (ankerite) cement between other grains as a pore filling cement. Dol =Dolomite, Ank =Ankerite, Pla = Plagioclase feldspar, Kfd = K-feldspar, Kao = Kaolinite, Pyr = Pyrite and Qtz = Quartz.

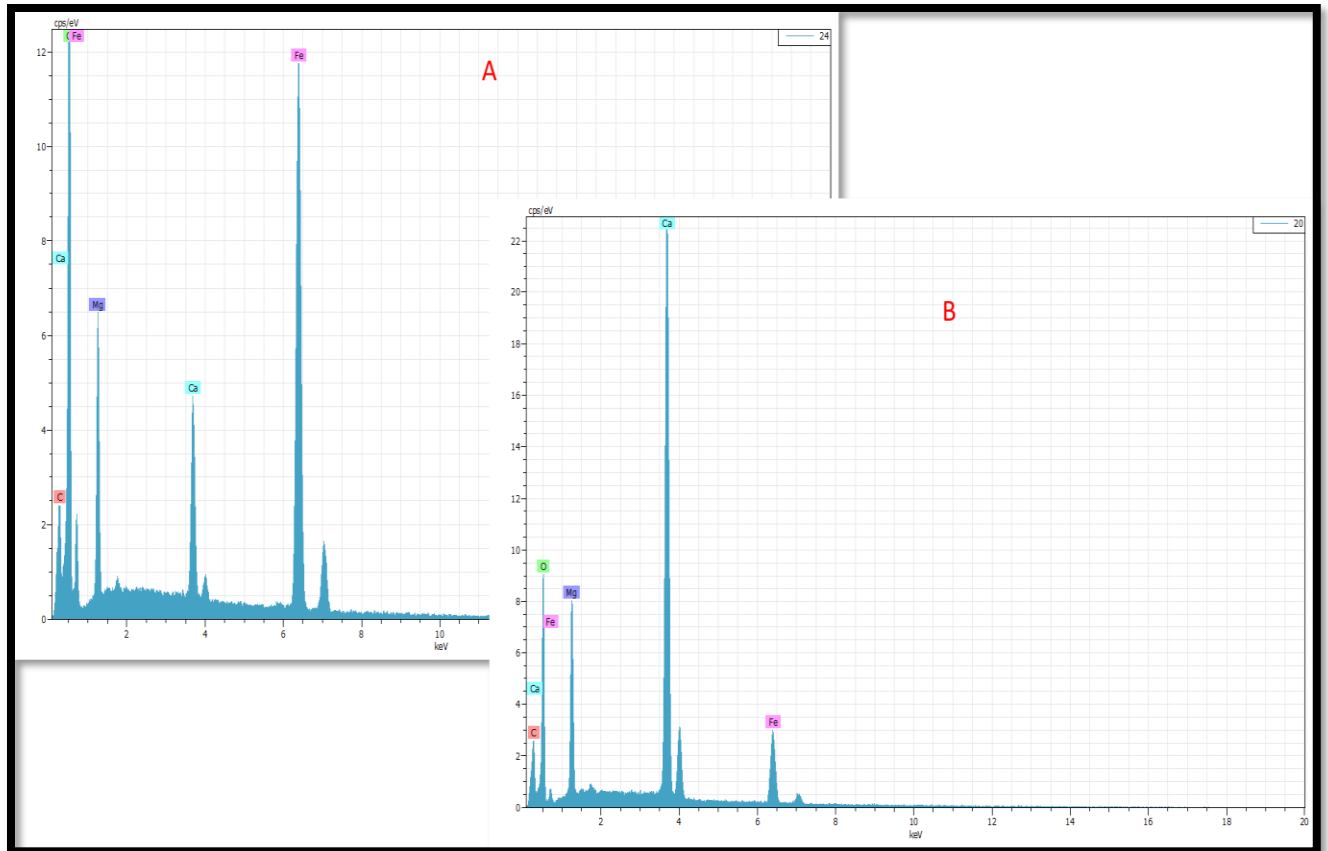


Figure 6.4: EDS image from sample depth 2983.57 m showing spectrum for (A) ankerite $[Ca(Fe,Mg,Mn)(CO_3)_2]$. (B) Dolomite Fe-bearing $[Ca(Mg,Fe)(CO_3)_2]$ referred as Ferroan - dolomite.

6.2.4 Authigenic clays

Point counting results shows the significant amount of authigenic clays found in most of the samples and it is interesting to make a similar estimation in the scanning electron microscopy. SEM results confirmed that the main content of the authigenic clay in studied sample is only kaolinite. It occurs as pore filling and also the authigenic clay has been observed replacing grains of muscovite or feldspars (Figure 6.5). The EDS analysis has confirmed the presence of kaolinite in the samples (Figure 6.6).

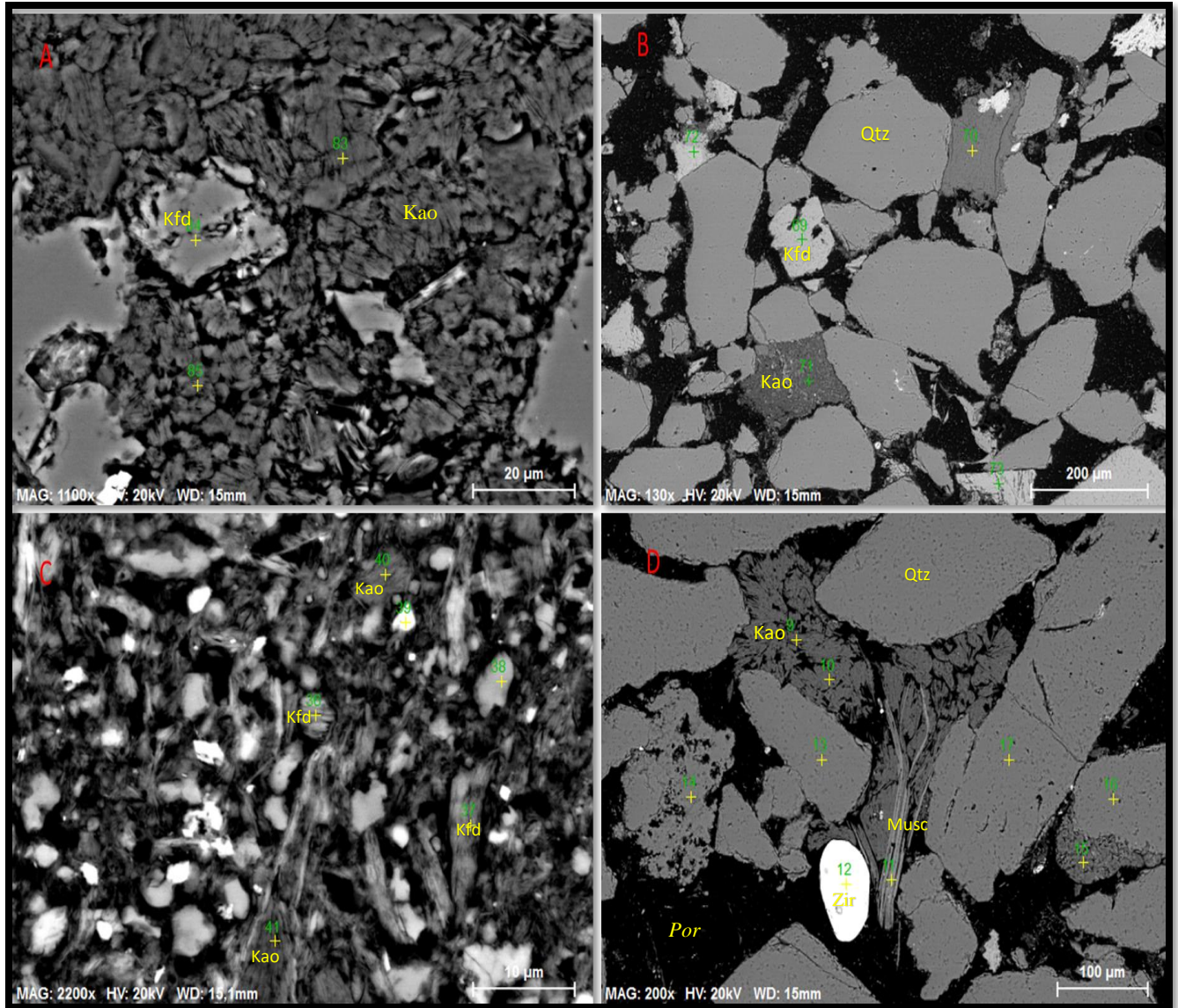


Figure 6.5: Backscattered electron image from sample depth (A) 4119.60 m showing kaolinite minerals from dissolution of feldspars. (B) 3112.94 m showing an overview of authigenic kaolinite with other grains (C) 3003.42 m showing the pore filled with kaolinite with some remnant of K-feldspars(D) 2976.45 m showing pore filling authigenic kaolinite which is probably from dissolution of Muscovite. Kao =Kaolinite, Kfd =K-feldspar, Musc =Muscovite, Qtz =Quartz, Zir =Zircon and Por =Porosity.

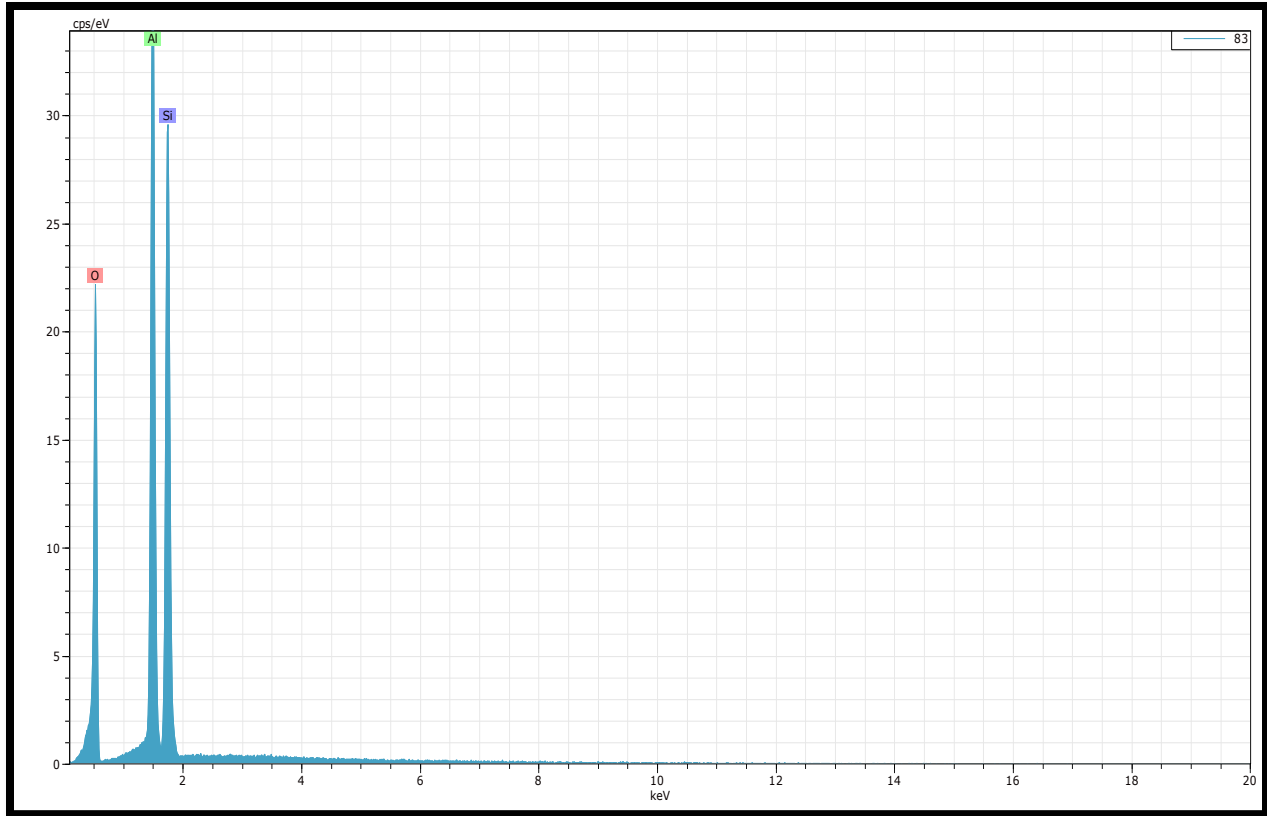


Figure 6.6: EDS image from sample depth 4119.60 m showing the spectrum for kaolinite ($Al_2Si_2O_5$)

6.2.5 Feldspar dissolution

Large dissolved feldspar grains are observed in thin section analysis forming secondary porosity. It is interesting to compare the amount of feldspar, especially K-feldspar, in connection with the amount of authigenic clay minerals. SEM results shows that most of the feldspar found in samples are K-feldspar. Some albite could be detected in the sample, but the abundance of this mineral is difficult to quantify as the albite has the nearly the exact same weight as the quartz grains, and thereby the same shade of grey in backscattered electron images. Albitization and dissolution of K-feldspar can be observed in [Figure 6.7](#). The EDS analysis of K-feldspar and albite is in [Figure 6.8](#).

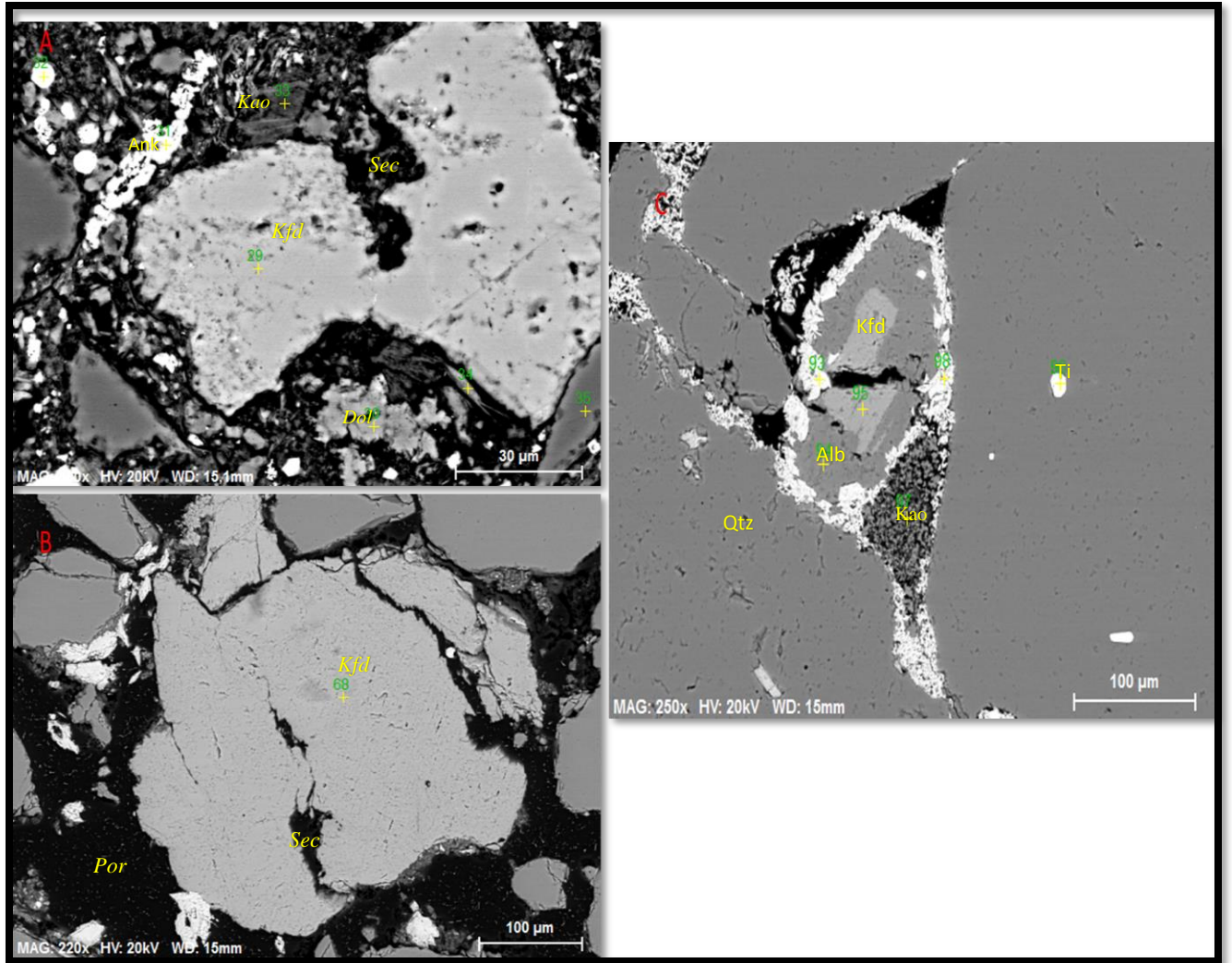


Figure 6.7: Backscattered electron image from sample depth (A) 3003.42 m showing dissolved K-feldspar grain in associated with authigenic kaolinite. (B) 3112.94 showing fractured K-feldspar grain creating secondary porosity (C) 4119.60 m showing formation of albite from K-feldspar, note the similar gray shade in quartz and albite grains. Alb = Albite, Ti = Titanium-oxide, Kfd =K-feldspar, Kao = Kaolinite, Qtz =Quartz, Dol = Dolomite, Ank = Ankerite, Por =Primary porosity and Sec = Secondary porosity.

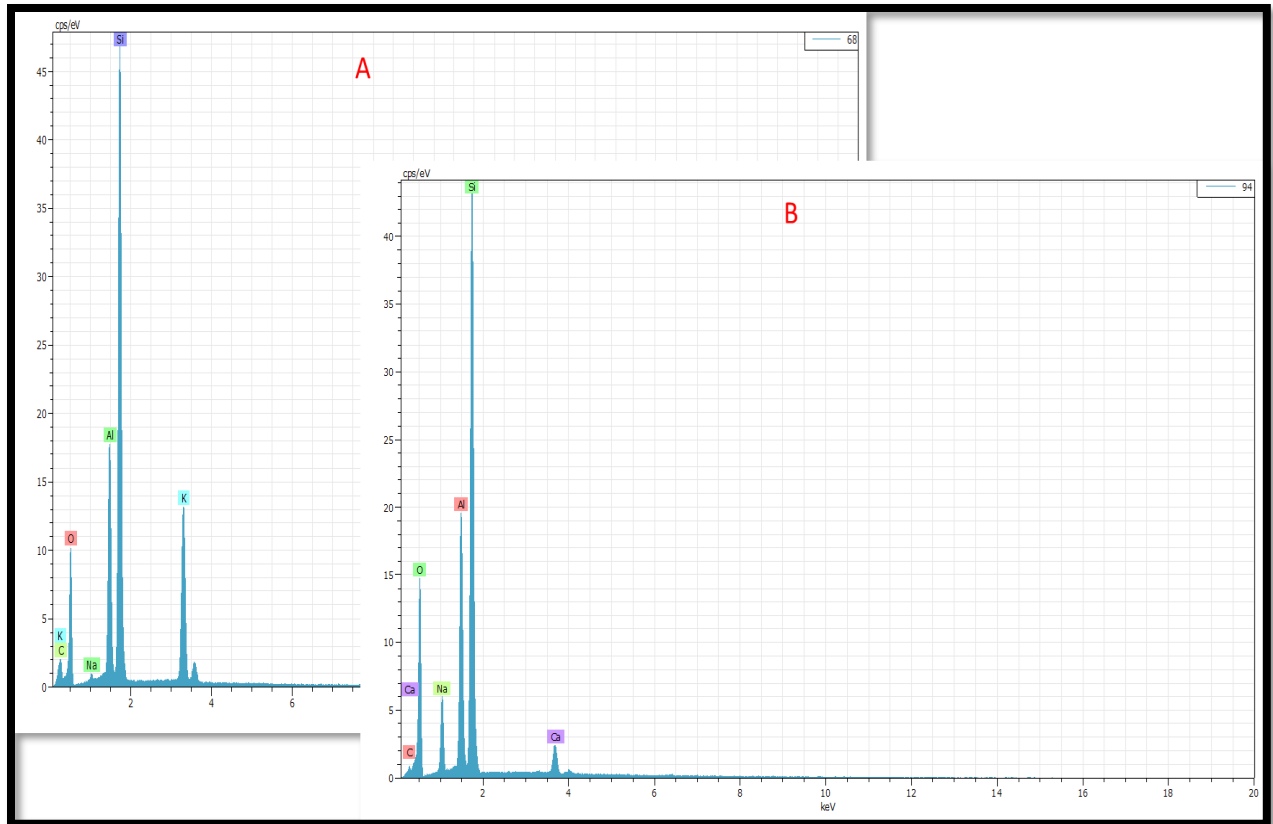


Figure 6.8: EDS image from sample depth (A) 3112.94 m showing spectrum for K-feldspar ($KAl_2Si_3O_8$) and (B) 4119.60 m for albite ($NaAlSi_3O_8$).

6.2.6 Opaque minerals

An abundance of opaque minerals has been observed in the thin sections as small black round crystals within pore filling and mostly could be referred as pyrite. SEM analysis was carried to identify different opaque minerals. They are observed as small bright spots in the backscatter electron images (Figure 6.9). The EDS analysis in Figure 6.10 reveals that the samples contains several grains of pyrite with some occurrences of zircon and titanium-oxide probably rutile.

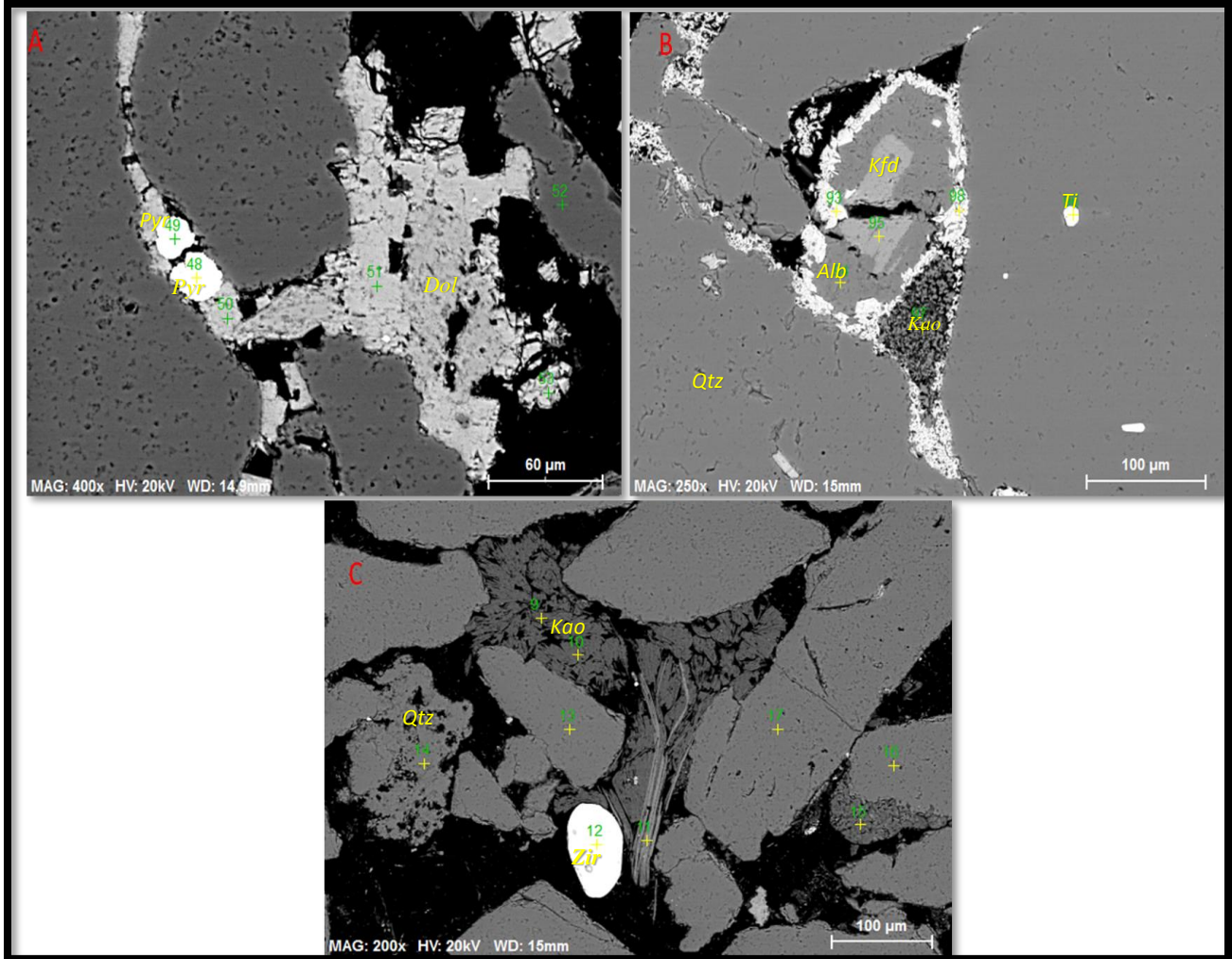


Figure 6.9: Backscattered electron image from sample depth (A) 3038.69 m showing pyrite minerals (B) 4119.60 m Titanium mineral (C) 2976.45 m showing Zircon mineral. Qtz = Quartz, Kfd = K-feldspar, Kao = Kaolinite, Dol = Dolomite, Alb= Albite, Pyr = Pyrite, Zir =Zircon and Ti = Titanium-oxide.

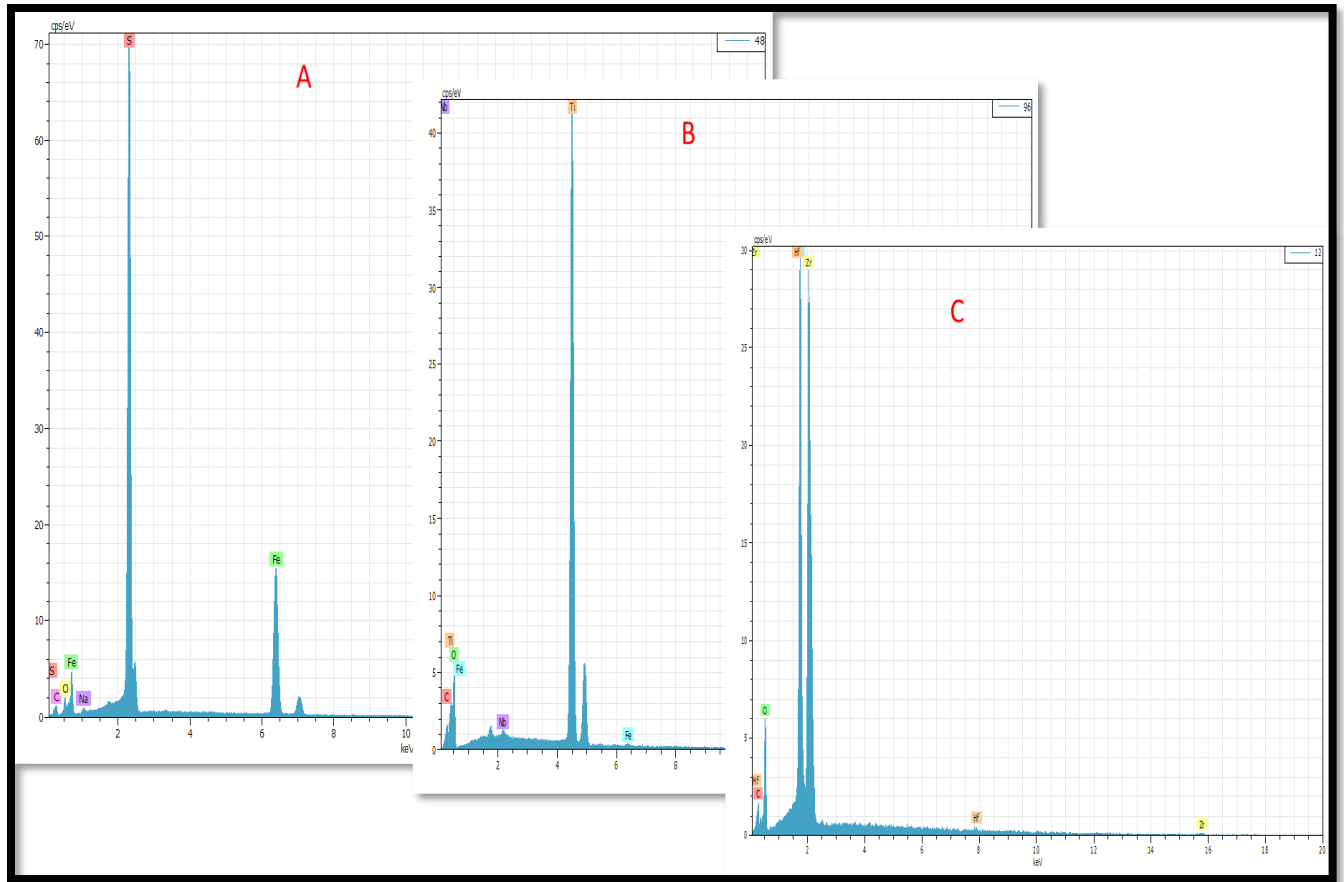


Figure 6.10: EDS image showing spectrum for (A) Pyrite (FeS_2) from sample depth 3038,69 m (B) Titanium-oxide (TiO_2) from sample depth 4119.60 m (C) Zircon (ZrSiO_4) from sample depth 2976.45 m.

6.2.7 Other minerals

Some amount of minerals other than the frequently found minerals (quartz, feldspar, carbonate and kaolinite) have been observed in the scanning electron microscope and identified by the EDS analysis. A backscatter electron image (**Figure 6.11**) and EDS image (**Figure 6.12**) show the presence of glauconite and muscovite in the Nise Formation. Presence of glauconite mineral proves that Nise Sandstone is from marine deposit (**Odin and Matter, 1981**). The muscovite grains in the samples, still hold the morphology of muscovite, but are largely replaced by kaolinite.

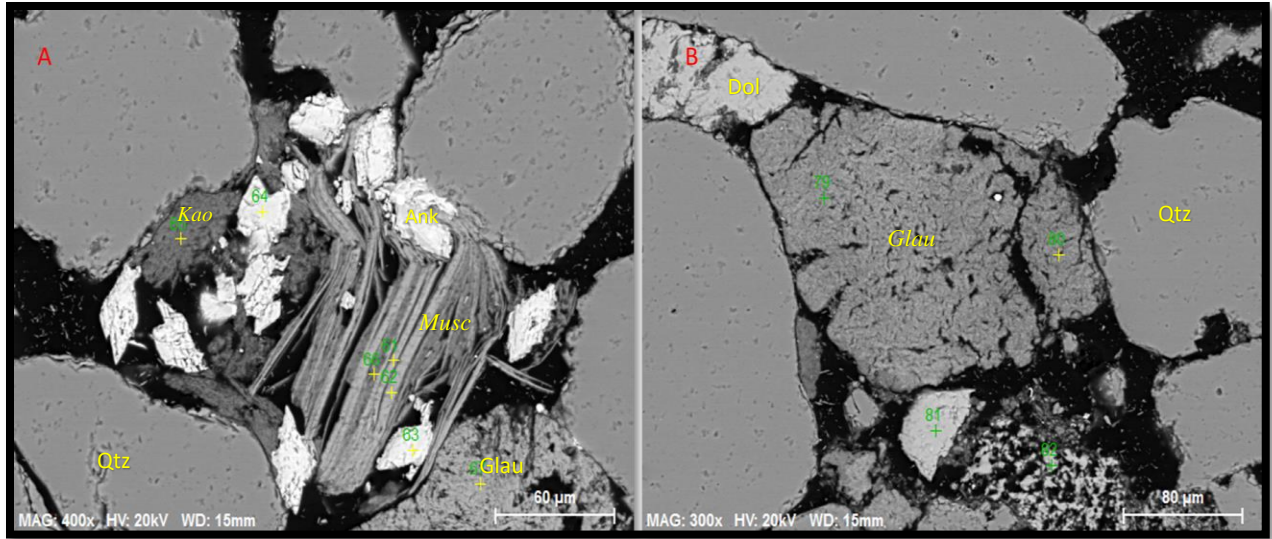


Figure 6.11: Backscattered electron image from sample depth 3112.94 m (A) showing altered muscovite associating with kaolinite minerals and ankerite cement (B) showing cracked glauconite mineral between the quartz grains. Glau = Glauconite, Musc = Muscovite, Qtz = Quartz, Ank = Ankerite, Dol = Dolomite and Kao = Kaolinite.

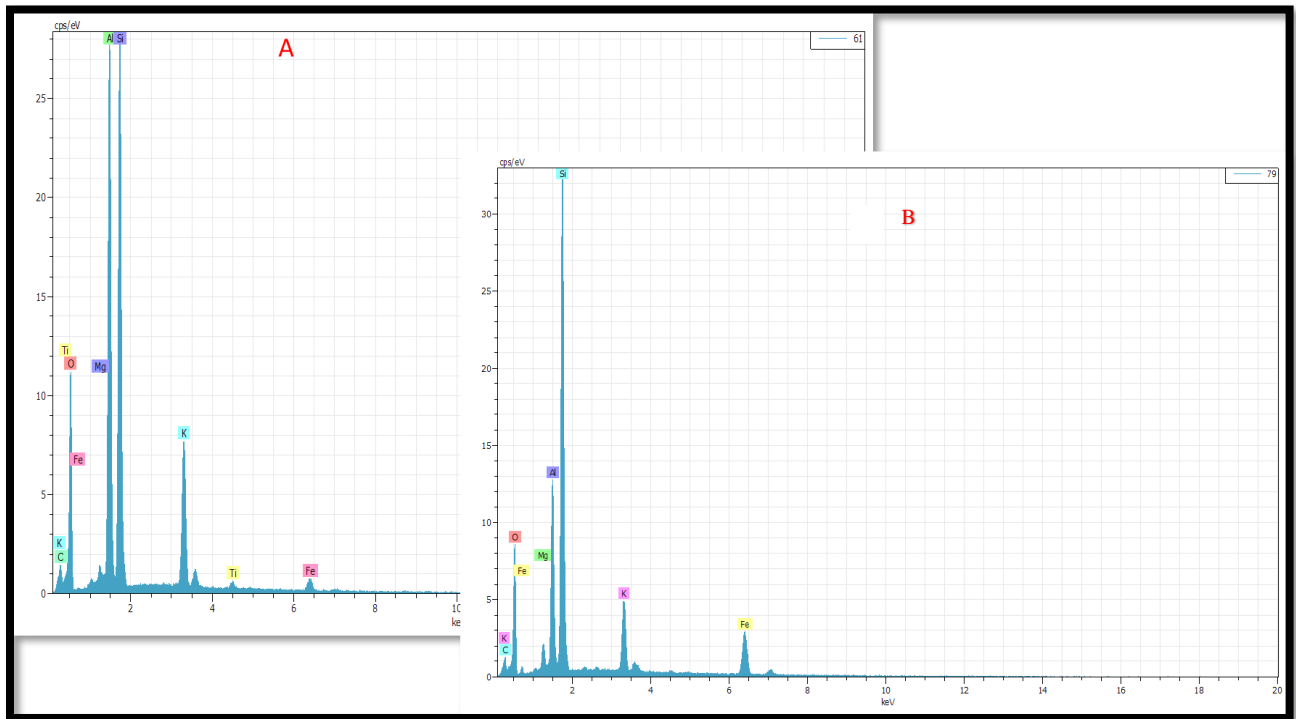


Figure 6.12: EDS image from sample depth 3112.94 m showing spectrum for (A) Muscovite $[KAl_2(Si_3Al)O_{10}(OH,F)_2]$ and (B) Glauconite $[K(Fe^{3+}, Al, Fe^{2+}, Mg)_2(SiAl)_4O_{10}(OH)_2]$.

Chapter 7: Discussion

7.1 Introduction

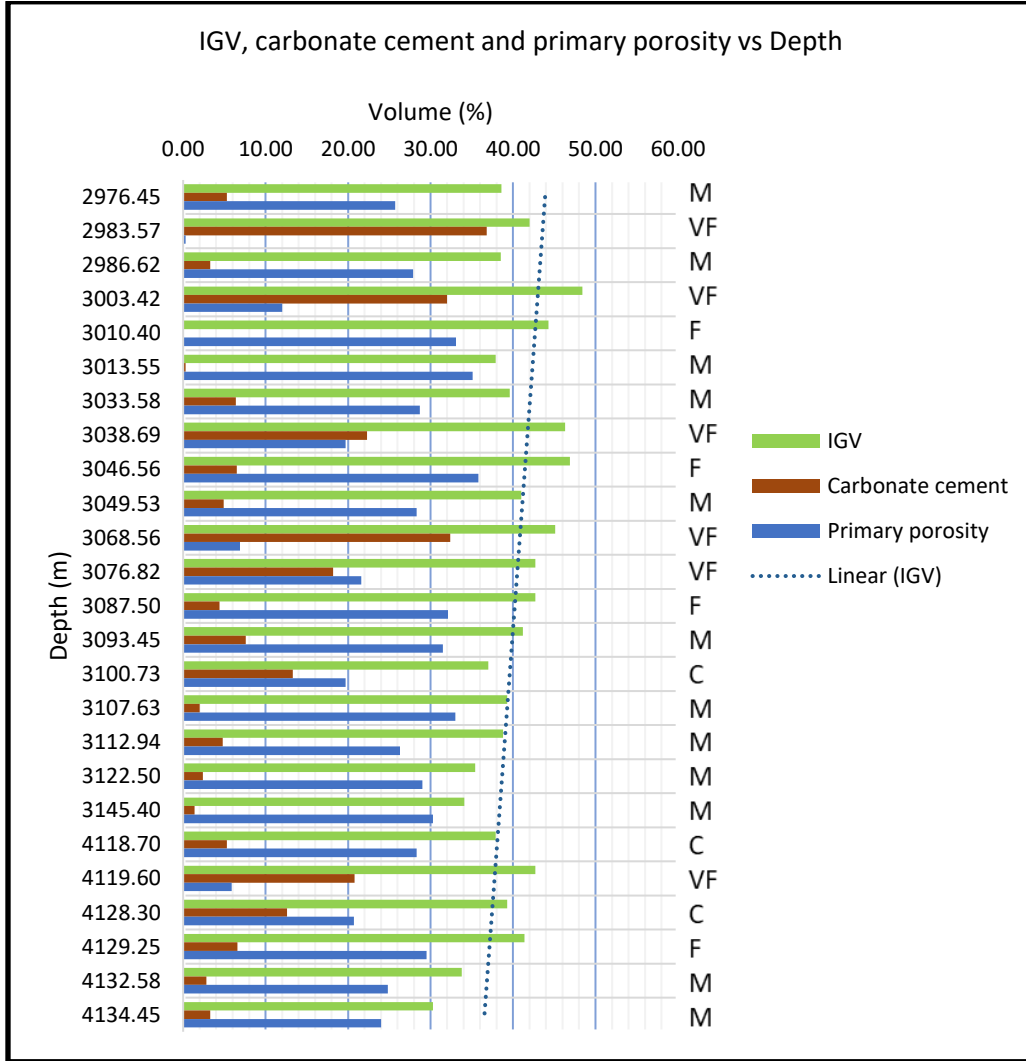


Figure 7.1: An overview of calculated IGV, carbonate cement and primary porosity in relation to the depths with respective grain size. Generally, IGV decrease with depth.

From the analysis of results generated in the previous chapters, several factors are found which affect the reservoir quality of sandstones starting from deposition to the burial during diagenesis of the sandstone. After studying the samples it seems possible to group the studied interval (2976.45– 4134.45 m) into different groups according to their grain size. Four groups (Very fine (VF), Fine (F), Medium (M) and Coarse (C)) have been identified from the petrographic study. F, M and C are high porosity samples while VF are very low porosity samples. With help of SEM, low porosity samples (VF) were confirmed to contain high amount of carbonate cement ([Figure 7.1](#)).

7.2 Mechanical compaction

7.2.1 Intergranular volume

The intragranular volume (IGV) is calculated from the point count data and is defined as the sum of intragranular porosity, cement and detrital matrix, and equals the maximum intragranular pore space before chemical cementation.

The IGV values calculated for this study by point counting ranges between 30.3% to 48.4%, showing that some of the samples have undergone more mechanical compaction (with low IGV) as compared to the samples having high IGV (40 - 48%). By analyzing the point count table ([Table 5.1](#)) and [Figure 7.1](#), a relation between carbonate cement and intergranular volume (IGV) can be made. It has been observed that samples with significant amount of carbonate cement (18.2 - 36.8%) have preserved the IGV (42 – 48.4%). Maximum preserved IGV (48.4%) has been measured from sample at 3003.42 m, containing 32% carbonate cement. It seems that this early carbonate cement reduces the effect of mechanical compaction by stiffening the grain frame work. Although a high percentage of carbonate cement destroys the intergranular porosity in samples where carbonate cementation was less than 18.2 %, the intergranular porosity was preserved and resulted to higher IGV.

The above results agree with earlier studies of mechanical compaction which states that mechanical compaction determines the intergranular volume (IGV) before the chemical compaction starts ([Paxton et al. 2002](#)). In the absence of carbonate cement, well sorted sediments are significantly affected by mechanical compaction during the first (0 - 2 km) of its burial. Quartz cementation starts at 2 - 3 km depth (80 - 100°C) in sedimentary basins with normal geothermal gradient. This quartz cementation stabilizes the grain framework and stops the further mechanical compaction ([Bjørlykke and Jahren 2010](#)).

In the petrographic classification ([Figure 5.4](#)) the majority of the samples were classified as subarkose (contain more than 5% feldspars). Possibly suggesting that high feldspar content increases the mechanical compaction, resulted in comparatively lower IGV values in some of the samples. It has already been discussed that the amount of feldspars is underestimated in point counting results because of the untwinned albite content. It is difficult to differentiate the untwinned albite and quartz grains during rapid point counting in an optical microscope. So high feldspar content probably increases the mechanical compaction, resulted in comparatively lower IGV values in some of the samples.

It has been observed that sandstones with a large proportion of secondary porosity from dissolved grains, will have a slightly steeper porosity depth curve due to the increased stress at grain contact ([Ramm, 1992](#)). The amount of secondary porosity in the samples was plotted against the IGV values, but no such correlation could be seen ([Figure 5.15](#)), suggesting that the amount of secondary porosity has not had a significant effect on the IGV of the sandstones.

The IGV-values were plotted against the corresponding amounts of detrital matrix in order to investigate the relationship between the two parameters. The cross plot showed no trend between the matrix content and the IGV ([Figure 5.14](#)). Clay matrix at grain contacts are preferred areas of quartz grain dissolution and precipitation of quartz cement on adjacent clay free-grain ([Bjørlykke, 2010](#)), increased content of matrix could therefore potentially lead to lower IGV and higher amounts of authigenic quartz cement. Neither the cross plot of the IGV and detrital clay matrix nor quartz cement, displayed a trend to support this ([Figure 5.14](#) and [Figure 5.16](#)).

7.2.2 Textural characteristics

Variations in the IGV values may also be due to differences in the texture of the sandstones, such as sorting, grain size and shape.

Sorting

It has been experimentally proven that well sorted sandstones are less readily compacted than poorly sorted sandstones (Chuhan et al., 2002; Fawad et al., 2011). The calculated IGV values from the studied samples increase with better sorting (Figure 5.11). This is believed to be caused by the rearranging of the grains during mechanical compaction, where smaller grains may fill the pore-space between the larger grains in the poorly sorted sands (Fawad et al., 2011). It should be noted that the samples examined in this study mostly range from moderate to well-sorted. This may have influenced the resulting trend, possibly an important factor in preserving the IGV value where none of the samples show less than 30% IGV.

Grain size

The calculated IGV values were the highest in the fine-grained sandstone samples (Figure 7.1), indicating that the mechanical compaction has been more significant in the coarse-grained sandstone samples. Similar connections have been reported by Chuhan et al. (2002) and Fawad et al. (2011), who represent the difference in compaction to be caused by increased pressure at grain contacts and subsequent grain-crushing due to fewer grain-contacts in the coarser samples. Some decrease IGV in fine-grained sandstones in relation to coarse-grained, may however also be expected due to the closer grain-packing associated with decrease in grain-size. The overall trend in the studied samples is decreasing IGV-values with increasing grain-size (Figure 5.12). The results show that majority of the samples are medium to fine grained, thus there is less pressure on individual contacts as compare to the coarse-grained sands.

Grain shape

Angular shaped grains are generally associated with high compaction, due to the small contact area and subsequent grain crushing (Fawad et al. 2011). The largest frequency of the samples in

this study are subangular to sub-rounded, thus grain shape is not expected to have had a large effect on the variation of IGV values in this study, and angularity did have a noticeable trend with the IGV values ([Figure 5.13](#)).

Influence on reservoir quality

In general the intra-granular space is well preserved in the studied samples, represented by high IGV values, indicating that the mechanical compaction has not been very significant. The preserved IGV may have been favored by early carbonate cement, moderate to well sorting, grain-roundness and the small grain size. Sandstone layers that differ from these characteristics occur within the formations, leading to local variation in IGV.

7.3 Chemical compaction

7.3.1 Carbonate cement

Majority of the observed carbonate cement in SEM analysis is ankerite and Fe-dolomite. Point count data ([Table 5.1](#)) shows that presence of carbonate cement varies throughout the sample interval. From point count it has been observed that there is little or no quartz cement in samples with higher carbonate cement (samples depth 2983.57, 3003.42, 3038.69, 3076.82 and 4119.60 m) suggesting that carbonate cement predate the quartz cement, as little overgrowth is present in carbonate cemented areas.

Influence on reservoir quality

This early carbonate cementation hinders the quartz overgrowth and helped to reduce the mechanical compaction. However it also destroyed the reservoir quality by filling the pores. These carbonates cemented intervals act as a barrier to fluid flow during hydrocarbon production ([Saigal and Bjørlykke, 1987](#)).

variation in authigenic kaolin amount contains the lowest amounts of kaolin both in the results from the point-count and in the SEM-analysis.

Influence on reservoir quality

Abundance of kaolin in the pore-space, as seen in many of the samples will take up pore-space and thus reduce the porosity in the sandstones. However, it is not believed that a large amount of kaolin will have a significant impact on the permeability of the reservoir, as fluids can easily flow around the authigenic morphology of kaolin. From this study, the content of kaolin observed is too small to have larger effect in the reservoir quality of Nise Formation.

7.3.3 Authigenic quartz cement

During the point count analysis, quartz is the main mineral present in the samples with quartz cement as authigenic mineral phase varies from 0.3 – 5.1%. In this study quartz cement did not appear to be abundant or well developed in any of the samples as carbonate cement.

Comparison of IGV and the content of quartz cement ([Figure 5.16](#)), showed no trend between the amount of quartz cement and calculated IGV. This indicates that after the onset of quartz cementation the continued precipitation of quartz is mainly related to a function of temperature integrated over time and grain surface area ([Walderhaug, 1994b](#)) and not to grain to grain pressure solution. If the phenomenon of grain-to-grain pressure solution occurs, it would cause the IGV to decrease with depth as the quartz cementation increases ([Oelkers et al., 1996](#); [Sheldon et al. 2003](#)).

[Figure 5.6](#) shows the quartz cement and porosity distribution according to depth. Sample with quartz cement show loss in primary porosity and some samples that do not follow this relationship. The reason for their low porosity in spite of lower quartz cement content is found to be carbonate cementation. A minor amount of quartz overgrowth has led to excellent reservoir quality with high porosity value average (24.41%). The possible scenarios for preventing quartz overgrowth are discussed below.

7.3.4 Effect of Temperature history

The quartz cementation process is controlled by the precipitation rate, and temperature is the main control on the quartz cementation because the rate of precipitation of quartz relies exponentially on temperature (Walderhaug, 1994a). Let consider the burial history temperature curves from Norwegian sea wells in Figure 7.2. The wells numbered 6704/12, 6706/11 and 6610/3 have had temperatures higher than 100°C for the last 40 million years and the wells numbered 6707/10 have only recently exceeded 100°C.

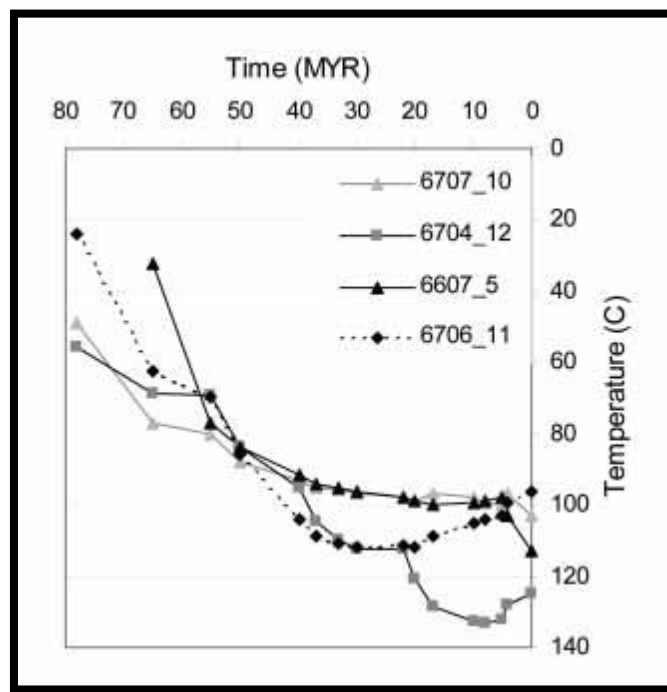


Figure 7.2: Burial history temperature curves of wells in the Norwegian Sea (Lien et al., 2006).

Lien et al. (2006) observed a trend of significantly lower porosity values for a given depth by samples from wells 6704/12-1 (Gjallar Ridge) and 6706/11-1 (Vema Dome) despite of having the same facies, lithology and stratigraphy as well 6707/10-1 (Nyk High) which have higher porosity. Therefore, the difference has to be explained by the effect of temperature history. The high porosity well has sediments with lower thermal exposure, hence contains very limited quartz overgrowths than the low porosity wells which contain high amount of quartz overgrowth due to higher thermal exposure at similar depths.

According to this observation, [Lien et al. \(2006\)](#) suggested alternative sources of high temperature in the low porosity wells in the Vøring Basin; (1) probably the sediments have been more deeply buried, exposed to higher temperatures and later uplifted, or (2) the subsurface heat flow has been higher in the wells with more quartz cement compared to the other wells. As, well 6704/12-1 is located on the Gjallar Ridge, high temperatures are related to the volcanic margin nearby and associated heat flow from deeper magmatic bodies ([Fjeldskaar et al., 2003](#)). Well 6706/11-1 is located on the Vema Dome which was a Cretaceous depocenter inverted during post-breakup compression ([Mogensen et al., 2000](#)). Consequently, the present study agrees that limited quartz overgrowth in the studied samples is due to lower thermal exposure that the sediments were not affected by the progressive and intense thermal subsidence to develop mesogenetic conditions such as extensive quartz overgrowth.

7.3.5 Grain coating

No preservation of porosity and permeability from grain coating could be recognized in the studied samples. Authors as [Ehrenberg \(1993\)](#) and [Bloch et al. \(2002\)](#) have documented occurrence of clay coatings in shallow marine sandstone on the Norwegian shelf and concluded that clay-coated grains could preserve reservoir quality during deep burial of shallow marine sediments. Still, the occurrence of clay coats in deep marine settings such as in the Vøring Basin is not well documented in the literature, and the origin of grain coats in deep-water sandstones is poorly understood.

An exception is described by [Lien et al. \(2006\)](#) who observed clay-coated grains of chlorite/smectite in the deep marine Agat sandstones, that had prevented quartz cementation and resulted in high porosity sandstones. But the clay coating was proved to be inherited clays from the shelf- and shallow-marine sediments. The Agat sandstones are sourced from re-deposited shelf- and shallow-marine Cretaceous sediments from western Norway ([Martinsen et al. 2005](#); [Fonneland et al. 2004](#)).

7.3.6 Overpressure

The fluid overpressure in the study area is expected to be high, corresponding with the great burial depths. In the samples with a limited amount of authigenic quartz cement, the great vertical stress associated with the burial depth should have caused significant grain crushing (Bjørlykke and Jahren, 2010) and a decrease in IGV corresponding to the lowest quartz cementation. However grain-fractures were rarely seen in the thin-section analysis and the IGV and quartz cement plot showed no trend (Figure 5.16). This indicates that in want of frame-enforcing quartz cement a high fluid overpressure may have reduced the effective vertical stress on the grains, preventing some of the mechanical compaction and preserve intergranular porosity.

7.3.7 Early Hydrocarbon emplacement

The effect of hydrocarbon emplacement is regarded as insignificant in this study, due to the water-wet properties of quartz rich sand as most of the sampled sandstones were classified as subarkoses. The effect of hydrocarbon emplacement is dependent on oil wet rocks, in order to retard nucleation of quartz cement , as has been previously concluded by Walderhaug (1990) and Aase and Walderhaug (2005).

Influence on the reservoir quality

In this study chemical compaction by quartz cement cannot be considered as the main porosity reducing mechanism as the content is too low to reduce quality. The observations show relatively high porosity values and excellent reservoir quality of Nise Sandstone Formation is due to the limited quartz cement and to textural and mineralogical matured sandstone.

Chapter 8: Conclusion

- ❖ In granular rocks, the Intergranular Volume (IGV) is a very good indicator of mechanical compaction. High IGV values in the studied samples (40.21% average) indicate that mechanical compaction is not very significant in Nise Sandstones.
- ❖ Higher IGVs observed in samples with higher carbonate content indicates the emplacement of early carbonate cement which in turn stiffen the grain framework before the onset of chemical compaction.
- ❖ The mechanical compaction has been the greatest in the coarse-grained samples and samples with a lack of sorting. Grain shape has not led to differences in the IGV-values, as the majority of the samples have a similar angularity and no effect on IGV.
- ❖ Sometimes higher IGV values may indicate inaccurate point count and this may be related to badly prepared thin-sections. As ripped out grains may have been mistaken for pore-space causes the higher counts in the porosity that could result in the higher IGV values.
- ❖ The Nise Sandstones are deposited in basin-floor fan (turbidites) system isolated with respect to meteoric flushing, thereby reducing the possibility for kaolin precipitation. The presence of small amounts of kaolinite in the studied sandstones suggests limited meteoric waters percolation into these deep marine turbidites.
- ❖ Reservoir quality improvement occurred due to the development of secondary porosity owing to dissolution of silicate grains, primarily feldspars, however the net gain in porosity by feldspar dissolution is insignificant due to precipitation of authigenic clay.

- ❖ Upper Cretaceous sandstones deposited in the Vøring Basin are sourced from East Greenland, the longer transport distance led to mature mineralogical composition hence prohibited substantial porosity destruction by mechanical compaction and the degree of sorting (moderate- to well-sorted) was achieved from hyper-concentrated to concentrated density flows and turbidity flows which deposited clay free sediments.

- ❖ Relatively high porosity values and the excellent reservoir quality in the studied samples is due to the limited quartz cements. Mesogenetic quartz overgrowth had little impact on the reservoir quality since the sediments in the study area experienced relatively low thermal exposure (less than 100°C) during burial resulting in limited amount of quartz overgrowth and preservation of porosity.

Chapter 9: References

Aase, N., E., Bjorkum, P.A. and Nadeau, P.H. 1996. The effect of grain-coating micro quartz on preservation of reservoir porosity. AAPG Bulletin 80, 1654-1673.

Aase, N.E. and Walderhaug, A. 2005. The effect of hydrocarbons on quartz cementation: diagenesis in the Upper Jurassic sandstones of the Miller Field, North Sea, revisited. Petroleum Geoscience 11, 215-223.

Adams, A.E., MacKenzie, W.S. and Guilford, C. 1986. Atlas of sedimentary rocks in thin section.: Ferdinand Enke Stuttgart Federal Republic of Germany. Pages: 103.

Berner, R. A. 1980. Early diagenesis: A theoretical approach, Princeton University Press.

Bishop, A.N., Kearsley, A.T. and Patience, R.L. 1992. Analysis of sedimentary organic materials by scanning electron microscopy; the application of backscattered electron imagery and light element X-ray microanalysis. Organic Geochemistry 18, 431-446.

Bjørlykke, K. 1984. Formation of secondary porosity; how important is it? AAPG Memoir 37, 277-286.

Bjørlykke, K. 1998. Clay mineral diagenesis in sedimentary basins; a key to the prediction of rock properties; examples from the North Sea Basin. Clay Minerals 33, 15-34.

Bjørlykke, K. Nedkvitne, T. Ramm, M. and Saigal, G. 1992. Diagenetic processes in the Brent Group (Middle Jurassic) reservoirs of the North Sea – An overview. In: Morton, A.C., Haszeldine, R.S., Giles, M.R. and Brown, S. (eds.), Geological Society Special Publication 61, Geology of the Brent Group, p. 263–287.

Bjørlykke, K. and Avseth, P. 2010. Petroleum geoscience: from sedimentary environments to rock physics, Heidelberg: Springer. IX, 508 s. pp.

Bjørlykke, K. and Jahren, J. 2010. Sandstones and Sandstone Reservoirs. Petroleum Geoscience: Springer Berlin Heidelberg, 113-140.

Bjørlykke, K. 2010. Well Logs: A Brief Introduction, in K. Bjørlykke, ed., Petroleum Geoscience: From Sedimentary Environments to Rock Physics, Springer Verlag, p. 361-373.

Blystad, P., Brekke, H., Faereth, R.B., Larsen, B.T., Skogseid, J., and Tørrudbakken, B., 1995. Structural elements of the Norwegian continental margin, Norwegian Petroleum Directorate, Bulletin 8.

Brekke, H., 2000. The tectonic evolution of the Norwegian Sea Continental Margin with emphasis on the Vøring and Møre Basins, in Dynamics of the Norwegian Margin, 167, 327-378, Published for the Geological Society by Blackwell, Oxford.

Brekke, H., Dahlgren, S., Nyland, B. and Magnus, C. 1999: The prospective of the Vøring and More basins on the Norwegian Sea continental margin. In Fleet, A. J. & Boldy, S. A. R. (eds.) Petroleum Geology of NW Europe: Proceedings of the 5th Conference: London, Geological Society, London, 261-274.

Brekke, H., Sjulstad, H.I., Magnus, C., Williams, R.W., 2001. Sedimentary environments offshore Norway - an overview, in Sedimentary environments offshore Norway – Palaeozoic to Recent, 10, 7-37, eds. Martinsen, O.J. and Dreyer, T., Elsevier Science B.V., Amsterdam.

Bloch, S., Ler Robert, H. and Bonnell, L. 2002. Anomalously high porosity and permeability in deeply buried sandstone reservoirs; origin and predictability. AAPG Bulletin 86, 301-328.

Bukovics, C. and Ziegler, P. A. 1985. Tectonic development of the Mid-Norway continental margin. *Marine and Petroleum Geology*, 2, 2-22.

Caja, M.A., Marfil, R., Estupiñán, J., Morad, S., Mansurbeg, H., Garcia, D., and Amorosi, A. 2008. Diagenesis and porosity evolution of Cretaceous turbidite sandstones: Vøring Basin, mid-Norway passive margin. *Geo-Temas* 10, 1567-5172.

Campbell, C. J. and Ormaasen, E. 1987. The discovery of oil and gas in Norway: An historical synopsis. *Geology of the Norwegian Oil and Gas Fields*, 1-37.

Chuhan, F.A., Kjeldstad, A., Bjorlykke, K. and Hoeg, K. 2002. Porosity loss in sand by grain crushing; experimental evidence and relevance to reservoir quality. *Marine and Petroleum Geology* 19, 39-53.

Cohen, M. and Dunn, M. The hydrocarbon habitat of the Haltenbanken–Trænabanken area offshore Mid-Norway. *Petroleum Geology of North West Europe. Proceedings of the 3rd Conference, 1987.* 1091-1104.

Dalland, A., Worsley, D. and Ofstad, K. 1988. A lithostratigraphic scheme for the Mesozoic and Cenozoic succession offshore for the Mesozoic and Cenozoic succession offshore mid- and northern Norway. *Norwegian Petroleum Directorate Bulletin*, 4, 65.

Dickinson, G. 1953. Geological aspects of abnormal reservoir pressures in Gulf Coast Louisiana. *AAPG Bulletin*, 37, 410-432.

Doré, A. G. and Lundin, E. R. 1996. Cenozoic compressional structures on the NE Atlantic margin; nature, origin and potential significance for hydrocarbon exploration. *Petroleum Geoscience*, 2, 299-311.

Dott, R.H. 1964. Wacke, greywacke and matrix- what approach to immature sandstone Classification? *Journal of sedimentary petrology* 34, no. 3, 625-632.

Ehrenberg, S.N. 1993. Preservation of anomalously high porosity in deeply buried sandstones by grain-coating chlorite; examples from the Norwegian continental shelf. AAPG Bulletin 77, 1260-1286.

Ehrenberg, S. N., Gjerstad, H. M. and Hadler-Jacobsen, F. 1992. Smorbukk Field: a gas condensate fault trap in the Haltenbanken province, offshore mid-Norway. Giant oil and gas fields of the decade 1978-1988, 323-348.

Ehrenberg, S. N., 1995. Measuring sandstone compaction from modal analyses of thin sections: how to do it and what the results mean. Journal of Sedimentary Research 65, 369-379.

Emery, D. Smalley, P. C. and Oxtoby, N. H. 1993. Synchronous oil migration and cementation in sandstone reservoirs demonstrated by quantitative description of diagenesis: Philosophical Transactions of the Royal Society of London, v. 344, p. 115–125.

Faleide, J. I., Tsikalas, F., Breivik, A. J., Mjelde, R., Ritzmann, O., Engen, Ø., Wilson, J. and Eldholm, O. 2008. Structure and evolution of the continental margin off Norway and the Barents Sea 31, 82-91.

Faleide, J. I., Bjørlykke, K. and Gabrielsen, R. H. 2010. Geology of the Norwegian Continental Shelf. Petroleum Geoscience: From Sedimentary Environments to Rock Physics, 467-499.

Fawad, M., Mondol, N.H., Jahren, J. and Bjørlykke, K. 2011. Mechanical compaction and ultrasonic velocity of sands with different texture and mineralogical composition. Geophysical Prospecting, no-no.

Fjeldskaar, W., Johansen, H., Dodd, T.A. & Thompson, M. 2003: Temperature and maturity effects of magmatic underplating in the Gjallar Ridge, Norwegian Sea. In Düppenbecker, S., & Marzi, R. (Eds.), Multidimensional basin modeling. American Association of Petroleum Geologists/Datapages Discovery Series 7, 71-85.

Fjellanger, E., Surlyk, F., Wamsteeker, L. C. and Midtun, T. 2005. Upper cretaceous basin-floor fans in the Vøring Basin, Mid Norway shelf. Norwegian Petroleum Society Special Publications 12:135-164.

Folk, R. L. 1951. Stages of textural maturity in sedimentary rocks. *Journal of Sedimentary Research*, 21, 127-130.

Folk, R.L. (1974) *Petrology of Sedimentary Rocks*. Hemphill Publishing Co., Austin, 170 p.

Fonneland, H.C., Lien, T., Martinsen, O.J., Pedersen, R.B. and Kosler, J. 2004: Detrital zircon ages: a key to understanding the deposition of deep marine sandstones in the Norwegian Sea. *Sedimentary Geology* 164, 147-159.

Forbes, P., Ungerer, P., A., Kuhfuss, F. and Eggen, S. 1991. Compositional Modeling of Petroleum Generation and Expulsion: Trial Application to a Local Mass Balance in the Smorbukk Sor Field, Haltenbanken Area, Norway (1). *AAPG Bulletin*, 75, 873-893.

Fuchtbauer, H. 1983. Facies controls on sandstone diagenesis. *Sediment Diagenesis*. Springer.

Færseth, R.B. & Lien, T. 2002. Cretaceous evolution of the Norwegian Sea – a period characterized by tectonic quiescence. *Marine and Petroleum Geology*, 19, 1005-1027.

Gabrielsen, R. H., Faleide, J. I., Pascal, C., Braathen, A., Nystuen, J. P., Etzelmuller, B. and O'donnell, S. 2010. Latest Caledonian to Present tectonomorphological development of southern Norway. *Marine and Petroleum Geology*, 27, 709-723.

Giles, M.R., Stevenson, S., Martin, S.V., Cannon, S.J.C., Hamilton, P.J., Marshall, J.D. and Samways, G.M. 1992. The reservoir properties and diagenesis of the Brent Group; a regional perspective. *Geological Society Special Publications* 61, 289-327.

Gluyas, J.G., Robinson, A.G., Emery, D., Grant, S.M. and Oxtoby, N.H. 1993. The link between petroleum emplacement and sandstone cementation. *Petroleum Geology of Northwest Europe Proceedings of the Conference 4*, 1395-1402.

Haddad, S. C. Worden. R. H Prior, D. J. and Smalley, P. C. 2006. Quartz cement in the Fontainebleau sandstone, Paris Basin, France: Crystallography and implication for mechanisms of cement growth: *Journal of Sedimentary Research*, v. 76, p. 244–256.

Heald, M. and Larese, R. 1974. Influence of coatings on quartz cementation. *Journal of Sedimentary Research*, 44.

Heald, M. and Renton, J. 1966. Experimental study of sandstone cementation. *Journal of Sedimentary Research*, 36.

Henriksen, S., Fichler, C., Grønlie, A., Henningsen, T., Laursen, I., Løseth, H., Ottesen, D. and Prince, I. 2005. The Norwegian sea during the Cenozoic. *Norwegian Petroleum Society Special Publications*, 12, 111-133.

Heum, O. R., Dalland, A. and Meisingset, K. K. 1986. Habitat of hydrocarbons at Haltenbanken (PVT-modelling as a predictive tool in hydrocarbon exploration, offshore Norway). *Habitat of hydrocarbons on the Norwegian continental shelf. Proc. conference, Stavanger, 1985*, 259-274.

Jackson, J. and Hastings, D. 1986. The role of salt movement in the tectonic history of Haltenbanken and Traenabanken and its relationship to structural style. *Habitat of hydrocarbons on the Norwegian continental shelf*, 241-257.

Karlsen, D. A., Nedkvitne, T., Larter, S. R. and Bjørlykke, K. 1993. Hydrocarbon composition of authigenic inclusions: Application to elucidation of petroleum reservoir filling history. *Geochimica et Cosmochimica Acta*, 57, 3641-3659.

Karlsen, D. A., Nyland, B., Flood, B., Ohm, S. E., Brekke, T., Olsen, S. and Backer-Owe, K. 1995. Petroleum geochemistry of the Haltenbanken, Norwegian continental shelf. Geological Society, London, Special Publications, 86, 203-256.

Karlsen, D. A., Skeie, J. E., Backer-Owe, K., Bjørlykke, K., Olstad, R., Berge, K., Cecchi, M., Vik, E. and Schaefer, R. G. 2004. Petroleum migration, faults and overpressure. Part II. Case history: The Haltenbanken Petroleum Province, offshore Norway. Geological Society, London, Special Publications, 237, 305-372.

Karlsen, D. A. and Skeie, J. E. 2006. Petroleum migration, faults and overpressure, part i: calibrating basin modelling using petroleum in traps — a review. Journal of Petroleum Geology, 29, 227-256.

Kittelsen, J.E., Hollingsworth, R.R., Marten, R.F. and Hansen, E.K. 1999: The first Deepwater well in Norway and its implications for the Cretaceous play, Vøring Basin. In Fleet, A.J. & Boldy, S.A. (eds.): Petroleum Geology of Northwest Europe: Proceedings of the 5th Conference, Geological Society, London, 275-280.

Knaust, D. 2009. Characterization of a Campanian deep-sea fan system in the Norwegian Sea by means of ichnofabrics. Marine and Petroleum Geology, 26, 1199-1211.

Lien, T. Midtbø, R.E. and Martinsen, O.J. 2006: Depositional facies and reservoir quality of deep-marine sandstones in the Norwegian Sea. Norwegian Journal of Geology, Vol. 86, pp. 71-92

Lundegard, P.D., 1992. Sandstone porosity loss -a “big picture” view of importance of compaction. Journal of Sedimentary Research 62, 250-260.

Marchand, A. M. E. Haszeldine, R. S. Macaulay, C. I. Swennen, R. and Fallick, A. E. 2000. Quartz cementation inhibited by crestal oil charge: Miller deep water sandstone, U.K. North Sea: Clay Minerals, v. 35, p. 210–210.

Marchand, A. M. E. Haszeldine, R. S. Smalley, P. C. Macaulay, C. I. and Fallick, A. E. 2001. Evidence for reduced quartz cementation rates in oil-filled sandstones: *Geology*, v. 29, p. 915–918, doi:10.1130/0091-7613(2001) 029<0915:EFRQCR>2.0.CO₂.

Martinsen, O.J., Lien, T. and Jackson, C. 2005: Cretaceous and Palaeogene turbidite systems in the North Sea and Norwegian Sea basins: source, staging area and basin physiography controls on reservoir development. In Dorè, A.G. & Vining, B.A. (Eds.), *Petroleum Geology: North-West Europe and Global Perspectives – Proceedings of the 6th Petroleum Geology Conference*, Geological Society, London, 1147-1164.

Mondol N. H., Bjørlykke K., Jahren J. and Hoeg K. (2007). Experimental mechanical Compaction of clay mineral aggregates - changes in physical properties of mudstones during burial. *Marine and petroleum geology*, v. 24, p. 289-311.

Mogensen, T.E., Nyby, R., Karpuz, R. and Haremo, P. 2000: Late Cretaceous and Tertiary structural evolution of the northeastern part of the Vøring Basin, Norwegian Sea. In Nøttvedt, A. et al. (Eds.), *Dynamics of the Norwegian Margin*. Geological Society, London, Special Publication 167, 379-396.

Morad, S., Ketzer, J.M., and De, R.L.F., 2000. Spatial and temporal distribution of diagenetic alterations in siliciclastic rocks; implications for mass transfer in sedimentary basins. In: Best Jim, L., Fielding, C., Jarvis, I., Mozley, P. (Eds.), *Millennium Reviews*. International Association of Sedimentologists, pp. 95e120.

Mosar, J. 2000: Depth of extensional faulting on the Mid-Norway Atlantic passive margin. *Norges geologiske undersøkelse Bulletin* 437, 33-41.

Mørk, M.B.E., Leith, D.A. and Fanavoll, S. 2001. Origin of carbonate-cemented beds on the Naglfar Dome, Vøring Basin, Norwegian Sea. *Marine and Petroleum Geology* 18, 223-234

Odin, G.S. & Matter, A. (1981). De glauconiarum origine. 1981. *Sedimentology*, 28, 611-641.

Oelkers, E.H., Bjorkum, P.A. and Murphy, W.M. 1996. A petrographic and computational investigation of quartz cementation and porosity reduction in North Sea sandstones. *American Journal of Science* 296, 420-452.

Osborne, M.J. and Swarbrick, R.E. (1997) Mechanisms for generating overpressure in sedimentary basins: A reevaluation. *AAPG Bulletin*, 81, 1023-1041.

Osmundsen, P., T., Sommaruga, A., Skilbrei, J., R., Olesen, O., 2002. Deep structure of the Mid Norway rifted margin, *Norwegian Journal of Geology*, 82, 205-224.

Patience, R. L. 2003. Where did all the coal gas go? *Organic Geochemistry*, 34, 375-387.

Paxton, S.T., Szabo, J.O., Ajdukiewicz, J.M. and Klimentidis, R.E. 2002. Construction of an intergranular volume compaction curve for evaluating and predicting compaction and porosity loss in rigid-grain sandstone reservoirs. *AAPG Bulletin* 86, 2047-2067.

Peltonen C., Marcussen O., Bjørlykke K. and Jahren J. (2008). Mineralogical control on Mudstone compaction: a study of Late Cretaceous to Early Tertiary mudstones of the Vøring and More basins, Norwegian sea. *Petroleum geoscience* 14(2), p. 127-138.

Provan, D. M. J. 1992. Draugen Oil Field, Haltenbanken province, offshore Norway. Giant oil and gas fields of the decade 1978-1988, 371-382.

Ramm, M. 1992. Porosity-depth trends in reservoir sandstones: theoretical models related to Jurassic sandstones offshore Norway. *Marine and Petroleum Geology* 9, 553-567.

Ramm, M. and Bjørlykke, K. 1994. Porosity/depth trends in reservoir sandstones; assessing the quantitative effects of varying pore-pressure, temperature history and mineralogy, Norwegian Shelf data. *Clay Minerals* 29, 475-490.

Ramm, M., Forsberg, A. W. and Jahren, J. S. 1997. Porosity--Depth Trends in Deeply Buried Upper Jurassic Reservoirs in the Norwegian Central Graben: An Example of Porosity Preservation Beneath the Normal Economic Basement by Grain-Coating Micro quartz

Ren, S., Faleide, J. I., Eldholm, O., Skogseid, J. and Gradstein, F. 2003. Late Cretaceous–Paleocene tectonic development of the NW Vøring Basin. *Marine and Petroleum Geology*, 20, 177-206.

Rittenhouse, G. 1971. Mechanical compaction of sands containing different percentages of ductile grains: a theoretical approach. *AAPG Bulletin*, 55, 92-96.

Rothwell, N., Sorensen, A., Peak, J., Byskov, K. and Mckean, T. 1993. Gyda: Recovery of Difficult Reserves by Flexible Development and Conventional Reservoir Management. *Offshore Europe*.

Selley, R. 1978. Porosity gradients in North Sea oil-bearing sandstones. *Journal of the Geological Society*, 135, 119-132.

Sheldon, H.A., Wheeler, J., Worden, R.H. and Cheadle, M.J. 2003. An Analysis of the Roles of Stress, Temperature, and pH in Chemical Compaction of Sandstones. *Journal of Sedimentary Research* 73, 64-71.

Skogseid, J., Pedersen, T., Eldholm, O. and Larsen, B.T., 1992a. Tectonism and magmatism during NE Atlantic continental break-up: the Voring Margin. In: B.C. Storey, T. Alabaster and R.J. Pankhurst (Editors), *Magmatism and the causes of continental break-up*. *Geol. Soc. Spec. Publ.*, 68: 305–320.

Skogseid, J., Pedersen, T., Eldholm, O., Larsen, B.T., 1992b. Tectonism and magmatism during NE Atlantic continental break-up: the Vøring basin, in *Magmatism and the Causes of Continental Break-up*, 305-320, eds. Storey, B.C., Alabaster, T., Plankhurst, R.J., Geological Society, London, Special Publications.

Skogseid, J., Planke, S., Faleide, J.I., Pedersen, T., Eldholm, O., Neverdal, F., 2000. NE Atlantic continental rifting and volcanic margin formation, in *Dynamics of the Norwegian margin*, 167, 295-326, published for the Geological Society by Blackwell, Oxford.

Smelror, M., Dehls, J., Ebbing, J., Larsen, E., Lundin, E. R., Nordgulen, Ø., Osmundsen, P. T., Olesen, O., Ottesen, D., Pascal, C., Redfield, T. F. and Rise, L. 2007. Towards a 4D topographic view of the Norwegian Sea margin. *Global and Planetary Change*, 58, 382-410.

Smith, G. 1985. Geology of the deep Tuscaloosa (Upper Cretaceous) gas trend in Louisiana. *Habitat of Oil and Gas in the Gulf Coast: Proc. of the Fourth Annual Research Conf., Gulf Coast Section Society of Economic Paleontologists and Mineralogists Foundation*. 153-190.

Storvoll, V. and Brevik, I. (2008). Identifying time, temperature and mineralogical effects on Chemical compaction in shales by rock physics relations. *The leading edge*, p. 750-756.

Storvoll, V., Bjorlykke, K., Karlsen, D. and Saigal, G. 2002a. Porosity preservation in reservoir sandstones due to grain-coating illite; a study of the Jurassic Garn Formation from the Kristin and Lavrans fields, offshore mid-Norway. *Marine and Petroleum Geology* 19, 767-781.

Swarbrick, R. E. 1999. "Diagenesis in North Sea HPHT clastic reservoirs—Consequences for porosity and overpressure prediction." *Marine and Petroleum Geology* 16(4): 337-353.

Taylor, T.R., Giles, M.R., Hathon, L.A., Diggs, T.N., Braunsdorf, N.R., Birbiglia, G.V., Kittridge, M.G., Macaulay, C.I. and Espejo, I.S. 2010. Sandstone diagenesis and reservoir quality prediction: Models, myths, and reality. AAPG Bulletin 94, 1093-1132.

Thomson, A. 1979. Preservation of porosity in the deep Woodbine/Tuscaloosa trend, Louisiana.

Tucker, M. 1988. Techniques in sedimentology.: Blackwell Sci. Publ. Oxford United Kingdom. Pages: 394.

Walderhaug, O. 1990. A fluid inclusion study of quartz-cemented sandstones from offshore mid-Norway; possible evidence for continued quartz cementation during oil emplacement. Journal of Sedimentary Research 60, 203-210.

Walderhaug, O. 1994a. Precipitation rates for quartz cement in sandstones determined by fluid-inclusion microthermometry and temperature-history modeling. Journal of Sedimentary Research 64, 324-333.

Walderhaug, O. 1994b. Temperatures of quartz cementation in Jurassic sandstones from the Norwegian continental shelf; evidence from fluid inclusions. Journal of Sedimentary Research 64, 311-323.

Wentworth, C.K. 1922. A scale of grade and class terms of clastic sediments. J. Geol., v. 30, p.377-392.

Whitley, P. K. 1992. The Geology of Heidrun - a Giant Oil and Gas-Field on the Mid-Norwegian Shelf. Giant oil and gas fields of the decade 1978-1988, 54, 383-406.

Williams, L.A., Parks, G.A. and Crerar, D.A. 1985. Silica diagenesis; I, Solubility controls. Journal of Sedimentary Petrology 55, 301-311.

Worden, R.H. and Morad, S. 2000. Quartz cementation in oil field sandstones: a review of the key controversies. Quartz cementation in sandstones, Special publications of international association of sedimentologists, 29, 1-20.

Worden, R. H. and Morad, S. 2009. Quartz cementation in oil field sandstones: a review of the key controversies. Quartz cementation in sandstones, blackwell publishing ltd.: 1-20.

http://factpages.npd.no/ReportServer?/FactPages/PageView/wellbore_exploration&rs: (Last accessed 30th June 2019).

<https://www.npd.no/en/facts/publications/co2-atlases/co2-atlas-for-the-norwegian-continental-shelf/5-the-norwegian-sea/5.1-geology-of-the-norwegian-sea/> (Last accessed 30th June 2019).

